GROUNDWATER VELOCITY FIELD: STOCHASTIC ANALYSIS OF MAJOR GROUNDWATER FLOWPATHS AND IMPLICATIONS FOR CONTAMINANT TRANSPORT WITHIN THE GA EAST AND ADENTAN DISTRICTS, GHANA

BY

GODFRED BRIGHT HAGAN

(10070819)

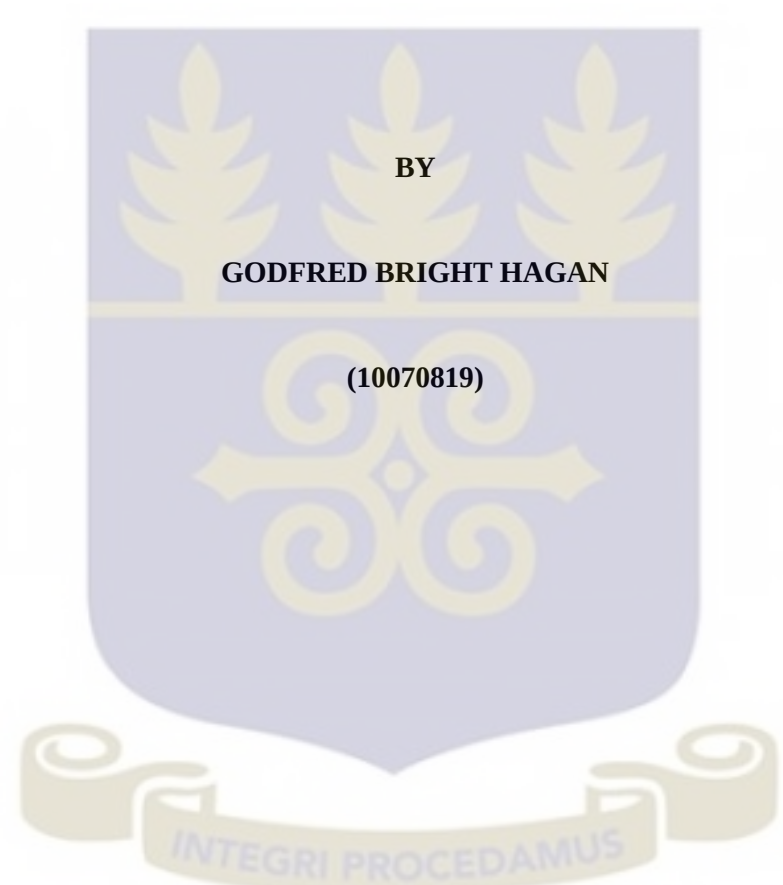

THIS THESIS IS SUBMITTED TO THE UNIVERSITY OF GHANA, LEGON, IN PARTIAL FULFILLMENT OF THE REQUIREMENT FOR THE AWARD OF DOCTOR OF PHILOSOPHY, PHYSICS DEGREE

JULY 2016

DECLARATION

I, Godfred Bright Hagan, hereby declare that except for the references to other peoples' works, which have been duly acknowledged, this thesis is the result of my own research work towards earning a Ph.D. as a student of the University of Ghana, Legon, under the supervision of the Supervisory Committee as detailed below.

…….. Date ……

GODFRED BRIGHT HAGAN
(Candidate)

……. Date ……

DR. V.C.K. KAKANE
(Principal Supervisor)

…… Date ……

PROF. S.M. YIDANA
(Supervisor)

…….. Date ……

PROF. J.K.A. AMUZU
(Supervisor)

DEDICATION

Partly to every Ph.D. student on the globe who is overwhelmed with the frustrations that come with Ph.D. research; and possibly contemplating giving up. I had my fair share of the frustrations and contemplated giving up too, just like you and many others who have travelled this path, but I finally made it. So DON'T GIVE UP!

I finally made it, thanks to the priceless assistance of a wonderful lady. Her commitment to the success of this work was beyond my comprehension. She was not in any way obliged to assist me, but she freely and willingly did so. **Lizzy**, I am honoured to dedicate this work to you. Cheers!

"HOPE and FEAR cannot occupy the same space at the same time. Invite one to stay."

Inspired by

MAYA ANGELOU

And I strongly suggest, you invite **HOPE** to stay.

ACKNOWLEDGEMENT

My foremost and utmost gratitude goes to the Almighty God for the gift of life and His guidance thus far in my professional pursuit.

Special appreciation to my supervisors – Dr. V.C.K. Kakane, Prof. S.M. Yidana, and Prof. J.K.A. Amuzu – for their patience and guidance throughout this work. This work could not have been completed successfully without their immense efforts. May the Almighty God remain gracious to you all. Amen. Prof. Yidana, I cannot thank you enough for your guidance and encouragement throughout the period of my postgraduate study.

Tons of gratitude go out to the staff of the Community Water and Sanitation Agency (CWSA) at the Greater Accra Region for the courtesies extended to me. Special thanks goes to Mrs. Safuratu Muhammed Andani (Regional director), Mrs. Rita Serwaa Cetteh (Hydrogeologist), and Mr. Kofi Mensah Sebuabe (the former Water and Sanitation Engineer). Serwaa, thank you very much for the countless times you had to assist me comb through piles of documents for useful data.

I received tremendous assistance from Mr. Kwame Johnson and Ms. Mary Mahama (of the Ga East Municipal Assembly), and Mr. Sylvester Sapaat (of Mdumolga Hydrogeological Development and Services Ltd.) for my field trips. Thank you all for your acts of kindness.

I am very grateful to Very Rev'd. R.A. Andam for his love, encouragement and sound counsel over the years. I am also grateful for the kind support and assistance received from Dr. F.G. Ofosu (GAEC) over the years. Again, my special gratitude goes out to Mrs. Angela Awere-Kyere (Procurement Officer, University of Ghana) for offering me a printer to aid my research.

My deep appreciation goes to Nii Amartey Amarteifio (formerly with the GIS Lab at the Department of Geography and Resource Development, University of Ghana) for assisting with my map works.

Mention must also be made of the support and encouragements I received from my colleagues at the Department of Physics. Special thanks to Dr. M.N.Y.H. Egblewogbe for proof reading my entire work. My brother, thank you very much! JAMH, thank you for your friendship. You were there for me every step of the way. You will surely taste your own Ph.D. success too. I salute Mr. Pamphile Tossou and his son, Emmanuel, for their tremendous support and friendship.

Dr. G.K. Nkrumah-Buandaoh, you took a very crucial step together with my neighbour (Dr. S.A. Anamzoya), and that singular act of yours turned things around for the better for me on this journey. I will forever be grateful to you both!

My gratitude also goes to the following faculty, staff, and students of the Department of Earth Science, University of Ghana, for their invaluable assistance: Dr. T.E.K. Armah, Dr. P.A. Sakyi, Dr. (Mrs.) Y.S.A. Loh, Mrs. T. Tietaah (Librarian), Messrs. S. Nunoo, D. Kwayisi, O.F. Fynn, and Ms. M.O. Addai.

Special *aseda* 'thanks' to Prof. K. Oduro-Afriyie and Dr. E.A.B. Effah Kaufmann for instilling in me the necessary values for my chosen career; and to my big brother – Dr. C.K.I. Appah (Department of Linguistics, University of Ghana) – for offering me expert editorial services.

I also want to acknowledge the goodwill from my trustworthy friends – Mrs. Bliss Acheampong (nee Arko-Boham), Mrs. Haziel Vera Cheataa-Plange, Ms. Gladys Poku, Dr. E. Mensah, Dr. B. Arko-Boham, and Rev'd. K. Boamah. I cherish our friendships! *Meda hom nyinara ase beberee* 'I thank you all very much.'

Finally, I wish to express gratitude to my lovely family – Edith (spouse), Liya (daughter), Ezra (son), Ewurabena (mum), and Percy (brother). I love you all for your endless support and prayers.

ABSTRACT

The hydrogeological system of the Ga East and Adentan Districts of the Greater Accra Region of Ghana was studied using numerical modelling on the Groundwater Modelling System platform (version 10.0). Historical hydrogeological data and groundwater monitoring data on twenty wells drilled in 2012 were relied on in conceptualising the hydrogeological system of the study area. A single aquifer system made up of quartzite-schist formation was identified. The borehole logs reveal four lithologies, laterite, schist, quartzite, and clay. Subsequently, a calibrated steady-state groundwater flow model was developed for the terrain. The aquifer hydraulic conductivity estimates for about 90% of the terrain are lower than 15.0 m day^{-1}. The observed outliers were attributable to the fractured and jointed quartzite within the weathered zone, which enhanced the conduits within the materials for rapid flow of groundwater. The estimated velocity field is in the range of 0.002 m day^{-1} to 11.2 m day^{-1}, with about 90% of the area having velocities below 0.85 m day^{-1}. The spatial distribution of the velocity field tied in well with the hydraulic conductivity field observed for the terrain. The estimated velocity field makes contaminant transport significant in the domain. For instance, contaminants/pollutants leached into the aquifer zone through recharge by rainfall from the landfill sited at Pantang will travel at approximately 0.85 m day^{-1} towards Oyarifa, Teiman and Ayimensa communities along an identified flowpath. Seven principal groundwater flowpaths were identified using the particle tracking technique. The travel times along the flowpaths from recharge to discharge locations ranged from 7 years to 833 years. The

cross-section cutting technique revealed cases of local and intermediate flow systems, and identified potential recharge areas. The effective aquifer recharge through precipitation ranges from 2.70×10^{-5} m day^{-1} to 8.10×10^{-5} m day^{-1}, representing 1.2% and 3.6% of the average annual precipitation in the area. The water budget shows that the flow system conserved mass, an indication that the flow model was indeed calibrated under steady-state conditions. The water budget also indicates that the current abstraction levels of groundwater can be sustained by recharge through rainfall to the aquifer system with minimal net drawdown in the hydraulic head. Stochastic simulations carried out on the calibrated model indicates that the model is unique for the aquifer recharge, hydraulic conductivity and hydraulic head. Three management scenarios which are centred on variations in groundwater recharge and abstraction were simulated to investigate the sustainability of the groundwater resource. The first scenario indicates that the existing recharge rates can sustain up to a three times increase in the current rates of abstraction of groundwater for both domestic and commercial purposes. The second scenario shows that, when the current rates of recharge decline by half or more, there would be considerable drawdown if the current abstraction rates were to be sustained solely by groundwater resource. The third scenario reveals that, with rainfall being the main source of recharge to the aquifer, a reduction in the current rainfall figures coupled with an increase in the current abstraction rates by three to five times would result in considerable drawdown.

LIST OF ABBREVIATIONS

CWSA-GAR	Community Water and Sanitation Agency in the Greater Accra Region
GAR	Greater Accra Region
GIS	Geographical Information System
GMS	Groundwater Modelling System
GoG	Government of Ghana
HK	Horizontal Hydraulic Conductivity
LPF	Layer Property Flow
MLGRD	Ministry of Local Government and Rural Development
MODFLOW	Modular Finite Difference groundwater flow simulation code
NSMC	Null Space Monte Carlo
PCG2	Pre-conditioned Conjugate Gradient 2
PEST	Parameter Estimation
PHC	Population and Housing Census
RMS	Root Mean Squared
S-T	Solute-Transport
TDS	Total Dissolved Solids
TIN	Triangulated Irregular Network
UTM	Universal Transverse Mercator

LIST OF TABLES

LIST OF FIGURES

TABLE OF CONTENTS

CHAPTER ONE

GENERAL INTRODUCTION

1.0 Introduction

This chapter ushers in this study by considering the following: the background of the study (section 1.1); the problem statement and relevance of the study (section 1.2); the objectives of the study (section 1.3); the methodology adopted in achieving the stated objectives (section 1.4); description of the study area (section 1.5); an overview/structure of the thesis (section 1.6); and the summary to this chapter (section 1.7).

1.1 Background of the study

The principles of groundwater flow and chemical transport (Domenico & Schwartz, 1998; Fetter, 2001; Freeze & Cherry, 1979) have largely been discussed in accordance with the general principles of fluid mechanics under a set of constraints and boundary conditions. Since the subsurface is accessible only through drilling, details of flow and associated phenomena are studied through models which are derived through the combination of the Darcy law and the conservation of mass (Fetter, 2001). There are a variety of versions of the governing equations of groundwater flow and these are copiously documented in the literature (Fetter, 2001; Freeze & Cheery, 1979).

Solutions to such equations provide useful information on the dynamics and fate of groundwater resources and assist in the management of the resource.

A variety of numerical codes have been developed over the years to assist in characterising subsurface fluid behaviour. They are all based on the fact that fluid flow is governed by differences in potential, as suggested by Hubbert (1940) and elaborated by Freeze and Cherry (1979). Solutions to numerical equations include spatial differences of flow and chemical transport. The generalised equation governing the flow of groundwater of constant density and viscosity through heterogeneous, anisotropic porous materials under transient conditions, given in equation (1.1), is of the form of the Laplace equation in three dimensions (Fitts, 2002).

$$K_x \frac{\partial^2 h}{\partial x^2} + K_y \frac{\partial^2 h}{\partial y^2} + K_z \frac{\partial^2 h}{\partial z^2} \pm W = S_s \frac{dh}{dt}, \tag{1.1}$$

For cases in which the assumptions of constant spatial fluid density and viscosity are not valid, the Laplace equation is modified to the form of equation (1.1) to accurately model fluid flow. Here K_i, W, and S_s, respectively, represent the hydraulic conductivity in the direction i, sources/sinks, and aquifer specific storage. Also, h is the hydraulic head (which dictates the groundwater potential).

Tóth (1962, 1963) was the first to analytically solve the simplified version of the Laplace equation to characterise subsurface flow and succeeded in identifying three different flow systems. Later, Freeze and Witherspoon (1966, 1967) solved the same

equations numerically under a set of boundary conditions. Since then, several attempts have been made and the accuracy of numerical predictions has been enhanced over the years. Large scale solutions of equation (1.1) and its several derivatives can be achieved only through numerical techniques and this requires the definition of boundary and initial conditions. In the light of this, the spatial and temporal representation of a numerical solution hinges on the accuracy and validity of the boundary and initial conditions.

Various investigators (e.g. Bethke, 1989; Connel, 2007; Farthing et al., 2004; Kai-Yuan, 2014; Panday & Huyakorn, 2004; Zhang & Werner, 2009; Zhou et al., 2003) have employed numerical modelling to investigate surface/subsurface flow phenomena under a variety of assumptions. In many cases, some of the assumptions of boundary and initial conditions could not stand the test of critical analysis. It is on the basis of this that the uniqueness of numerical models has been questioned in the past (e.g. Franke & Reilly, 1987; Moltyaner et al., 1993) as several sets of solutions are possible under the same set of boundary conditions.

However, Ophori (1999) argues that if models are sufficiently well calibrated with sufficient field data, they are sufficiently unique and provide useful decision support systems for managing the resource. The present research tests the uniqueness of numerical models calibrated with finite difference technique for the same terrain using the same boundary. The focus is on the effectiveness of the available numerical codes to adequately characterise groundwater flow conditions.

Numerical hydrogeology is a growing field in Ghana and the rest of the West African sub-region. In the past, due to paucity of data and the lack of appropriate expertise in the area, models were not popularly used as decision support systems. Where numerical models have been developed, they have largely been calibrated under steady state conditions (e.g. Attandoh et al., 2013; Lutz et al., 2007; Yidana, 2011; Yidana et al., 2014).

The uniqueness of the current study (being the first of its kind in the study area) lies in the fact that it focuses on the representation of the numerical solution for the terrain under the known boundary conditions. The results will guide the choice of numerical code and the solution techniques appropriate to the local terrain.

1.2 Statement of the problem

The supply of pipe-borne water in the Ga East and Adentan municipalities is insufficient and erratic. As a result, most households are exploiting groundwater by drilling boreholes and digging wells. The problem, however, is the lack of adequate and useful information on the dynamics and fate of the groundwater resources in the municipalities to assist in their proper management. The Ga East municipality, in particular, lacks proper sanitation and this challenge has been compounded with the recent decision to commission a landfill site within the municipality at Pantang.

Some households in the municipality have in recent times detected stains in their cooking utensils and have attributed these to their use of groundwater in the area. Such staining

could have been caused by one or several trace elements in excess concentrations in the groundwater. Thus, domestic use of such water over a long period of time can pose severe health risks.

The current work, therefore, seeks to study the details of flow in this terrain using numerical models to provide the needed adequate and useful information for the proper management of groundwater resources in the Ga East and Adentan municipalities. Providing such information can assist in the efforts being made by the Community Water and Sanitation Agency in the Greater Accra Region (CWSA-GAR). In accordance with *The CWSA Act 1998* (Act 564) establishing the CWSA, the Agency is committed to effective facilitation of the provision of sustainable potable water and related sanitation services as well as hygiene promotion in rural communities and small towns through resource mobilisation, capacity building and standards setting with the active participation of major stakeholders.

1.3 Objectives of the study

The main objective of this research is to develop a stochastic flow model over the Ga East and Adentan municipalities to generate a groundwater velocity field to predict travel times along flow paths. The specific objectives include the following:

- conceptualising the hydrogeological system
- developing a numerical simulation for groundwater flow systems, based on finite difference approach under specific boundary conditions

- determining an optimal approach to numerical approximation of subsurface flow in the study area
- developing a velocity field to assess possible impacts of anthropogenic activities such as refuse disposal sites on groundwater quality.

1.4 The methodology

To achieve the objectives stated above, this study will consider the following key aspects:

- conceptualisation of the hydrogeology of the area, using historical hydrogeological and groundwater monitoring data;
- identification and resolution of numerical groundwater flow equations to approximately characterise the physical groundwater flow system in the domain;
- calibration of the model to estimate key aquifer parameters;
- identification of flow systems and potential recharge areas in the modelled domain, using the cross-section cutting approach;
- simulation of the velocity field for the terrain to assess the impact of contamination transport in the study area.

1.5 The study area

The Ga East and Adentan municipalities are located at the northern part of the Greater Accra Region (GAR), between latitudes 5° 37’ 50” N to 5° 49’ 40” N and longitude

0° 16' 30" W to 0° 4' 30" W (Figure 1.1). The administrative capital of the Ga East Municipal Assembly is Abokobi, while that of the Adentan Municipal Assembly is Adentan. The Ga East municipality lies to the west of the Adentan municipality and the two municipalities share boundaries to the south with the La-Nkwantanang-Madina municipal. To the north, the Ga East municipal shares boundary with Akuapim South Municipal while the Adentan municipal shares boundary with the Tema Metropolis. The Ga East municipal shares boundary with Ga West municipal to the west; the Adentan municipal shares boundary with Ashiaman municipal to the east (Ministry of Local Government and Rural Development (MLGRD), 2006).

The Ga East and Adentan municipalities used to be classified as rural fringe but due to population and urban sprawl, they can now be considered as urban/peri-urban fringe (Adarkwa, 2012). They are rapidly urbanising, especially in the areas bordering Accra-Tema. As a result of the urban sprawl, the two municipalities have grown beyond the serviceable area of the Ghana Water Company. This has made many people resort to the use of groundwater by drilling boreholes or digging wells within their compounds. Besides individuals harnessing groundwater within the municipalities, a number of water sachet producing companies are also sited within the municipalities. The challenge, however, is the lack of adequate and useful information on the dynamics and fate of the groundwater resources in the municipalities to assist in the proper management of resource. The two municipalities therefore form a good case study for this research. A landfill, for instance, was recently located within the Ga East municipality at Pantang.

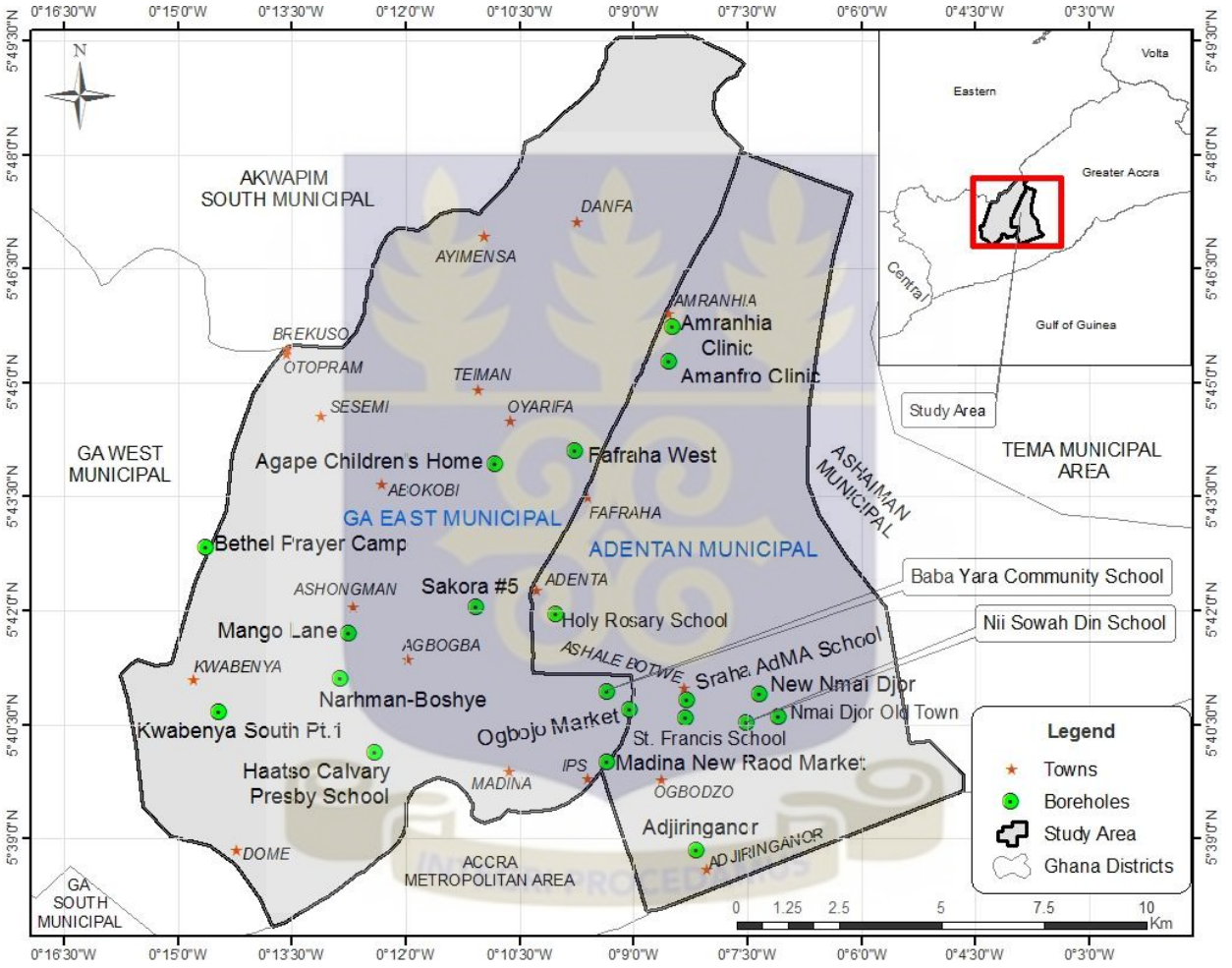

Figure 1.1 Map of the study area illustrating the twenty boreholes (wells) locations

(Source: Modified from the Geological Survey of Ghana, Accra)

1.5.1 The geology of the study area

The study area is predominantly Dahomeyides (Dahomeyan and Togo Structural Units) with minimal trait of the Accraian formation (Figure 1.2). The Dahomeyan structural unit is found in the southwestern part of Ghana (Dapaah-Siakwan & Gyau-Boakye, 2000; Mani, 1978). Mani's work, as well as that by Dapaah-Siakwan and Gyau-Boakye, show that this structural unit underlies the plains of Accra and moves eastwards into parts of the Volta Region of Ghana.

The Dahomeyan, which is neoproterozoic, is made up of the garnet quartzite, quatz-sericite schist, quartzo-feldspathic and augen gneisses, granulites and granitoids, and the migmatitic assemblage found at the eastern portion of the suture zone in southeastern Ghana. The Dahomeyan is generally northeast trending lithologic belts with low to medium angled dips to the southeast. Along the western boundary of the belt, the gneisses are in fault contact and overthrust onto rocks of the Buem-Togo Belt. The Dahomeyan shares a thrust folded contact with the Togo structural unit towards the west (Tairou et al., 2012).

The Togo structural unit, which is part of the Togo range, consists of quartzites; phyllites and phyllonites; quartz and sericite schists; shales; and siliceous limestones. Ar40/Ar39 (Muscovites) dating showed the Togo structural unit is 579.4 ± 0.8 Ma (Attoh et al., 1997). According to Kesse (1985), the Togo unit is highly folded, faulted and metamorphosed. The main structural grain in the Togo structural unit is the NE-SW with dips to the west (Kesse, 1985). The Togo range is bounded by two major thrust faults. One with the Dahomeyan contact at its eastern margin and the other at

its western contact with the Cape Coast granitoids complex rocks, the Voltaian, and the Buem sediments (Kesse, 1985).

The Togo range also consists of north to northeast trending rocks. These rocks are strongly tectonised phyllite, quartzite and serpentinite. These rocks were previously referred to as the Togo Series by Kesse (1985), but later as the Togo Tectonic Unit by Blay (1991). The unit grades from east to west from phyllite and chlorite schist upwards into quartzite, micaceous quartzite and sandstone (Grant, 1969).

The study area actually lies within the western quartzite, phyllite and chlorite schist of the Togo Structural Unit and its boundary with the Dahomeyan Gneisses.

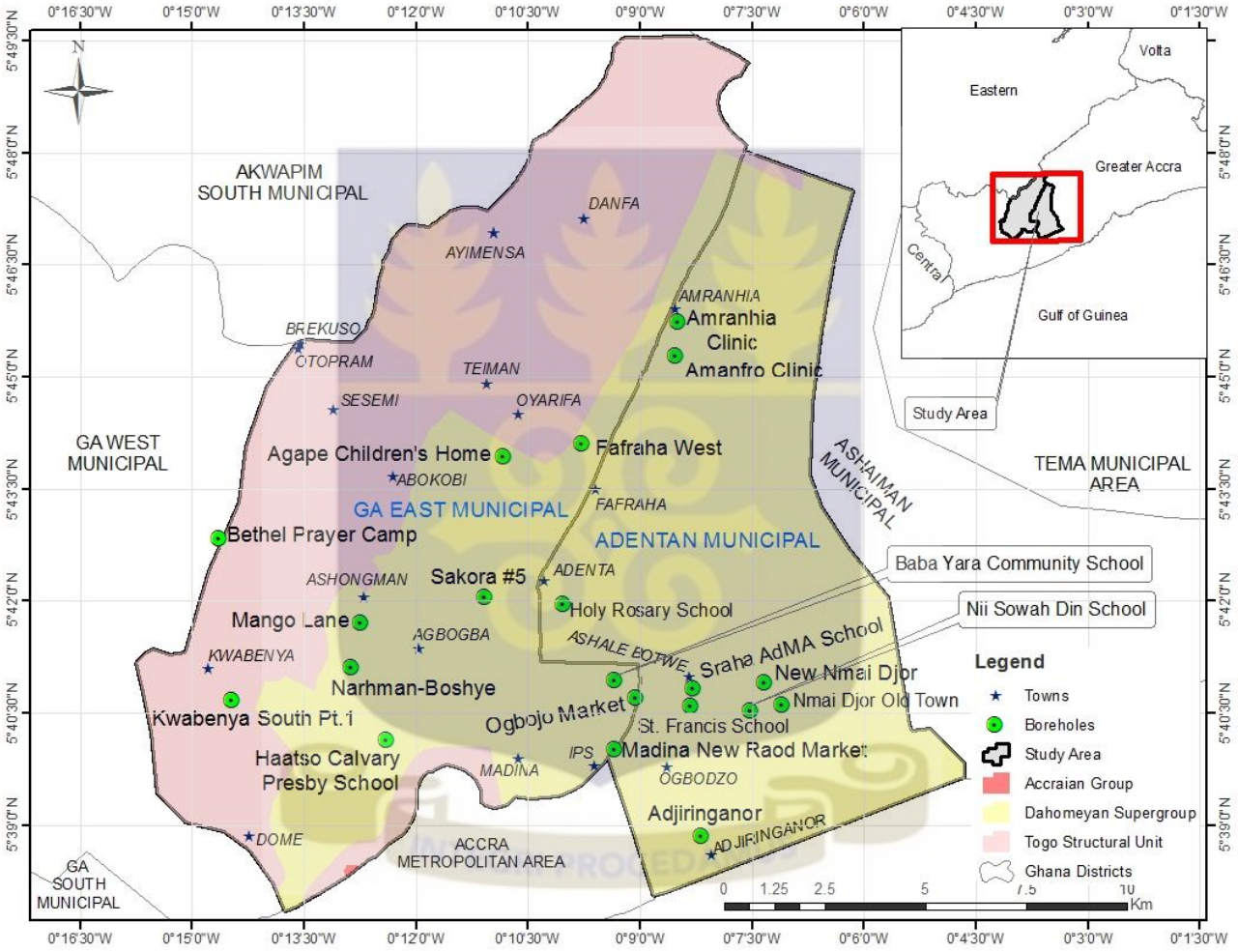

Figure 1.2 Geological map of the study area

(Source: Modified from the Geological Survey of Ghana, Accra)

1.5.2 The geography of the study area

1.5.2.1 Climate

The area under study has a semi equatorial type climate due to its position relative to the equator. Relative humidity averages 92%. The annual rainfall in the area ranges from 90 cm to 110 cm (Dickson & Benneh, 1988).

Rainfall is seasonal in the study area with the heaviest rainfall typically recorded in the months of June and July. The rainfall pattern is bi-modal; the first, usually the heaviest, occurs from May to about July while the second occurs between August and November (MLGRD, 2006).

The average annual temperature ranges between 25.1 ^{o}C in August and 28.4 ^{o}C in February and March. February and March are normally the hottest months (MLGRD, 2006).

1.5.2.2 Vegetation

The study area has two main types of vegetation, viz. shrub lands and grassland. The shrub lands occur mostly in the western outskirts and in the north towards the Aburi hills (MLGRD, 2006). The northern and the northwestern parts of the area are mostly forested. The mountains and highlands host a typical African sub-tropical deciduous forest. There are a lot of tall trees which usually form a canopy cover for short shrubs beneath. Dickson

and Benneh (1988) reported that it was difficult to find outcrops in such thickly forested areas.

The grassland which occurred to the southern parts has now been encroached upon by human activities including settlements (MLGRD, 2006). The southern part also hosts a thick cover of weathered lateritic materials. This forms a cover over the highly consolidated rocks beneath. Thus, a large portion of the study area except the northwestern segment can be described as poorly vegetated.

1.5.2.3 Topography, relief and drainage

The northwestern parts of the study area comprise mountains and other highlands interspersed with lowlands. The highest points in the area include the mountains at Otopram, about 1150 ft (350.52 m) above mean sea level. Another is the hill at Quarters, east of Comet properties. The hill is about 1040 ft (316.99 m) above mean sea level. It hosts one of the main television transmission masts of the Ghana Broadcasting Corporation. The lowest points in the study area are towards the southern boundary. Atwuo-Okuman is only about a 100 ft (30.48 m) above mean sea level.

The main rivers in the study area are the Ado, Labor and Onyasia rivers. The rivers generally flow from the northern part of the study area and to the south. The Ado and Labor rivers flow in southwesterly direction of the study area. River Onyasia in the

southern-most part of the study area also flows towards the south. The rivers have a generally dendritic pattern, and they meander between the lowlands.

1.6 Overview of the thesis

The rest of the thesis is structured as follows. In chapter two, I discuss appropriate and relevant literature and underscore the relevance and appropriateness of this study. The issues dealt with are the principles governing groundwater flow and the relevance of the hydraulic head and potential field to groundwater flow; related studies in parts of Ghana; theories of groundwater flow; numerical methods and models for the study of groundwater flow; and data requirements for numerical models.

Chapter three is on the methodology adopted for this study. I deal with the hydrogeological characterisation of the domain using historical hydrogeological and groundwater monitoring data. Next, I describe the development of the numerical model, its calibration, and sensitivity analysis performed on the calibrated model. Following these, I discuss the need for carrying out stochastic simulations on the model, and proceed to describe the various management scenario analysis conducted on the model.

Chapter four focusses on the presentation, analysis, and discussions of pertinent results from this study based on the methodology adopted. The key aspects delved into are the general groundwater levels and flow patterns in the domain; hydraulic conductivity

estimates at calibration and the velocity field; recharge rate estimates at calibration; parameter sensitivity analysis; groundwater budget in the domain; stochastic simulations on the calibrated model for the domain; and analysis of management scenarios.

The final chapter, five, presents a summary of the research work done, highlighting significant results and their implications. I also outline recommendations to the two municipal assemblies, and further work in this field of research in the study area and the rest of the GAR.

1.7 Chapter summary

In this introductory chapter, I have dealt with the problem statement and relevance of the study which was informed by the discussion on the background of this study. I also outlined the key and specific objectives of the study, based on which a tailored methodology have been stated. Next, I described the study area touching on aspects that are relevant to the subject of this study. Finally, the structure of the rest of the thesis is presented.

CHAPTER TWO

LITERATURE REVIEW

2.0 Introduction

In this chapter, I review relevant literature on the subject of the present study. The chapter is divided into four main sections. Section 2.1 reviews the principles governing groundwater flow and establishes the relevance of the hydraulic head and potential field to groundwater flow. Section 2.2 outlines some related studies in parts of Ghana, and makes the case for this present study. Section 2.3 examines the theories of groundwater flow whilst section 2.4 discusses numerical methods and models for the study of groundwater flow, and data requirements for numerical models. Section 2.5 summarises the chapter.

2.1 Principles of Groundwater Flow

Accordingly to Fitts (2002), in almost any investigation involving groundwater, questions arise about how much water is moving and how fast it is flowing. Answers to such questions are based on groundwater flow analyses, which in turn are based on some straightforward physical principles that govern subsurface flow.

Principles of groundwater flow and transport have been extensively researched, as reported in studies by, among others, Freeze and Cherry (1979), Todd (1980), Domenico and Schwartz (1998), and Fetter (2001). In groundwater flow studies, analogies are often drawn between the general flow and heat and electricity transport. *Heat transport* occurs from regions of high temperature to those of low temperature, whilst *Electricity flow* (or transport) occurs from a high electric potential to a low electric potential. The rate of transport in either case is proportional to the potential gradient between the two given locations (Spitz & Moreno, 1996). Groundwater flow takes a similar pattern to heat and electricity transport. Groundwater possesses energy (in mechanical, thermal and chemical forms) that varies spatially and hence, is forced to move from one region to another to eliminate the energy differentials (Appelo & Postma, 2010; Fetter, 2001; Hayatu et al., 2013; Konikow, 1996; Konikow & Reilly, 1998). The flow of groundwater is thus considered to be controlled by the laws of physics and thermodynamics.

There are a number of forces acting on groundwater (Fetter, 2001; Hálek & Švec, 1979). Fetter (2001) explains that there are three external forces that act on groundwater. The first is *gravity* which pulls it downward. The second is *external pressure* which is a combination of the atmospheric pressure acting above the zone of saturation and pressure from the weight of overlying water. The third force is *molecular attraction* which causes water to adhere to solid surfaces. When the water is exposed to air, this third force causes surface tension in the water. The phenomenon of capillarity is as a result of the two processes of water adhering to solid surfaces and surface tension in water (Fetter, 2001).

However, there are also frictional forces that tend to resist the flow of groundwater through porous media. These consist of the *shear stresses* acting tangentially to the surface of the solid and the *normal stresses* acting perpendicularly to the surface. There is also the *viscous force* within the fluid itself which tends to impede the movement of fluid molecules past each other (Fetter, 2001).

Considering a unit volume of groundwater of nearly constant temperature, the total mechanical energy of the water would have three components – kinetic, gravitational potential and fluid-pressure energy (Fetter, 2001). Derivation of the mathematical expression for the total mechanical energy is given in Appendix A, but the mathematical expression is given in equation (2.1).

$$E_{tv} = \frac{1}{2}\rho v^2 + \rho g z + P \tag{2.1}$$

where

E_{tv} is the total mechanical energy per unit volume

ρ is the density of the unit volume of the water

v is the velocity

z is the elevation of the centre of gravity of the water above a datum

g is the acceleration due to gravity

P is the pressure

Dividing equation (2.1) by ρ, yields total mechanical energy per unit mass, E_{tm}, as shown in equation (2.2), which is referred to as the Bernoulli equation (Freeze & Cherry, 1979; Weight, 2008).

$$E_{tm} = \frac{v^2}{2} + gz + \frac{P}{\rho} \tag{2.2}$$

An ideal fluid has the three components of the total energy to be constant while real fluids do not. Real fluids are compressible and do suffer frictional flow losses. Dividing equation (2.2) by g for the case of an ideal fluid will result in the expression shown in equation (2.3).

$$\frac{v^2}{2g} + z + \frac{P}{\rho g} = \text{constant} \tag{2.3}$$

Analysis of equation (2.3) reveals that each of the terms has units of energy per unit weight ($\mathrm{J\,N^{-1}}$), which reduces to units in length dimension. This sum of the total mechanical energy per unit weight is referred to as the *hydraulic head, h*.

2.1.1 The Hydraulic Head and Potential Field

The *hydraulic head, h*, as given by equation (2.3), is the total mechanical energy per unit weight of fluid. It is a specific measurement of fluid pressure above a geodetic datum (Fetter, 2001). Groundwater velocities are often very low; hence the velocity term in

equation (2.3) can be dispensed with. Thus, from equation (2.3), the total hydraulic head, h, is given by the expression shown in equation (2.4).

$$h = z + \frac{P}{\rho g} \tag{2.4}$$

Considering a fluid at rest, the pressure at a point is equal to the weight of the overlying water per unit cross-sectional area as expressed in equation (2.5).

$$P = \rho g h_p; \qquad h_p = {}^{P}/_{\rho g} \tag{2.5}$$

where

h_p is the height of the water column that provides a *pressure head*.

Thus, the total head, h, in terms of the pressure head h_p, is as given in equation (2.6) and illustrated in Figure 2.1, where the variable z is the *elevation head*.

$$h = z + h_p \tag{2.6}$$

Equation (2.6) is one of the very fundamental relationships in groundwater studies. It shows that the hydraulic head at a point in the hydrogeological system is made of two components: the pressure head (h_p) and the elevation head (z).

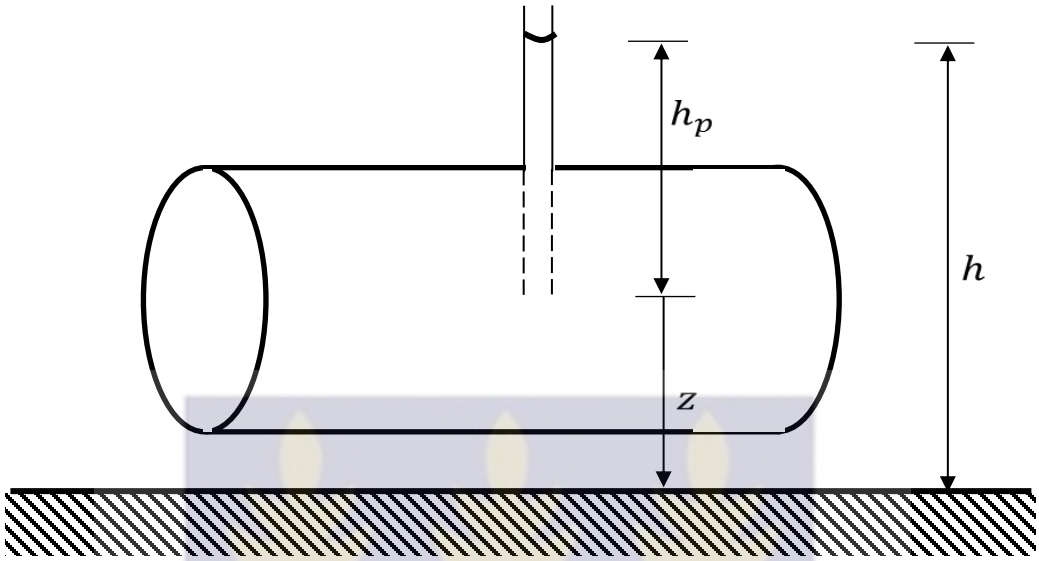

Figure 2.1 Components of the hydraulic head h, above a datum

(Source: Modified from Fetter, 2001)

Force Potential (or simply, *Potential*), $\emptyset$, is the term given to the total mechanical energy per unit mass in equation (2.2) above. Whenever water moves from one place to another, work is done. The work performed in moving a unit mass of fluid is a mechanical process and is known as the potential (Weight, 2008). It is considered to be the driving force behind groundwater flow. The Force Potential is thus, as shown in equation (2.7). Substituting for P from equation (2.5) in equation (2.7) yields the expression given in equation (2.8).

$$\emptyset = gz + \frac{P}{\rho} \tag{2.7}$$

$$\emptyset = g(z + h_p);\ \emptyset = gh \tag{2.8}$$

Equation (2.8) is very important in hydrogeology and groundwater flow studies and was first derived by Hubbert (1940). It indicates that *the potential* at a point in a hydrogeological system can be computed from the hydraulic head, h, and acceleration due to gravity g, at that point. Since acceleration due to gravity is almost constant everywhere on earth, the *potential field* (equation (2.8)) is determined largely by the hydraulic head (Freeze & Cherry, 1979). Thus, it is the total hydraulic head that controls the movement of groundwater.

From the preceding discussions, it is worth noting that the distribution of hydraulic head through an aquifer (or in a field) determines the groundwater flow direction. The flow is along the hydraulic gradient. The relative levels of the hydraulic head between two stratigraphic units in a formation will determine the relative vertical flow between them. Groundwater will flow vertically from the unit with higher head to that with relatively lower head. At any depth in an aquifer, the hydraulic head corresponds to the water table height; thus, when measuring the water level it does not make any difference how far the piezometer penetrates the aquifer (Figure 2.2).

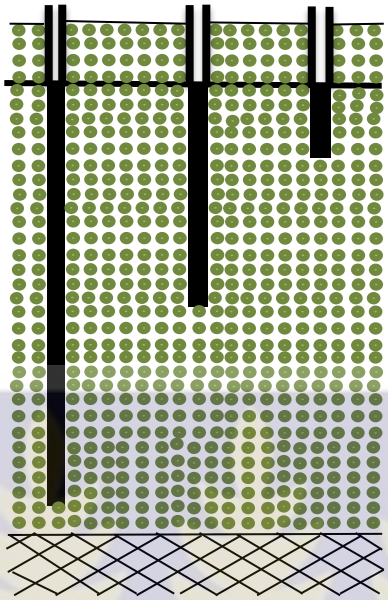

Figure 2.2 Illustration of water levels observed in piezometers

A pipe driven/placed in the subsoil with no leakage around it and having all entrance of water into it through the open bottom is what is referred to as *piezometer*. When the pipe has perforations/slots in its lower part (screen), it is referred to as an observation well or borehole. Observation boreholes in a region can, therefore, be used to determine the 3-D distribution of the hydraulic head.

A *potentiometric surface map* is a groundwater level map for a confined aquifer. It provides an indication of the directions of groundwater flow in the aquifer. For an unconfined aquifer, such a map is referred to as a *water table map* (Freeze & Cherry, 1979). The hydraulic head at a point in the potentiometric map is the level that the groundwater would rise in a borehole drilled to penetrate it. In a hydrogeological system, areas of high hydraulic head are referred to as *recharge areas*,

while areas of low hydraulic head are *discharge areas*. In other words, groundwater flows from recharge areas to discharge areas in the flow regime.

Having established the relevance of the hydraulic head and the potential field to groundwater flow, it is appropriate at this stage to review some recent works on the development of groundwater flow geometry in Ghana.

2.2 Application of numerical models in the development of groundwater flow geometry in Ghana

The use of numerical models to conceptualise the hydrogeological system of aquifers in parts of Ghana is an emerging field of research. For most of the terrains investigated, groundwater flow models have been developed and calibrated under steady-state conditions using the Groundwater Modelling System (GMS). From the scanty works conducted in this field of research in Ghana, a number of related studies are presented in the following discussion.

One of the pioneering works in the application of numerical models to groundwater flow studies in Ghana was undertaken by Lutz et al. (2007). A steady-state flow model was developed using the GMS package to conceptualise the aquifer conditions in the Nabogo Basin, a sub-catchment of the White Volta River Basin in northern Ghana. The developed model covered a limited duration because of the scarcity of available data, hence, the predictions and findings of the research were limited. However, the result of the study

was intended to form the basis for a more robust evaluation of groundwater resources in the area. Currently, extensive studies are ongoing on the White Volta using numerical models.

Similar steady-state models have been developed and calibrated to describe groundwater flow conditions in other parts of Ghana (*inter alia*, Attandoh et al., 2013; Banoeng-Yakubo et al., 2008; Yidana, 2011; Yidana et al., 2011; Yidana et al., 2014; Yidana et al., 2015a, b). The study carried out by Banoeng-Yakubo et al. (2008) defined the flow direction in southeastern Ghana as being a generally NE-SW preferred flow. This observation was corroborated by the work of Yidana et al. (2011).

The research conducted by Yidana et al. (2011) on some crystalline aquifers in southeastern Ghana was an improvement on the study carried out by Banoeng-Yakubo et al. (2008). However, in terms of the volume of data used and the robustness of the numerical codes used for the simulation, both works fell short of developing a velocity field and conducting stochastic analysis on the calibrated model to enhance confidence in the model.

Attandoh et al. (2013) characterised the general groundwater flow pattern in a crystalline rock aquifer system in southern Ghana. The results indicated a NE-SW direction of preferred flow, which was consistent with the findings of Yidana (2011) on the southern Voltaian sedimentary aquifers in the Afram Plains area, and that of Yidana et al. (2011)

on the crystalline basement aquifer system in southeastern Ghana. The study, however, had similar limitations to those by Yidana et al. (2011), highlighted earlier. The research by Yidana (2011) applied particle tracking to identify six distinct flowpaths for chemical transport and proceeded to simulate the travel times along the flowpaths. However, no detailed velocity field was developed for the terrain. Stochastic analysis was also not conducted on the calibrated model.

In a more recent study, Yidana et al. (2015a) used a calibrated steady-state model to characterise the flow geometry of the crystalline aquifer system in Lawra. The results pointed to a NW groundwater flow pattern, which is consistent with the NNW-SSE orientation of the Lawra belt. In yet another recent study by Yidana et al. (2015b), a flow model was calibrated under steady-state conditions to simulate the flow pattern in some crystalline aquifer systems in the Afigya Sekyere South District. The resulting NE-SW preferred flow pattern in the area conformed to the structural trend observed in some crystalline rock aquifers of the Birimian in the Densu Basin and the Southern Voltaian in the south by Yidana et al. (2014) and Yidana (2011), respectively.

However, this suggested flow pattern was different from that observed for the crystalline rock aquifer system in the northern part of the Voltaian by Attandoh et al. (2013). This observation was attributed to the fact that, in the Lawra area, the general structural controls on the flow are much more local entities which do not follow the general NE-SW regional structural pattern. As with all the discussed studies, these works by Yidana

et al. (2015a, b) stopped short of developing a velocity field for the areas, and conducting stochastic analysis on the calibrated models.

It can be deduced from the list and description of the related research works that, this field of research has not been explored in the current study area under investigation. This underscores the relevance and appropriateness of this study, especially that groundwater is largely harnessed in the Ga East and Adentan municipalities for both domestic and commercial use.

This study will develop and calibrate a groundwater flow model under steady-state conditions for the domain using the GMS platform. Hydrogeological characterisation of the domain would be undertaken using available historical hydrogeological and groundwater monitoring data from CWSA-GAR, and a flow geometry simulated for the identified aquifer system in the area. Hydraulic conductivity and recharge estimates for the terrain will be simulated, as was the case for most of the related studies presented. In addressing the limitations of the related works discussed earlier, a velocity field will be developed for the area. Particle tracking will be used to identify prominent flowpaths. The lengths of the flowpaths and the travel times along them will be simulated to facilitate developing the velocity field. Stochastic analysis will be carried out on the calibrated flow model to address that limitation with the other models discussed to enhance confidence in the current model to be developed. Additionally, a cross-section cutting approach will

be employed to identify the flow systems in the domain; a procedure that has not been explored by existing models, as discussed earlier.

The results of this study is intended to provide sufficient information for developing the groundwater vulnerability fields for the area. Additionally, the findings would provide the needed adequate and useful information for the proper management of groundwater resources in the area. This should lead to developing a robust transient groundwater flow model to predict the effects of climate change scenarios on groundwater budgets in the area.

2.3 Theories governing groundwater flow

2.3.1 Darcy law

The preceding section has established the fact that groundwater flow geometry is primarily tied to the spatial distribution of the hydraulic head and the potential field. The *hydraulic conductivity* is another essential parameter in groundwater flow studies. It reveals the character and quality of an aquifer and influences observed flow patterns, as will be demonstrated in the developed model for this study (section 4.2).

The process of groundwater flow is generally considered to be governed by the relations expressed in Darcy's law and the law of conservation of mass. For any control volume of porous medium in any given time, a general equation of the law of conservation of mass

for the volume may be expressed as equation (2.9), which is also referred to as the *continuity equation* (Konikow & Reilly, 1998).

$$\begin{bmatrix} (rate\ of\ mass\ inflow) \\ -(rate\ of\ mass\ outflow) \end{bmatrix} + \left[(rate\ of\ mass\ \frac{production}{consumption})\right]$$

$$= [(rate\ of\ mass\ accumulation)] \qquad (2.9)$$

Darcy's law relates the rate of flow of water through porous media to the properties of the water, the properties of the media, and the gradient of the hydraulic head (Konikow & Reilly, 1998). The law states that for any two points, a hydraulic gradient is created between them when the groundwater levels are different at the two locations. The flow between these two points depends on the magnitude of the hydraulic gradient.

The ratio of the hydraulic head to the length of the porous media ($\frac{dh}{dl}$) is referred to as the *hydraulic gradient* (Fetter, 2001). The flow direction is from areas where the hydraulic head is high to areas where the head is low. This is indicated by the negative sign in equation (2.10). Darcy's law can be expressed in terms of the force potential, using equation (2.8), as in equation (2.10) (Hubbert, 1940).

$$Q = -\frac{KA}{g}\frac{d\emptyset}{dl} \qquad (2.10)$$

Darcy's law generally holds when the resistive forces of viscosity predominate. Thus, the law is applicable to very slowly moving ground waters (laminar flow) which is the most natural condition for groundwater. According to Lindquist and Rose (as cited in Fetter, 2001), laminar groundwater flow prevails at Reynolds number between 1 and 10. However, it is difficult to detect turbulence in groundwater. Its occurrence in groundwater has been reported at a Reynolds number ranging from 60 (Schneebeli, 1955 as cited in Fetter, 2001) to 600 (Hubbert, 1956). The Reynolds number relates the four factors that determine whether the flow will be laminar or turbulent (Hornberger et al., 1998). This is expressed in equation (2.11).

$$R = {}^{\rho v d}/_{\mu} \qquad (2.11)$$

where

R is the Reynolds number, dimensionless

ρ is the fluid density

v is the discharge rate

d is the diameter of the passageway through which the fluid moves

μ is the viscosity

Turbulent flow in groundwater might occur in areas of rock with large openings, such as basalt flows, and areas of steep hydraulic gradients, such as the vicinity of a pumping well.

2.3.2 Seepage velocity

When water flows at a velocity v through a pipe or open channel of cross-sectional area A, the specific discharge Q, is as expressed in equation (2.12). The velocity can therefore be expressed as equation (2.13).

$$Q = vA \tag{2.12}$$

$$v = \frac{Q}{A} \tag{2.13}$$

From equations (2.10) and (2.13), the velocity can equally be expressed as equation (2.14)

$$v = \frac{Q}{A} = -K\frac{dh}{dl} \tag{2.14}$$

It is worth noting, that the cross-sectional area of flow in an open pipe is equivalent to the area of the end of the pipe. However, if the pipe is filled with a porous medium (say, sand), the open area of flow would be much smaller than the cross-sectional area of the pipe.

The cross-sectional area of flow for a porous medium is the product of the *effective porosity* of the aquifer material and the physical dimensions, where the effective porosity is that part of the pore space through which saturated flow occurs. To obtain the velocity

at which groundwater is actually moving, the velocity in equation (2.14) is divided by the effective porosity, n_e, to account for the actual open space available for the flow (Konikow, 1996). The resulting velocity is referred to as the *seepage velocity*, v_x. It represents the average rate at which groundwater flows between two points (Konikow & Reilly, 1998; Fetter, 2001). The seepage velocity is given in (2.15).

$$v_x = \frac{Q}{n_e A} = -\frac{K}{n_e}\frac{dh}{dl} \tag{2.15}$$

The foregoing equation shows clearly that the seepage velocity is controlled by the hydraulic conductivity. The calibrated model developed for this study establishes this relationship (section 4.2).

It is worth mentioning that the seepage velocity of groundwater is highly variable, even if aquifer properties are relatively homogeneous as a result of complex boundary conditions (Konikow, 1996). Thus, for the same system, no one numerical method chosen for the simulation model will be ideal or optimal over the entire domain of the problem. For this reason, significant numerical errors may be introduced somewhere in the solution. However, the numerical codes incorporated in the GMS version 10.0 (Aquaveo, 2014) used to develop and calibrate the model for this study is sufficiently robust to circumvent this challenge. This makes the simulated velocity field in this study a reliable representation of the real system.

2.4 Numerical methods and models

Mathematical models can be used to represent the physics of groundwater flow. The mathematical models consist of partial differential equations. Darcy's law is the simplest mathematical model of groundwater flow. Most groundwater flow models are deterministic mathematical models. Such models generally require solutions to the partial differential equations. The equations can be solved mathematically using either analytical solutions or numerical solutions. Obtaining the exact analytical solution, generally, requires that the properties and boundaries of the flow system be highly and perhaps unrealistically idealised. For most field problems, the mathematical benefits of obtaining an exact analytical solution are probably outweighed by the errors introduced by the simplifying assumptions of the complex field environment that are required to apply the analytical model (Konikow & Bredehoeft, 1992; Konikow, 1996).

The alternative approach is the approximation of the partial differential equations numerically to properly describe the physics. By so doing, the continuous variables are replaced with discrete ones defined as nodes or grid blocks. Thus, the differential continuous equation defining hydraulic head everywhere in the system is replaced by a finite number of algebraic equations defining the hydraulic head at specific points. These algebraic equations are solved using matrix techniques. This approach constitutes a *numerical model*, which is one of the most important developments in hydrogeology (cf. Konikow, 1996).

Under steady-state conditions, the generalised equation governing the flow of groundwater of constant density and viscosity through a heterogeneous, anisotropic aquifer (equation 1.1) reduces to equation (2.16).

$$K_x \frac{\partial^2 h}{\partial x^2} + K_y \frac{\partial^2 h}{\partial y^2} + K_z \frac{\partial^2 h}{\partial z^2} = 0 \qquad (2.16)$$

The two major classes of numerical methods used in solving the groundwater flow equation are the *Finite-difference* and *Finite-element* techniques (Anderson & Woessner, 1992). Both techniques require that the area of interest be subdivided by a grid into a number of cells or elements that are associated with node points, where the equations are solved for unknown values (Konikow, 1996) and the nodes are either at the centres or peripheries of the cells.

2.4.1 The finite-difference and finite-element models

Two variations of the Finite-difference grid are *Block-centred grid* and *Mesh-centred grid*. The former has the node points in the centre of the grid while the latter has the node points at the intersection of grid lines. The boundary conditions influence the choice between the two. A Block-Centred grid is most convenient when the flux is specified across a boundary and a Mesh-Centred grid most useful for situations where the head is specified at the boundary (Fetter, 2001).

The basic grid is regular with the rows and columns at right angles to each other and the distance in the x direction, Δx, being equal to Δy in the y direction. In the computer codes, the locations of the nodes are designated with reference to node ij, where i represents the column and j represents the row. The notation for i is positive to the right and for j, it is positive upward (Fetter, 2001). Codes exist that incorporate the z direction to describe the 3-D flow of groundwater flow, such as equations (1.1) and (2.16).

The finite-difference equation for a steady-state system expressed in equation (2.16) is shown in equation (2.17) (Wang & Anderson, 1982).

$$K_x \frac{h_{i+1,j,k} + h_{i-1,j,k} - 2h_{i,j,k}}{\Delta x^2} + K_y \frac{h_{i,j+1,k} + h_{i,j-1,k} - 2h_{i,j,k}}{\Delta y^2} + K_z \frac{h_{i,j,k+1} + h_{i,j,k-1} - 2h_{i,j,k}}{\Delta z^2} = 0 \quad (2.19)$$

The value of $h_{i,j,k}$ can be obtained from equation (2.19). It represents the average of the heads at the four closest nodes in the nodal mesh. In a finite-difference mesh, there are tens to hundreds of nodes. Equation (2.19) is solved by the *iterative methods*. This study utilised the mesh-centred grid approach of the finite-difference technique.

Finite-element models have the aquifer divided into polygonal cells (triangular in shape rather than rectangular as in Finite-difference models). The triangles intersect at the nodes that represent the points at which the unknown values (heads, for example) will be

computed. The value of the head in the interior of each cell is determined by interpolation between the nodal points (Fetter, 2001).

Either approach has its merits and demerits, but generally, the finite-difference techniques are easier to program for a computer because the mathematical basis is less complex. However, finite-element models are considered to be superior to finite-difference models (e.g. contaminant transport simulation). Another advantage of finite-element models is the flexibility of the grid to mimic the geometry of an aquifer system much more than finite-difference models. Finite-element models also require fewer nodes (Fetter, 2001; Konikow, 1996; Konikow & Reilly, 1998).

2.4.2 Boundary and initial conditions

Boundary and *Initial conditions* provide additional information about a specified physical process. This information aids in obtaining a unique solution of the partial differential equation corresponding to the given physical process. Only boundary conditions are needed for steady-state problems, while both boundary and initial conditions are required for transient problems (Konikow, 1996).

The boundary conditions specify the interaction between the area under study and its external environment. Mathematically, the boundary conditions include the geometry of the boundary and the values of the dependent variable or its derivative perpendicular to the boundary (Konikow, 1996; Konikow & Reilly, 1998). Mercer and Faust (1981) Fetter

(2001), and Todd and Mays (2005) point out that, the boundary conditions for groundwater model applications are basically of three types, namely:

1. Specified value (head or concentration) referred to as *Dirichlet boundary condition*,
2. Specified flux (relating to a specified gradient of head or concentration) referred to as *Neumann boundary condition* and
3. Head-dependent flux or mixed boundary condition referred to as *Cauchy boundary condition*. This type is called mixed boundary condition because it relates boundary heads to boundary flows.

A careful consideration is required in specifying appropriate types of boundaries to a particular field problem. This is crucial to providing reliable results from the calibrated model.

2.4.3 Data requirements for numerical models

Kumar (2015) noted that, the first phase of any groundwater study consists of collecting all existing geological and hydrological data on the groundwater basin in question. The major constraint to numerical modelling is data paucity, which reduces the effectiveness of the results of the numerical simulation of the flow and solute transport. This is mainly due to economic and accessibility constraints. However, a properly calibrated model with

adequate data is an excellent decision support system for the effective management and optimization of groundwater and aquifers (Yidana et al., 2014).

The weakness of deterministic numerical models relates to the apparent non-uniqueness, especially where the data relied upon is scanty. This is based on the argument that, several sets of hydraulic conductivity and recharge values can result in calibrated models (Yidana & Chegbeleh, 2013). This challenge is further compounded where there is insufficient field investigations to properly conceptualise the physical domain, models can produce unreliable results leading to bad decisions. However, as suggested by Ophori (1999) and collaborated by Yidana and Chegbeleh (2013) and amply demonstrated in several applications of numerical models in hydrogeological studies, when models are carefully conceptualised, constructed and calibrated in a professional manner with adequate data, it is useful as a decision support tool in a variety of environmental applications.

In order for a model to make hydrological sense, it must be based on a rational hydrogeological conception of the study domain. Thus, to successfully transform a conceptual model into a numerical model, it is necessary to have a database that provides adequate information to allow for the application of requisite equations (Fetter, 2001). A numerical model is first used to synthesise the various data and then to test the assumptions made in the conceptual model (Kumar, 2015).

Most models begin with a groundwater flow model which requires knowledge about the physical configuration of the aquifer and important hydraulic properties (Moore, 1979; Fetter, 2001). Thus, the success of numerical groundwater flow models in predicting subsurface flow phenomena depends on how adequately the groundwater flow equation is properly approximated to represent the real situation on the ground and how much each section of the domain is adequately represented in the conceptualisation process (Yidana et al., 2014). The two major approaches to the numerical approximation of equation (1.1), which represents the flow of groundwater, both rely on the adequacy and accuracy of the information obtained from the domain of the basin being studied in order to adequately define boundary and initial conditions (Yidana et al., 2014).

The physical configuration includes the location, areal extent, and thickness of all the aquifers and confining layers. It also includes the locations of the surface water bodies and streams; and the boundary conditions of all aquifers. The important hydraulic properties include the variation of transmissivity or permeability and storage coefficient of the aquifers, the variation of permeability and specific storage of the confining layers, and the hydraulic connection between the aquifers and surface water bodies (Fetter, 2001; Kumar, 2015). Hydraulic energy indicated by water-table or potentiometric-surface maps as well as the amounts of natural aquifer recharge and natural streamflow are also needed (Fetter, 2001; Kumar, 2015).

Solute-transport models require, in addition to the flow model data, the following information: distribution of effective porosity, aquifer dispersivity factors, fluid density variations, and natural concentrations of solutes distributed throughout the groundwater reservoir. The locations and strengths of the sources of contamination are also needed. In addition, retardation factors for the specific solutes with the specific rocks and soils of the area are needed (Fetter, 2001). The flow model computes the direction and rate of fluid movement whereas the solute-transport model derives movement and retardation values of contaminants (Fetter, 2001).

Models need to be calibrated and verified. Deterministic groundwater simulation models impose large requirements for data to define all of the parameters at all of the nodes of a grid (Konikow, 1996). *Model calibration* involves taking estimates of the model parameters and solving the model to see how well it reproduces some known condition of the aquifer (Fetter, 2001).

The objective of the calibration procedure is to minimise differences between the observed data and calculated values (Konikow, 1996). Properly calibrated models provide good estimates of aquifer hydraulic parameters (Fitts, 2002). Such estimates are usually large-scale averages with levels of uncertainties attributable to the uncertainties in some of the known data, and the incomplete knowledge of the nature of the aquifer material. The degree of uncertainty is greatly reduced if the nature of the aquifer is fairly

known, and the lithological well logs are fairly accurate and representative enough of the study area.

Most models are initially calibrated against the steady-state groundwater heads, and this requires a water-table or potentiometric-surface map. A potentiometric map of an aquifer provides an indication of the directions of groundwater flow in the aquifer. Also, it is useful to undertake a *sensitivity analysis* during the calibration of the model. This involves varying the parameters in the model during calibration to determine how sensitive the model is to changes in the hydraulic parameters and boundary conditions. This sensitivity analysis will give an understanding of the uncertainty in the model based on the known uncertainty of the field values of the most sensitive parameters (Fetter, 2001).

Since the same result can be obtained by changing two variables simultaneously, it is appropriate to verify a model once it has been calibrated. The model is usually considered calibrated when it reproduces historical data within some acceptable level of accuracy (Konikow, 1996). Thus, *model verification* is achieved by history matching in which a transient response of the model is obtained and compared with a known transient condition in the aquifer. If the known history is not reproduced with a desired degree of accuracy, the model parameters can be changed to recalibrate the model with a new set of model parameters and the verification run repeated (Fetter, 2001).

According to Fetter (2001), in verifying against transient condition, the aquifer storage coefficient is the recommended parameter to be adjusted since it may not be used in the calibration against steady-state conditions. Once the model has been verified against a transient event, it needs to be checked against the steady-state condition to ensure that it is still calibrated.

Transient events for history matching can include pumping tests in addition to long-term water-level declines. At this stage, *model field verification* can be carried out by stressing the aquifer (say, by performing a pumping test; Anderson, 1986) to see if the model correctly predicts the response of the aquifer as it is stressed. Most computer models, however, are not subjected to field verification because it is time consuming and very expensive.

The processes of model calibration and verification frequently require many changes in the data parameters that tend to compromise the model. Scale and analog models may require rebuilding each time a change is made in data values. Numerical models, however, can be easily recomputed with the new data. This explains why numerical models have nearly replaced other types of models. It must be emphasised, though, that the more accurate the data that is initially input into a model, and the more detailed the data against which it is verified, the more reliable the model results (Fetter, 2001).

The issue of non-uniqueness of the results of calibrated numerical groundwater flow models was circumvented through carefully constructing the model taking into account the appropriate boundary conditions to assign supported by sufficiently representative datasets. Additionally, the use of the GMS version 10.0 (Aquaveo, 2014) also assisted in enhancing the confidence in the calibrated model for this study. The software package provides a calibration-constrained Monte Carlo analysis of the groundwater model. This stochastic simulation generates a set of models from the calibrated model where each model in the set is equally probable as a unique representation of the terrain (system) under investigation. Subsequently, several management scenarios were conducted on the set of unique realisations for the domain generated by the stochastic simulations to predict the possible changes in the flow pattern and hydraulic heads (section 3.6).

Additionally, the cross-section cutting procedure will be utilised to identify the flow system in the area. A velocity field will also be simulated for the terrain and utilised to assess the implications for contaminant transport in the area.

2.5 Chapter summary

In this chapter, I have discussed literature that is relevant to the present study. I dealt with issues like the principles and theories governing groundwater flow. Key among the principles and theories discussed were Darcy's law and the relevance of the hydraulic head and potential field to groundwater flow. I also reviewed some related studies in parts of Ghana, and proceeded to make the case for this present study. Following these, I

touched on numerical methods and models for the study of groundwater flow, and data requirements for numerical models. The finite-difference technique and the boundary conditions adopted for this study have been discussed. Additionally, measures adopted to resolve the issue of non-uniqueness of calibrated models to provide confidence in the flow model developed for this study have been discussed. Finally, the unique procedures adopted in this study to improve on earlier studies in this field of research in parts of Ghana have been presented and discussed.

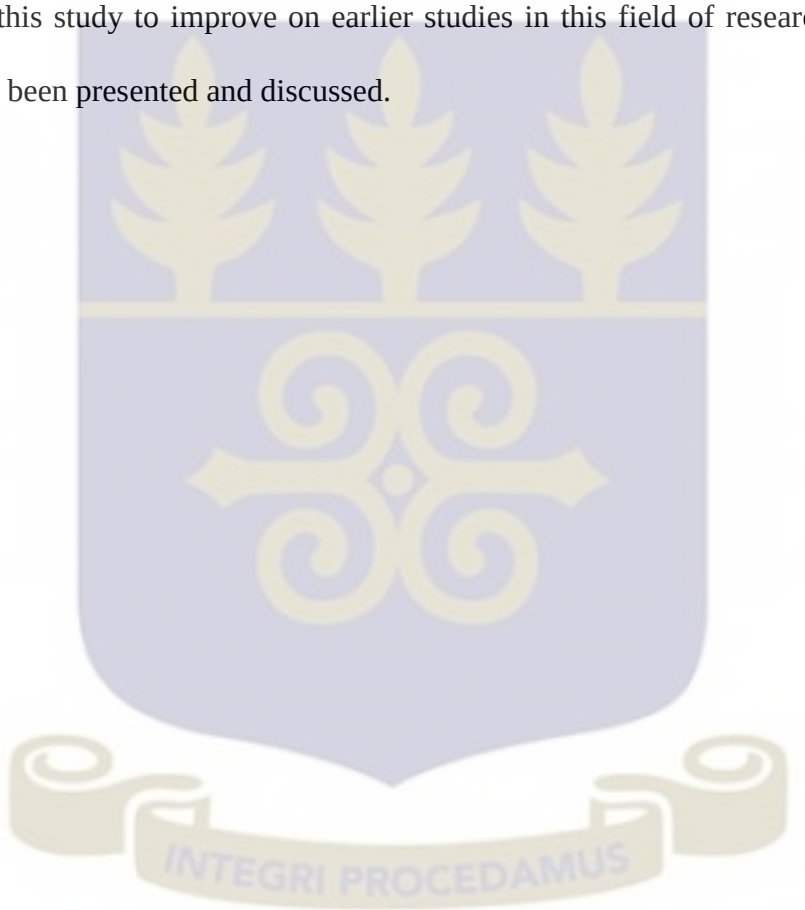

CHAPTER THREE

METHODOLOGY

3.0 Introduction

This chapter focuses on the approach to this study. The approach entails the following key aspects: hydrogeological characterisation of the domain using historical hydrogeological and groundwater monitoring data (section 3.1); development of the numerical model (section 3.2); calibration of the model (section 3.3); sensitivity analysis on the calibrated model (section 3.4); stochastic simulations on the model (section 3.5); and scenario analysis on the model (section 3.6). Section 3.7 summarises the chapter.

3.1 Characterisation of the hydrogeology of the domain

The hydrogeological characterisation of the study area was achieved using historical hydrogeological and groundwater monitoring data. Data on pumping test and borehole lithological logs of twenty wells drilled in the Ga East and Adentan municipalities under the Government of Ghana (GoG) 20,000 Borehole Drilling Project carried out in 2012 were accessed from the CWSA-GAR. The data captured information on the borehole IDs, their spatial positions (Figure 3.1) and locations, top and bottom elevations (in metres),

hydrogeological unit descriptions, lithology types, and well depths which ranged from 50 m to 90 m.

The lowest drill depth was recorded for the borehole at the Madina New Road Market while the deepest drill depth was recorded for boreholes at the Baba Yara Community School and Haatso Calvary Presbyterian School. A total of twenty wells (ten in each municipality) were logged showing rock types such as laterite, schist, quartzite and clay.

Maps on the geology, physical boundaries and drainage network of the study area were obtained from the Remote Sensing and Geographic Information System Laboratory of the University of Ghana. Field reconnaissance was undertaken to verify and confirm some of the information received from the two municipal assemblies and the CWSA-GAR.

These pieces of information were processed into acceptable formats for the characterisation and eventual conceptualisation of the hydrogeology of the domain. The conceptual framework was subsequently converted to a numerical model for steady-state simulations. The Modular Finite Difference groundwater flow simulation code, MODFLOW, (Harbaugh, 2005), incorporated in GMS version 10.0 (Aquaveo, 2014) was used for the numerical simulation.

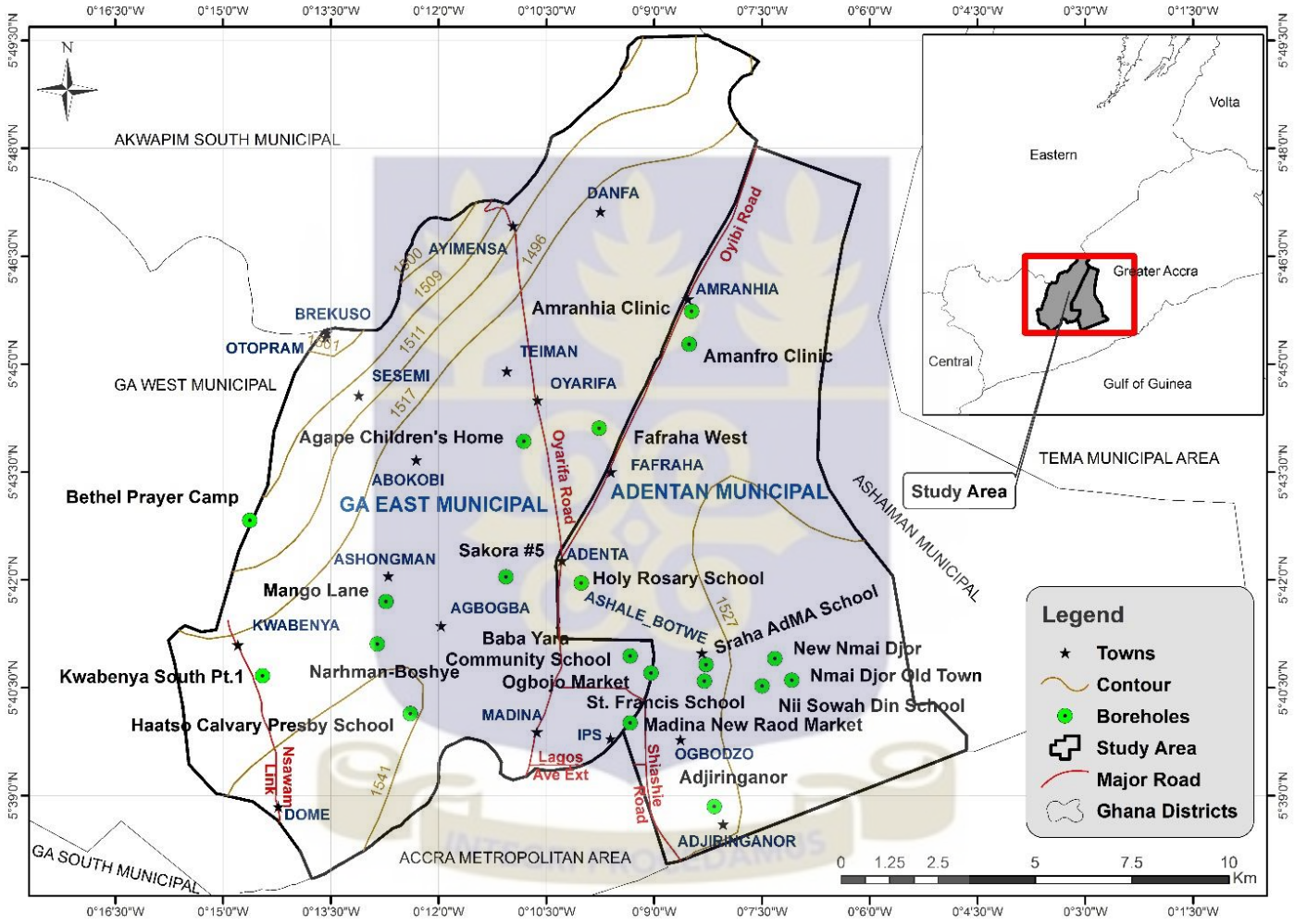

Figure 3.1 Map illustrating the borehole locations in the study area

(Map source: Modified from the Geological Survey of Ghana, Accra)

3.1.1 Lithostratigraphic and hydrostratigraphic units modelling

Lithostratigraphic units refer to the distinctive bodies of rock. These units focus solely on the specific types of rock; they may consist of a single rock type or a variety of rock types. Lithostratigraphy modelling involves generating the rock types in a domain from the near surface to the subsurface, sequentially from one location to the other, in the form of solids. It entails variation in various lithological units in terms of thickness, composition and their relation with the aquifer system. There are three basic methods in generating stratigraphy in the form of solids, viz. Horizons-to-Coverages, Horizons-to-TINs-to-Meshes, and Horizons-to-Solids (Aquaveo, 2010). This study utilised the Horizons-to-Solids algorithm approach because it provides a grid independent definition of layer elevations that can be used to immediately re-create MODFLOW grid geometry after any change to the grid resolution (Jones et al., 2002).

First, the coordinates of the twenty boreholes forming a representation of the entire study area were converted to Universal Transverse Mercator (UTM) in units of metres. These together with the elevations and other descriptions on the well logs were imported into MODFLOW. Next, a digitised geological map (Figure 3.2**)** of the domain was imported and registered within the GMS version10.0 (Aquaveo, 2014) to serve as base map coverage for the construction of the conceptual model using the Geographical Information System (GIS) map tools in GMS. The boundary of the map was delineated to form the boundary of the model.

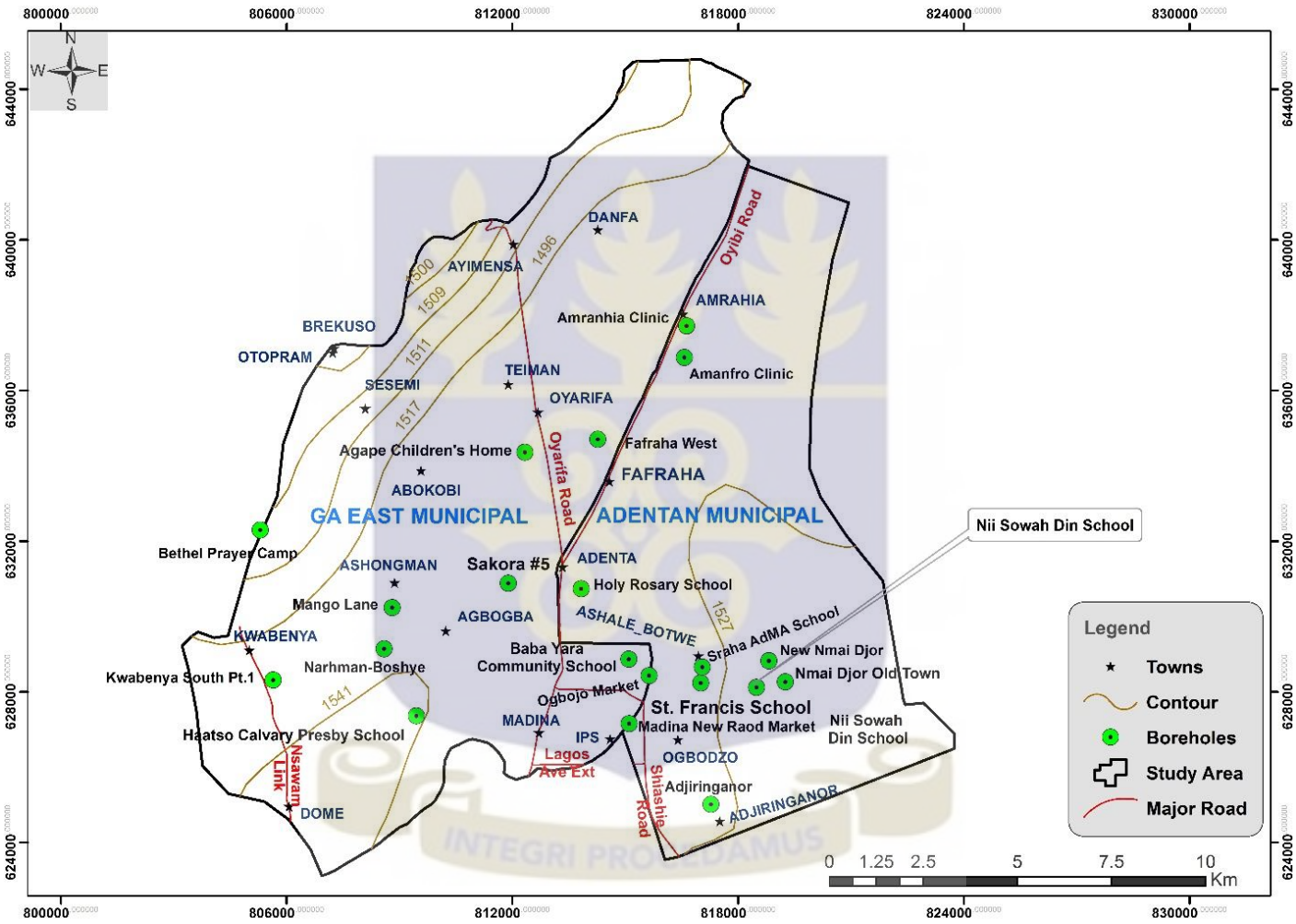

Figure 3.2 The registered digital map of the domain illustrating the borehole locations

(Map source: Modified from the Geological Survey of Ghana, Accra)

As noted in section 1.5, the study area is bounded in the west by Ga West municipal, north-west by Akwapim South municipal, east by Tema and Ashiaman municipal areas, and south by Ga South municipal and Accra metropolitan assembly. The various stratigraphic units are separated by defined surfaces. This was followed by defining a solid model of the domain using a series of extrusions and set operations. 3-D oblique views of the boreholes were created and colour-coded for quick reference. Horizons IDs were then assigned to the boreholes to represent the tops of geologic units in a depositional sequence. The rock types in the domain were grouped into four geologic units based on similar geological characteristics, viz. laterite, schist, quartzite and clay. Triangulated Irregular Network (TIN) was defined using a standard triangulation algorithm (Watson, 1981; Lawson, 1986; Field, 1991) to model terrains and the interfaces between stratigraphic units (Figure 3.3).

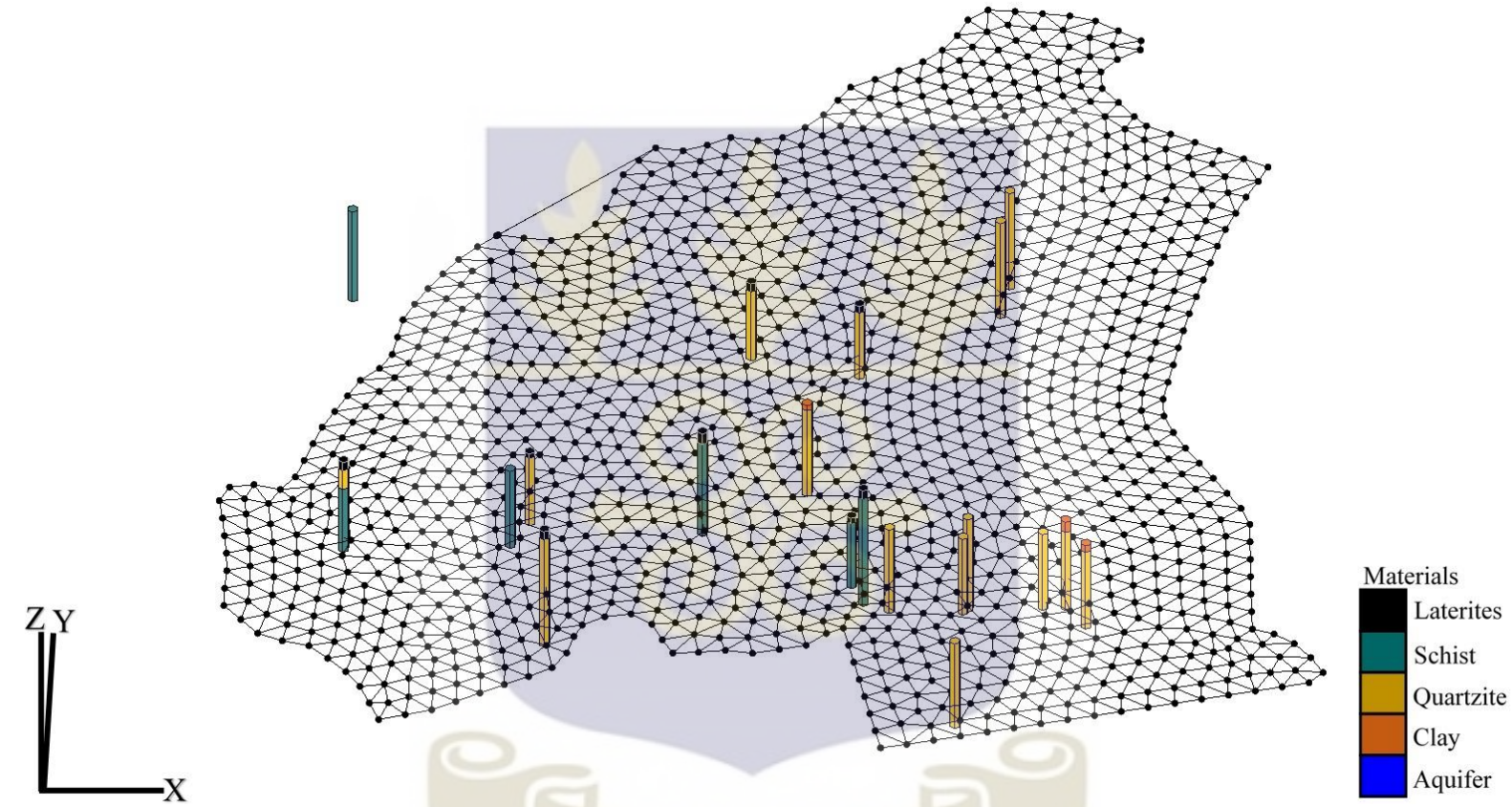

Figure 3.3 Horizon IDs for the various boreholes interpolated to the TIN

Horizon elevations from the borehole contacts were then interpolated to the TIN (top and bottom) using inverse distance weighted mode of algorithm, to define the horizon surfaces. Following this, the horizons were extruded and the solids were built, which defined the lithostratigraphic framework of the domain.

The next phase had the solid model converted into a hydrostratigraphic model. A *hydrostratigraphic unit* can be defined as a part of a rock that forms a distinct hydrologic unit with respect to the flow of groundwater (Maxey, 1964). Seaber (1988) redefined the term as "a body of rock distinguished and characterised by its porosity and permeability". Delineation of these units subdivides the geologic framework into relatively more or less permeable fragments and thus assists in the definition of the flow system. The hydrostratigraphic model was achieved by incorporating the aquifer zones, as scripted on the lithological well logs data. Using the thicknesses of each borehole and the depth of the aquifer zones, the depth of water tables per each well was delineated from the stratigraphic framework and used as the basis for the conceptualisation of the domain.

3.1.2 Conceptualisation of the hydrogeological framework

Model conceptualisation is the systematic description of the known physical features, and the groundwater flow and contaminant transport processes within an area of interest using all available data and knowledge of the region of interest (Kumar, 2002). This makes accurate conceptualisation very necessary in groundwater modelling. A good numerical

groundwater flow model proceeds from an adequate conceptualisation of the essential components of the hydrogeology of the terrain being modelled (Yidana et al., 2014).

The purpose of building a conceptual model is to simplify the field problem and organise the associated field data so that the system can be analysed readily (Anderson & Woessner, 2002). For this study, the conceptual model was developed using the map tools in the GMS version 10.0 (Aquaveo, 2014).

3.1.2.1 Model design and input of aquifer parameters

The domain was conceptualised as a single layer system since the hydrostratigraphy revealed by the well logs suggested insignificant differences amongst the groundwater bearing units penetrated by the wells. The bottom part of the domain, however, was conceptualised as a no-flow boundary since permeability generally decreases with depth. The aquifers generally range from semi-confined to confined, and were modelled under convertible condition. The vertical boundaries were modelled as general head boundaries so that they can adequately compute flows in and out of the domain. Coverages were generated and assigned initial values for the various aquifer parameters (viz. *Recharge*, *Horizontal Hydraulic Conductivity*, *General Head Boundary*, *Abstraction Well*, and *Observed Hydraulic Head*) as part of the conceptualisation process. Figure 3.4 illustrates the digitized boundary of the domain with the demarcated zones from which the aquifer parameters were assigned.

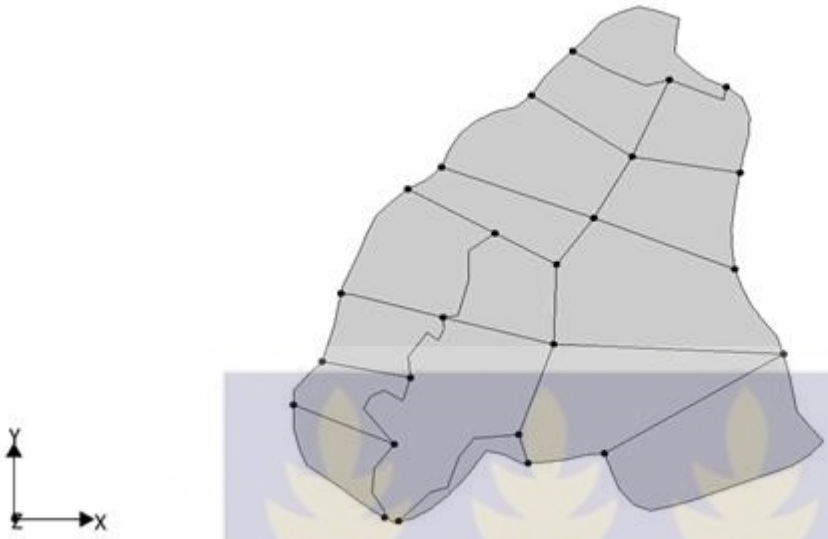

Figure 3.4 The sixteen demarcated zones within the domain

3.1.2.2 Drainage network (river coverage)

The study area has a number of perennial rivers and attributes whose networks were digitized and incorporated into the model as a river coverage. Elevations were assigned to the river networks haven extrapolated the contour height values for the study area from the general topography of the area using google earth. However, some streams within the domain could not be included in the model due to lack of sufficient and accurate data.

3.1.2.3 Recharge coverage

In estimating the recharge rates for the domain under investigation, a recharge coverage was set up using rainfall data for Accra, for the period January 2005 to December 2014, obtained from the Ghana Meteorological Agency. The annual average precipitation for the stated period was computed (as $825.60\ \text{mm yr}^{-1} \equiv 2.26 \times 10^{-3}\ \text{m day}^{-1}$) and

1% to 3% of the value was used as the initial input data for the recharge coverage. These calculated range of values were varied slightly and the model simulated during the calibration process. In the coverage for recharge, sixteen zones based on the lithology of the domain were created using the map tools in GMS version 10.0 (Aquaveo, 2014) in an attempt to capture the spatial variability of groundwater recharge. The sixteen zones were achieved by sub-dividing the area covered by each of the four identified lithologies. The spatial distribution of groundwater recharge estimated in the domain at the end of calibration is discussed in section 4.3.

3.1.2.4 Horizontal hydraulic conductivity (HK) coverage

The HK coverage, similar to that for recharge, was generated and assigned initial values based on the pump-test data associated with the boreholes, data on the well logs, and standard literature for the geology of the area. The vertical anisotropy was kept at default while the initial HKs were set in the range of 8.50 m day^{-1} to 12.00 m day^{-1} for the zones created. The HK field at calibration is discussed in section 4.2.

3.1.2.5 Abstractions coverage

All the wells used in this study are abstraction wells. The abstraction or discharge rates for the wells (in units of m^3 day^{-1}) from the pumping test results were imported into the abstraction coverage. Table 3.1 contains details of the abstraction rates associated with the various wells.

3.1.2.6 Observed hydraulic head coverage

Assigned to this coverage were the hydraulic head values for all the wells together with their spatial positions. The hydraulic heads (Table 3.2) were computed as the difference between the ground elevations and the static water levels for the individual wells.

Table 3.1 Initial abstraction rates for the various boreholes

Latitude Y	Longitude X	Community	Abstraction rates ($l\ day^{-1}$)	Abstraction rates ($m^3\ day^{-1}$)
811891.0	-630880.5	Sakora #5	5.0	7.20
814271.8	-634701.4	Frafraha West	10.0	14.40
805643.5	-628311.1	Kwabenya South Pt.1	10.0	14.40
805298.0	-632296.6	Bethel Prayer Camp	12.0	17.28
815106.6	-627151.7	Madina New Road Market	12.0	17.28
815098.2	-628864.1	Baba Yara Community School	7.0	10.08
808592.8	-629139.9	Narhman-Boshye	50.0	72.00
812333.5	-634356.7	Agape Children's Home	10.0	14.40
808809.2	-630232.2	Mango Lane	60.0	86.40
809451.3	-627357.8	Haatso Calvary Presby School	5.0	7.20
816631.0	-637716.8	Adjiringanor School	28.0	40.32
816573.6	-636874.2	Nii Sowah Din School	30.0	43.20
819258.9	-628263.6	Amanfro Clinic	24.0	34.56
818818.8	-628818.0	Holy Rosary School	65.0	93.60
818489.7	-628115.4	Amranhia Clinic	22.0	31.68
815633.2	-628430.2	New Nmai Djor	21.0	30.24
817045.7	-628652.3	Nmai Djor Old Town	20.0	28.80
817007.7	-628231.0	Ogbojo Market	45.0	64.80
813829.5	-630730.2	Sraha AdMA School	200.0	288.00
817279.2	-625013.3	St. Francis School	20.0	28.80

Table 3.2 Wells used for model calibration

Latitude Y	Longitude X	Community	Ground Elevation (m)
811891.0	-630880.5	Sakora #5	114
814271.8	-634701.4	Frafraha West	96
805643.5	-628311.1	Kwabenya South Pt.1	129
805298.0	-632296.6	Bethel Prayer Camp	216
815106.6	-627151.7	Madina New Road Market	135
815098.2	-628864.1	Baba Yara Community School	145
808592.8	-629139.9	Narhman-Boshye	100
812333.5	-634356.7	Agape Children's Home	119
808809.2	-630232.2	Mango Lane	81
809451.3	-627357.8	Haatso Calvary Presby School	134
816631.0	-637716.8	Adjiringanor School	113
816573.6	-636874.2	Nii Sowah Din School	112
819258.9	-628263.6	Amanfro Clinic	127
818818.8	-628818.0	Holy Rosary School	138
818489.7	-628115.4	Amranhia Clinic	129
815633.2	-628430.2	New Nmai Djor	114
817045.7	-628652.3	Nmai Djor Old Town	108
817007.7	-628231.0	Ogbojo Market	103
813829.5	-630730.2	Sraha AdMA School	100
817279.2	-625013.3	St. Francis School	117

3.1.2.7 Grid design

Developing the numerical model begins with the design of a suitable grid. The finer the grid, the better the modelling results. The conceptual model of the domain was discretized

into 10,000 cells with 100 rows and 100 columns. The model grid is oriented north-south and covered a total of 5223 active cells over a single layer (Figures 3.5a and 3.5b). Vertically, the domain was conceptualised as a single layer with spatially variable hydraulic properties.

There are several numerical codes available for the simulation of regional and local groundwater flow systems. MODFLOW, the code adopted for this study, is based on the finite differences approximation of equation (1.1). It is the general equation that describes the 3-D flow of groundwater of constant density and viscosity through a porous geologic material under transient conditions (Fetter, 2001). The choice of this code was based on the fact that it has been used found to produce reliable results in almost all terrains all over the world that it has been used (e.g. Ebraheem et al., 2003; Senthilkumar & Elango, 2004; Uddameri & Kuchanur, 2007; Lutz et al., 2007). In the case of the study area, checks on the total dissolved solids (TDS) content of the water does not suggest significant spatial variations in the groundwater density and viscosity in space. It was on this basis, and the fact that MODFLOW has been considerably well tested that it was considered appropriate for this study.

This study considers steady-state conditions for the calibrated model hence, the simulation was based on equation (2.16) and subsequently, on equation (2.17).

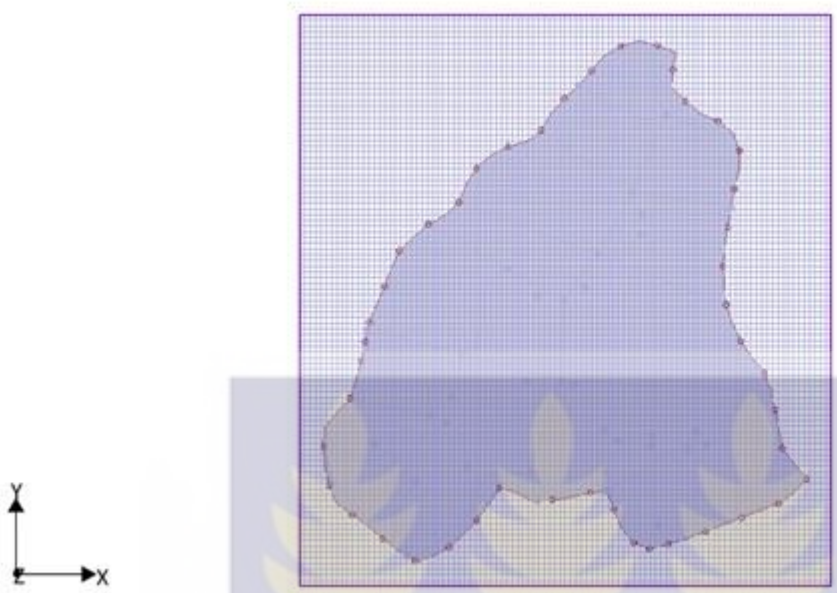

Figures 3.5a Map illustrating grid over the entire coverage area

Figures 3.5b Map illustrating grid over the active domain

3.1.2.8 General head boundary coverage

All the four vertical boundaries were conceptualised as *general head boundaries* with varying conductance and head stages. The general head boundary is a head-dependent or mixed boundary condition (Anderson & Woessner, 2002). It computes flow across a boundary based on the hydraulic head difference across it and the conductance of the material at the boundary. The flow rate, Q, across a general head boundary is expressed in equation (3.1), where C_d is the conductance of the material at the boundary and dh is the hydraulic head difference across the boundary.

$$Q = C_d dh \tag{3.1}$$

The top and bottom of the domain were conceptualised as semi-confined and confined, respectively to depict the situation on the ground. The confining conditions at the bottom reflect the impervious nature of the materials at the lower limits of the terrain. The semi-confining conditions at the top mimic the limited direct vertical recharge from precipitation. Arcs for the general head boundary were assigned as such in the conceptualisation process. The general head boundary assigns flows across boundaries depending on the relative levels of the groundwater table within and without the domain of the study area. Head stages were assigned to nodes at the ends of general head boundary arcs so that MODFLOW would compute head stages along the general head arcs.

Groundwater would flow across the boundary into or outside of the domain depending on the relative elevations of the hydraulic heads within the modelled domain and along the general head boundary. If the head just inside the model area is higher than the stage along the boundary, groundwater will flow outside of the model across the domain. On the other hand, if the stage is higher than the hydraulic head within the modelled domain, there would be net groundwater flow into the domain. The magnitude of the flow, Q, is as expressed in equation (3.1).

The general head boundary condition is the best condition applicable since there is no observable physical and geographical boundary limiting flow at the boundaries of the modelled domain (Todd & Mays, 2005). Thus, there would be no justification for assigning no flow boundaries. In addition, there has been no information of the general flux across the boundary for the study area; therefore, constant head boundaries would not be appropriate. The general head boundary is therefore the best boundary condition to assign under these circumstances. It would simulate lateral groundwater recharge or discharge across the boundaries, and provide an opportunity to compute lateral outward and/or inward flow of groundwater from adjoining areas.

3.2 Numerical modelling of the domain

The conceptual model was translated into a numerical model to simulate the general groundwater flow. The numerical simulation was performed using MODFLOW (Harbaugh, 2005) incorporated into GMS. A uniform rectangular grid system was

automatically set over the conceptual model to initiate the simulation under steady-state conditions. The top and bottom elevation data on the boreholes that were imported during the conceptualisation process were then mapped to MODFLOW top and bottom elevations, respectively, to define the thicknesses of the layers. Kriging was then used to interpolate to cover the entire domain.

There are three flow and five solver packages available in MODFLOW for solving the partial differential equation governing groundwater flow (equation 1.1). These packages are available in the Global Options folder and the choice of a set of flow and solver packages is dependent on the type of data available and the intended purpose of the simulation. Details of these packages are contained in Harbaugh (2005). In this study, the Layer Property Flow (LPF) and the Pre-conditioned Conjugate Gradient 2 (PCG2) packages were, respectively, opted for as the flow and solver packages for the simulation.

The LPF package is relatively simpler to use and has been well tested in recent times. It is the default package in GMS and supports two layer types: *convertible* and *confined*. In a confined layer, the transmissivity (which is computed from the hydraulic conductivity and cell elevations) is constant throughout the simulation. In the case of a convertible layer, the transmissivity varies with the hydraulic head throughout the simulation. There is the possibility of a cell converting to a no flow boundary when the water level goes below the bottom elevation of the layer. This allows MODLOW the flexibility of

assigning confined and unconfined conditions to locations based on the computed water levels. This formed the basis for choosing the convertible top boundary in this study.

Two main reasons govern the choice of a solver package in MODFLOW: the ability of the package to solve the differential equations for the problem being investigated and the time involved in executing the solutions (Hill, 1990). Another consideration is the memory space needed by each solver since different solvers have different computer memory requirements. Every solver employs iterative procedures in executing the solution for the differential groundwater flow equation.

There are two levels of iteration in MODFLOW: the *outer* and *inner* iteration procedures. The former is common to all solvers while the *inner iteration* is not. The inner iteration improves the accuracy of the results without altering anything in the equations. The outer iterations are repeated until a satisfactory solution is achieved at the convergence. The PCG2 solver package was preferred in this study because it incorporates both the outer and inner iterations (Hill et al., 2000) and has been tested over time and found to produce much more accurate results than the other solver packages (Harbaugh, 2005). Results of the numerical simulation are presented and discussed in section 4.1.1.

3.3 Calibration of the model

After the selection of the flow and solver packages, MODFLOW was then set to run on forward mode and calibration targets were set. The calibration target was set to give the

optimal agreement between the model computed data and the field observed data. A reasonable agreement between the observed and the model computed data should be reached in order for the model to be relied upon as a suitable numerical representation of the domain under study.

Every model ought to be calibrated before it can be used as a tool for predicting the behaviour of a considered system. The calibration interval was set at 1.0 m for this study. This suggests that, the model-computed and the field-observed hydraulic head data should not differ by more than 1 m at calibration. Based on this, MODFLOW then computed the other parameters (such as, the root mean square error, the mean absolute error, and the mean error) used to assess the level of calibration of the model. The graphical interface available in GMS version 10.0 (Aquaveo, 2014) also provided a visual assessment of the level of calibration.

The calibration was initially performed manually, by adjusting values of recharge and hydraulic conductivities for the sixteen zones created. The conductances were also varied within acceptable limits towards achieving the calibration target. When the model stabilised, the calibration was switched to the automatic approach via PEST, and the Pilot Point method (Hill et al., 2000) was used to simulate the hydraulic conductivity field. PEST is a model-independent parameter optimization program that inversely estimates parameters based on differences between simulated and observed measurements using a weighted least-squares method (Doherty, 2005). The Pilot Point approach makes it

possible to simulate a continuous hydraulic conductivity field for proper characterisation of the aquifer.

Pilot points are created in the conceptual model allowing for MODFLOW to then assign values from a defined range. MODFLOW then used a spatial interpolation technique to produce a smooth spatial distribution of the hydraulic conductivity field. Kriging was the preferred interpolation technique for this study, due to its versatility and not only depending on proximity but also takes into account the general spatial autocorrelation of the parameter (Hill et al., 2000). Distribution of the aquifer hydraulic conductivity field in the study area is presented and discussed in section 4.2.

The mean residual head and root mean squared residual head were used to determine the most optimal balance between the observed and computed hydraulic heads. Twenty wells were used. After about four months of calibration, the steady-state model was finally calibrated with a root mean squared weighted residual head as low as possible. The observed hydraulic head values of the twenty wells had a close fit with the computed hydraulic head values. The hydraulic head distribution of the calibrated model is presented and discussed in section 4.1.2. A plot of the model computed heads against the observed heads is also presented and discussed in the same section.

3.4 Sensitivity analysis

Sensitivity analysis is carried out in groundwater flow simulation to measure the stability of the model against subtle changes in some of the aquifer hydraulic parameters. The analysis is performed by adjusting the values of one parameter, whereas the remaining parameters are kept constant at calibrated level. The model is then simulated to measure the deviations in the hydraulic heads relative to the calibrated heads. The root mean square residual is observed after each run of the sensitivity analysis to determine the extent to which the model deviates from the calibrated value. A model that is highly sensitive to any of the model parameters is considered unstable, and thus unsuitable for predicting scenarios. However, in the case of automatic PEST, the sensitivity analysis is conducted automatically during the calibration. In this study, the sensitivity analysis on the model was carried out automatically through PEST. It was conducted for hydraulic conductivity and recharge. A histogram generated at the end of the model calibration to illustrate parameter sensitivities is presented and discussed in section 4.4.

3.5 Stochastic modelling of the domain

Moore and Doherty (2005, 2006) report that there is always a significant amount of uncertainty associated with a groundwater model. This uncertainty can be associated with the conceptual model or the field data or the input parameters of the model. Model parameters such as recharge and HK are particularly prone to uncertainties. This challenge brings up the issue of non-uniqueness of model calibrations (Ophori, 1999). The GMS version 10.0 (Aquaveo, 2014) used for this study provides a calibration-

constrained Monte Carlo analysis of the groundwater model, which makes it possible to obtain parameter sets that respect both the stochastic variability of the subsurface as well as the field measured values. In stochastic modelling, a set of models are constructed from the calibrated model where each model in the set is equally probable as a unique representation of the terrain (system) under investigation.

In this study, stochastic simulations were generated for nine hundred and ninety-five (995) realisations (i.e., a set of 995 unique models) using the PEST Null Space Monte Carlo approach. The null space comprises individual parameters, or combination of parameters that have no effect on model outputs under calibration conditions (Doherty, 2005). These combinations of parameters can therefore be added to any set of parameters which calibrates the model, to produce another set of parameters which also calibrates the model (Doherty, 2005). In this approach, the *stochastic randomize* option was turned on for the hydraulic conductivity parameter. Thus, the values at the pilot points that estimate the HK parameter should be varied during the Monte Carlo runs.

At the end of the simulation, the statistical analysis command was executed to generate new data sets (min, max, mean, and standard deviation) of HK, recharge and hydraulic head for each grid cell. The standard deviations in the hydraulic parameters indicating how much variability can occur in their input array and still result in a calibrated model are presented and discussed in section 4.6, together with the first and final unique models generated for the domain from the stochastic simulations.

3.6 Scenario analysis

Analysis of scenarios of stresses on aquifers is best simulated using a transient model because the transient model simulates changes in aquifer storage with time. In this study, however, the calibrated steady-state model was used to simulate the various management scenarios because of the absence of transient data to calibrate a transient model. The analysis was carried out on the set of unique realisations for the domain generated by the stochastic simulations. The following scenarios were carried out in the forward mode.

Three management scenarios were simulated based on a number of considerations. Increase in population with an accompanying increase in the per capita per day water usage was one such consideration. The final results of the 2010 Population and Housing Census (PHC, 2010) indicate that the Greater Accra Region population increased by 38.0 percent over the 2000 figure of 2,905,726. The general observation is that, the region is opening up significantly in the direction of the two municipalities under investigation. This has resulted in the creation of a new municipality (La-Nkwantanang-Madina).

Another consideration was global warming, which leads to increase in evapotranspiration. The anticipated effect is decline in the levels of surface water bodies culminating into greater dependence on groundwater resource. Also, urbanisation and the increasing complexities of lifestyles in the two municipalities would further increase the dependence on groundwater for both domestic and commercial activities. Hence, an increase in the current abstraction rates.

There was also the consideration to decrease the current recharge rates of the resource through rainfall. This was considered to simulate the possible effects that a decline in rainfall would have on the groundwater resource in the modelled domain.

The first scenario simulated the effects of increased groundwater abstractions from the twenty wells progressively by 10 percentage points, up to 100%, and then by 200%, 300%, and 400% above the current abstraction rates, under the same conditions of recharge at calibration. The model was simulated after each increase, and the flow patterns were observed for any possible changes on each of the unique realisations generated by the stochastic simulations. Results obtained from the simulation of the stated scenarios are presented and discussed in section 4.7. Also, additional illustrations of the results are presented in Appendix B.

The second scenario entailed successively decreasing the groundwater recharge rates at calibration by 10%, 20% up to 90% below the current recharge rates while keeping the current abstraction rates unchanged. Similarly, after each decrease the model was ran and the flow patterns were observed for any possible changes on each of the unique realisations generated by the stochastic simulations. Results obtained from the simulation of the stated scenarios are presented and discussed in section 4.7, and additional illustrations of the results presented in Appendix B.

For the third scenario, there was a 10% reduction in the current groundwater recharge rates with a subsequent progressive increase in the current abstraction rates by 10%, 20% up to 100%, and then 200%, 300%, and 400%. As indicated earlier, the model was simulated after each permutation and the effects on each realisation observed. Results obtained from the simulation of the stated scenarios are presented and discussed in section 4.7 and additional illustrations thereof presented in Appendix B.

3.7 Chapter summary

In this chapter, I have discussed the methodology adopted for this study. I have indicated that the hydrogeology of the domain was characterised using historical hydrogeological and groundwater monitoring data. I stated that the GMS platform (version 10.0) was used in studying the stratigraphy of the domain. The processes leading to the development and calibration of the numerical model have also been presented. I further indicated that sensitivity analysis and stochastic simulations were carried out on the calibrated model to enhance confidence in it, hence, the reliability of results generated from the model. Finally, I delved into the simulation of various management scenarios based on variations in groundwater recharge and abstraction to investigate the sustainability of the groundwater resource in the terrain. In the next chapter I present and discuss the results obtained from the study.

CHAPTER FOUR

RESULTS AND DISCUSSIONS

4.0 Introduction

This chapter consists of the presentation, analysis, and discussions of pertinent results from this study based on the methodology adopted, as discussed in the preceding chapter. The discussions focus on the following key aspects: general groundwater levels and flow patterns in the domain (section 4.1); hydraulic conductivity estimates at calibration and the velocity field (section 4.2); recharge rate estimates at calibration (section 4.3); parameter sensitivity analysis (section 4.4); groundwater budget in the domain (section 4.5); stochastic simulations of groundwater flow in the domain (section 4.6); and analysis of management scenarios (section 4.7). Section 4.8 summarises the chapter.

4.1 The general piezometric levels and groundwater flow patterns

4.1.1 The stratigraphy

The spatial distribution of the twenty boreholes used for this study is represented in Figure 4.1. The distribution is fairly even over the selected grid frame of the study area. The study identifies a single aquifer unit in the domain. The aquifer occurs in the weathered zone, made up of the quartzite-schist formations. There is a laterite-clay overburden, posing a semi-confined to confined aquifer system (Figure 4.2). The stratigraphy of the

domain (Figure 4.2) was successfully developed as a major step towards the development of the conceptual model of the study area. One of the main benefits of using solid models to define stratigraphy for MODFLOW models is that it provides a grid-independent definition of the layer elevations that can be used to immediately re-create the MODFLOW grid geometry after any change to the grid resolution (Jones et al., 2002). Figure 4.2 captures the four lithological units identified in the domain, viz. laterite, schist, quartzite, and clay.

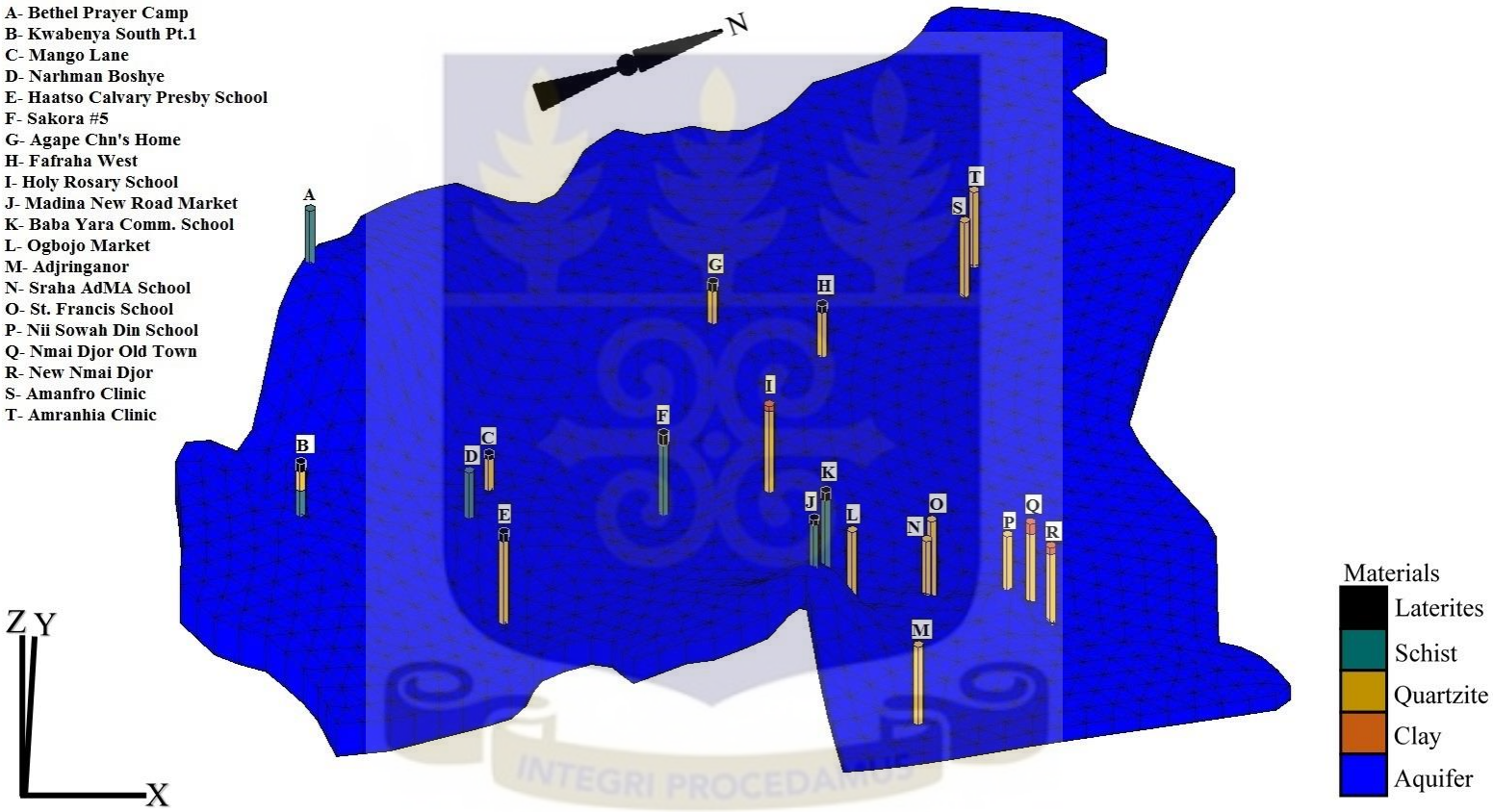

Figure 4.1 Spatial distribution of boreholes in the study area

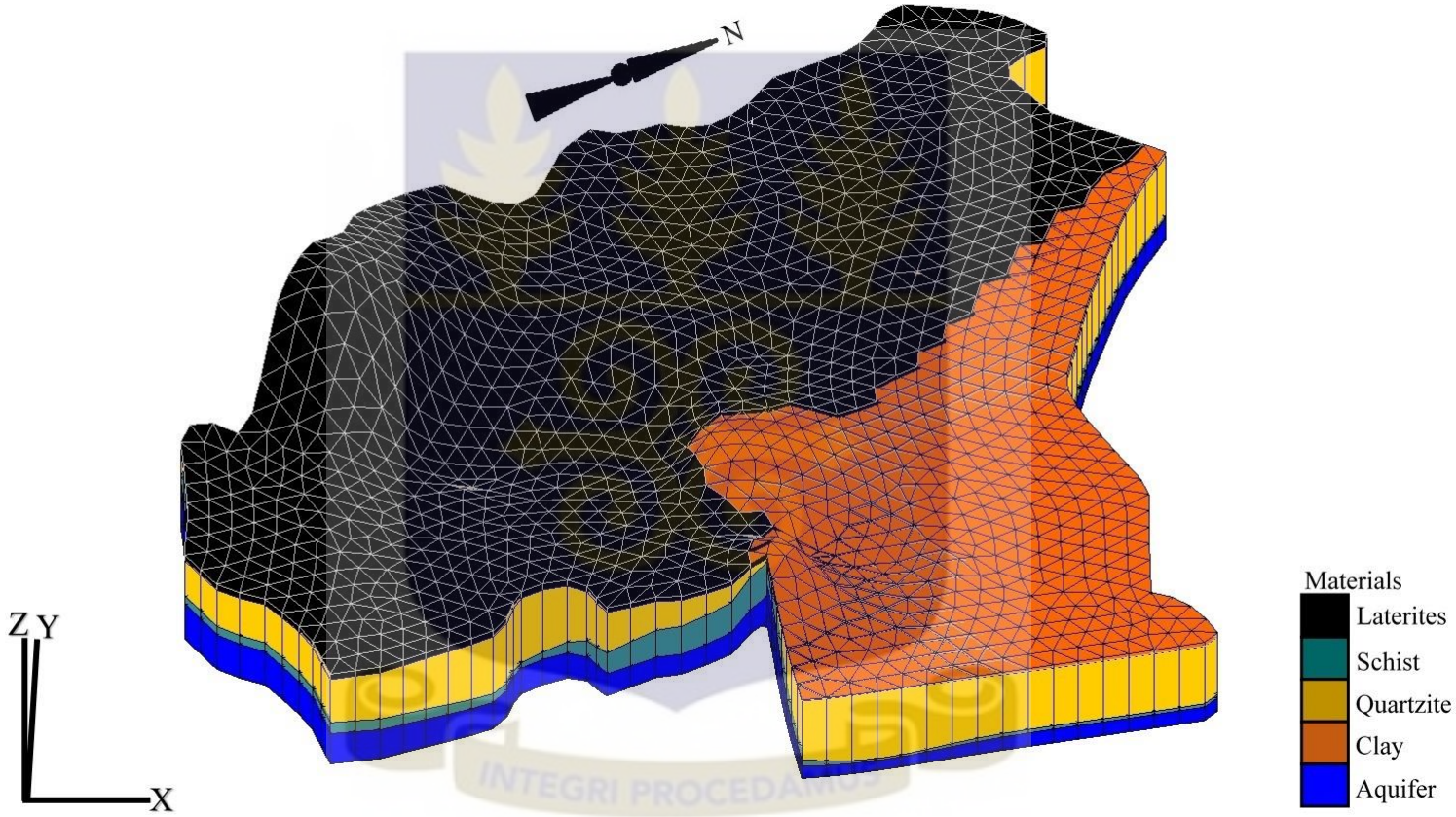

Figure 4.2 The solid stratigraphy of the domain capturing the four lithological units identified

The aquifer thickness ranges from 6.5 m to 31.5 m. The highest aquifer thickness occurs at Bethel Prayer Camp, which is located at the topmost elevation in the study area. The low aquifer thicknesses occur in the low topographic regions of the study area (for example, Adjiringanor). The estimation of aquifer thickness stems from the aquifer test results conducted in situ. Hence, a potential source of error in the estimation of aquifer thickness is the partial penetration of the wells in the aquifer (Fetter, 2001). A potential outcome, therefore, is that the estimated thicknesses of the aquifer could be smaller than they actually are. Also, both the amount of water pumped from the wells and the potential field caused by the drawdown could also be affected.

From Figure 4.2, schist and quartzite appear to cover the widest space, followed by laterite and then clay. The quartzite covers the northern portions of the study area and spreads through the eastern sections towards the south. The schist covers the north-western portions towards the south, and spreads towards the eastern portions. The laterite spreads from the central portions towards the south, while the clay is within the south-eastern potions.

Relating the identified lithological units to the established local and regional geology of the area, quartzite and schist locally belong to the Togo Structural Unit of Ghana (Attoh et al., 1997). The clay and laterite emerge from alterations of the phyllites belonging to the Togo Structural Unit.

The solid model was converted to MODFLOW data using the boundary-matching option. The most significant challenge in solid modelling approach is converting an arbitrary complex solid-model representation of stratigraphy to a MODFLOW-compliant grid with continuous layers. Boundary Matching is one of the approaches for performing this conversion (Jones et al., 2002). The goal of the boundary-matching approach is to ensure that each upper and lower boundary defined by the solid model is precisely matched by a layer boundary in the MODFLOW grid. The interior grid layers must also match the boundaries of the solids. The grid cell materials are set to match the material of the solid that the grid cell center is located in. The option results in a close fit between the grid and the solids.

Figure 4.3, the result of the entire process, illustrates the interpolated horizon surfaces depicting the top and bottom elevations. The top elevation of the aquifer in the terrain range from 40.0 m to 166.0 m, with the highest elevation occurring, predictably, at the Bethel Prayer Camp.

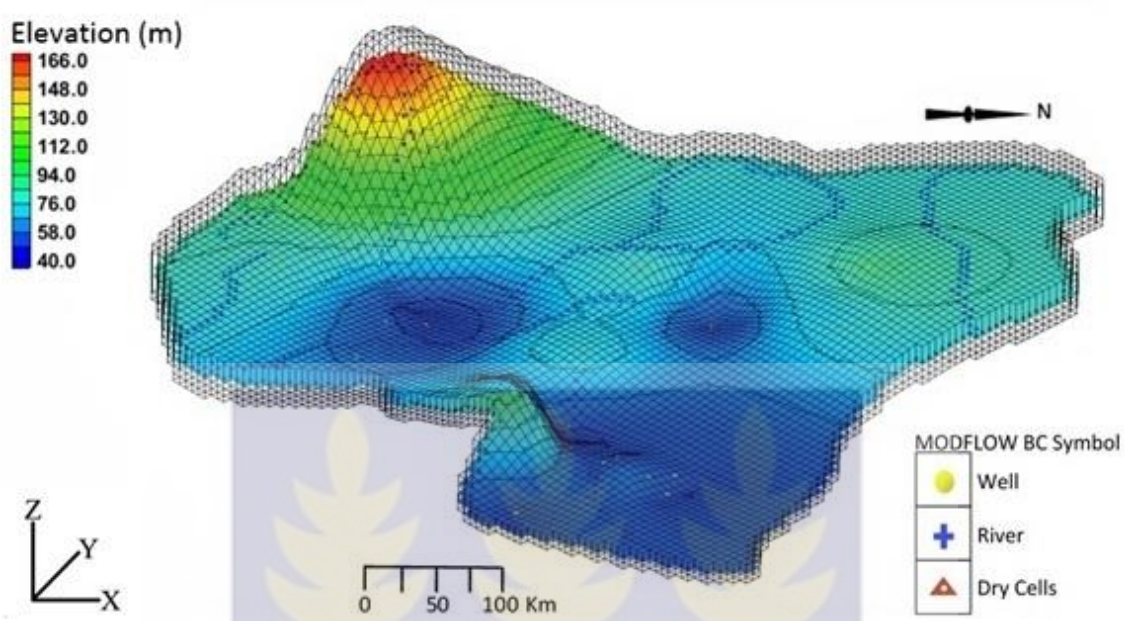

Figure 4.3 Summary of the interpolated horizon surfaces and discretization used for the model depicting the spatial distribution of the top and bottom elevations (oblique view)

4.1.2 Hydraulic head distribution

Todd (1959) and Domenico (1972) employed the famous Bernoulli equation to develop concepts of fluid potential and hydraulic head. The hydraulic head distribution in the study area was obtained through calibration of the steady-state model. The calibration interval was set to 1.0 m to generate minimal variations between the observed and computed heads. The potential field is one of the tools used to ascertain the groundwater potential in a domain (section 2.1.1). It is the distribution of the hydraulic heads in the domain that provides a clue about the potential field. From the calibrated steady-state model, the observed heads of twenty wells has a close fit with the computed hydraulic heads. Figure 4.4 captures the reasonable match between the two sets of data. The model

computed hydraulic heads match the observed heads with a root mean squared (RMS) weighted residual head of 3.84.

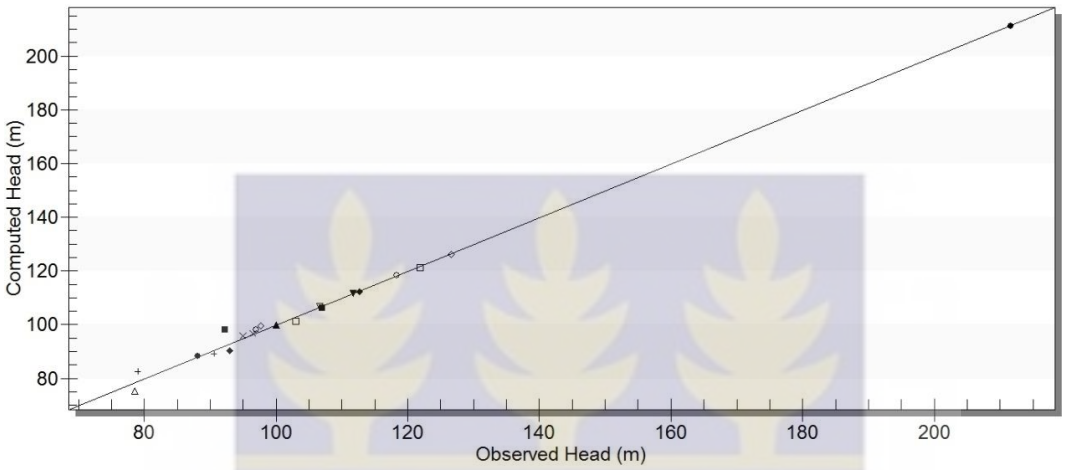

Figure 4.4 A linear plot of the relationship between model computed and observed hydraulic head data at calibration

From equation (2.8), we observe that the potential, which is the driving force behind groundwater flow, at a point is related to the hydraulic head, h, and the acceleration due to gravity, g (Freeze & Cherry, 1979; Hubbert, 1940). However, since acceleration due to gravity is almost constant everywhere on the earth's surface, the potential field is largely determined by the hydraulic head. In effect, it is the distribution of hydraulic head through an aquifer that controls/determines the groundwater flow direction. And in accordance with the laws of physics, the flow will advance from regions of high hydraulic heads (or potential) to that of low hydraulic heads (or potential).

Figure 4.5 illustrates the head distribution in the study area. It ranges from 53.0 m to 221.0 m. It is highest in the south-western sections of the study area, where the ground elevations are the highest (Figure 4.3). The hydraulic heads are, however, low in the topographic lows. Thus, groundwater flow will always take the shape of the surface topography. For instance, the flow geometry of groundwater beneath a hill will take the shape of the hill. The topographic highs serve as recharge areas where the vertical component of the hydraulic head is directed downwards. The converse is the case in discharge areas of the groundwater flow system. From the reasonably good match illustrated in Figure 4.4, it is safe to say that Figure 4.5 is an ample representation of the distribution of groundwater potential in the study area.

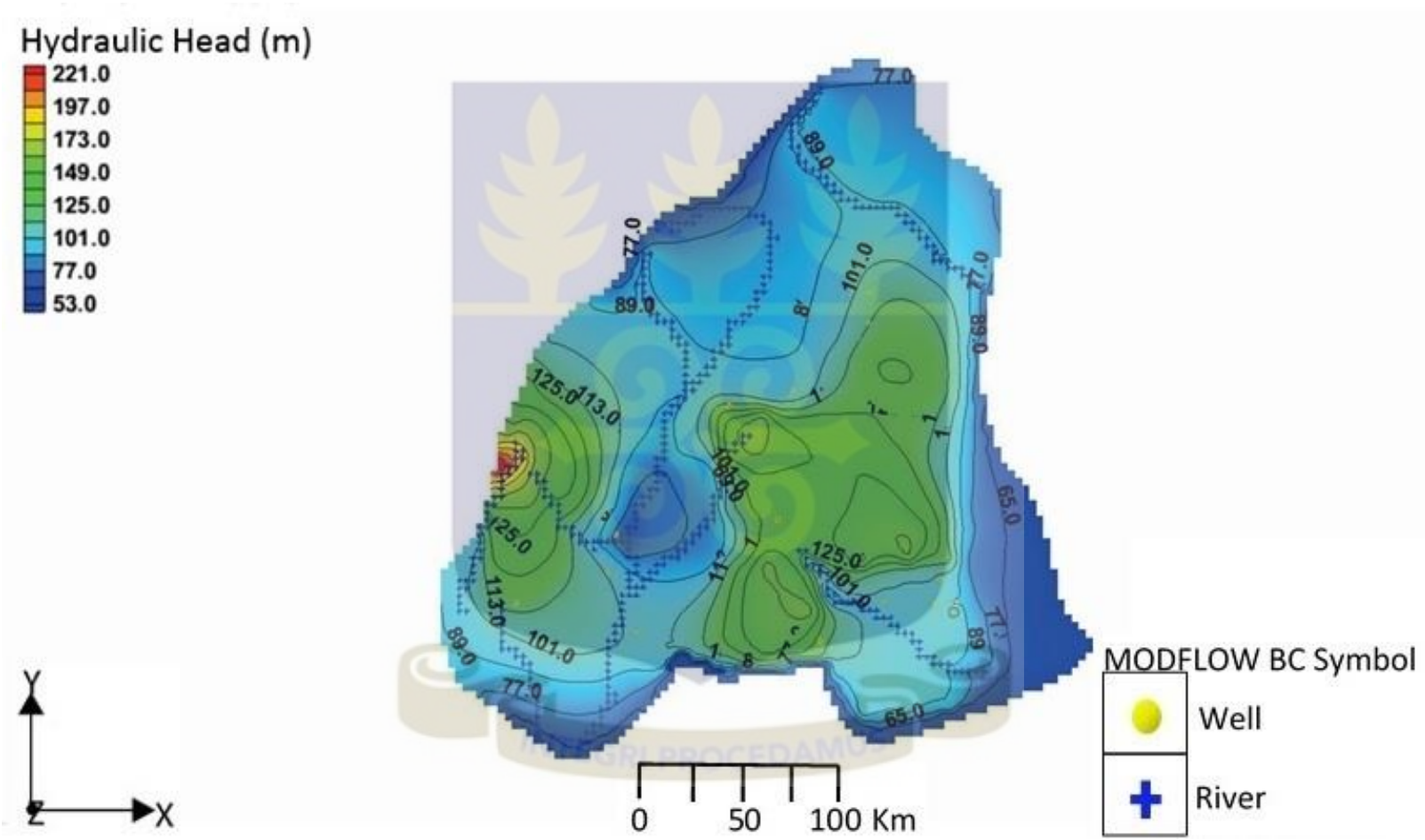

Figure 4.5 Distribution of the calibrated hydraulic heads (plan view) in the study area

4.1.3 The groundwater flow patterns

Figure 4.6 illustrates a cross-section through the potential field of the domain (Figure 4.5), revealing details of the groundwater flow systems. The cut proceeds from the SWW towards SW and terminates in the SE of the domain. At the west, the Bethel Prayer Camp area has rich recharge potential which discharges towards the SW at Mango Lane (an intermediate flow system). The Mango Lane area in turn serves as recharge and discharges at the Agbogba area (a local flow system). The Santeo area is a recharge area, and discharges towards the west at the Holy Rosary School area in Adentan (a local flow system) and to the east towards Ashiaman (an intermediate flow system). The general knowledge in groundwater hydraulics, that the flow geometry is controlled by the surface topography, is evidently supported by Figure 4.6.

The particle tracking technique under MODPATH was employed to assist in identifying the unique flowpaths in the study area. Particles were generated at the midsections of the modelled domain to forward track the flow for these areas. Pantang is located within the midsection of the study area, and the existence of a landfill in Pantang informed the decision to generate particles there. The intention is to monitor the trajectory of pollutants from the landfill. Particles were also generated at the western sections of the modelled domain where the altitude and hydraulic heads are high. In addition, a particle each was generated at the northern and southern sections to observe/capture the trajectory of chemicals/pollutants at the identified recharge zones at these sections of the domain (Figure 4.5).

The velocity field for the modelled domain was generated to appreciate the rate at which the various particles generated travel. Section 4.2.1 presents the analysis and discussions on the velocity field.

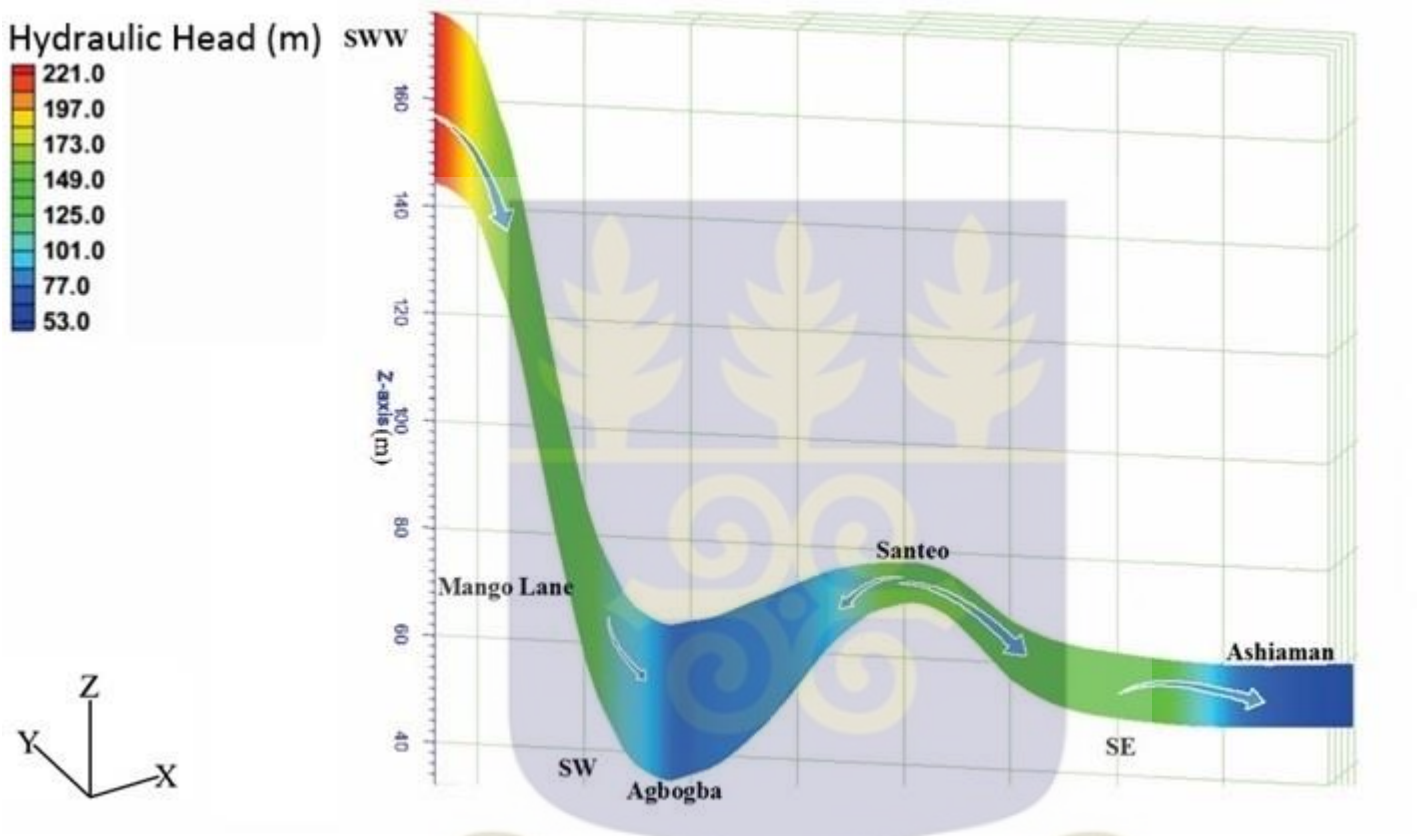

Figure 4.6 Cross-section of the potential field showing the flow systems and potential recharge and discharge areas in the terrain

4.2 The hydraulic conductivity field

One of the essential outputs of a properly calibrated groundwater flow model is the hydraulic conductivity field (Fetter, 2001). Hydraulic conductivity assists in conceptualising the general pattern of the transmissive properties of the aquifer and aids in understanding observed flow patterns.

The HK field in the domain was established through pilot point method. The estimated HK field at calibration is presented in Figure 4.7. The values range from 3.75 m day^{-1} to 105 m day^{-1}, with a mean of 13.1 m day^{-1}. Figure 4.7 shows that the HKs are lower than 15.0 m day^{-1} in much of the area. This is consistent with observed HK values for lithologies of the aquifer material (quartzite and schist), which have been identified (Lewis, 1989). The HK field is largely heterogeneous for most part of the terrain.

The hydrogeological properties of the aquifer in the study area are controlled by secondary permeabilities created in the wake of fracturing and/or weathering. Where the degree of secondary permeability is high, the HKs are high. The very high conductivity values observed in the western parts and towards the north are outliers which can be ascribed to the fractured and jointed quartzite within the weathered zone. They enhance the conduits within the materials for rapid flow of groundwater (Tairou et al., 2012).

The estimated HKs in this study has some resemblance to estimates obtained by Yidana et al. (2014) for portions of the Densu basin with similar lithologies. Their results ranged between 2 m day^{-1} to 37 m day^{-1}.

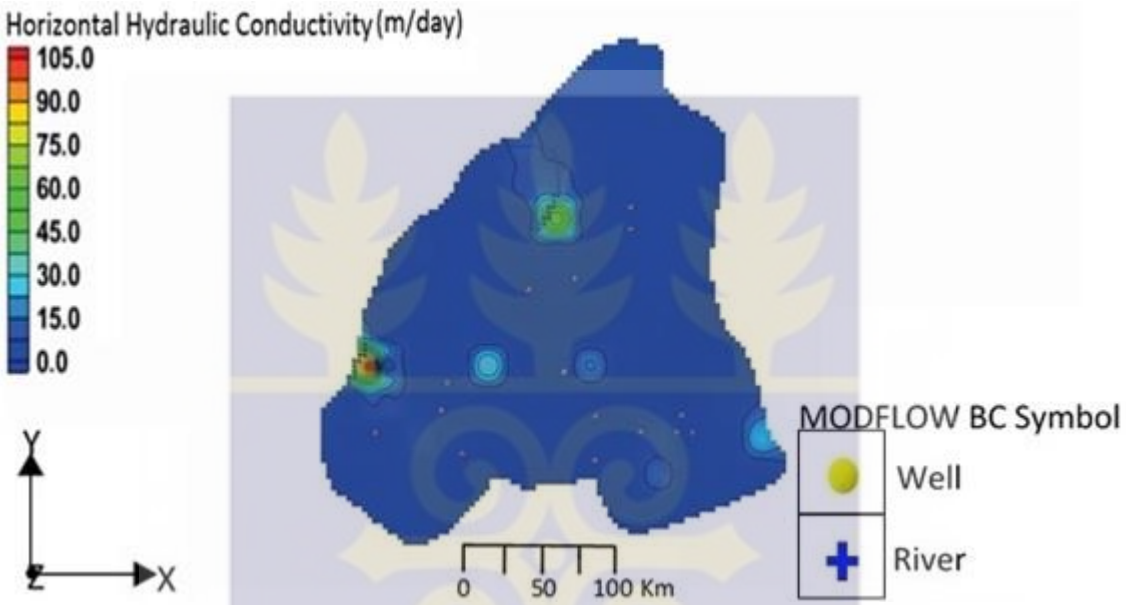

Figure 4.7 Distribution of the calibrated horizontal hydraulic conductivities (plan view) in the study area

From equation (2.15), it is observed that the hydraulic conductivity determines/controls the velocity field. This relationship is depicted by the distributions of the hydraulic conductivities and the velocities of the modelled domain. This observation will be further discussed in section 4.2.1.

4.2.1 The velocity field

Figures 4.8a and 4.8b illustrate the velocity field and seven flowpaths from the particle tracking simulations, respectively. Travel times from the perceived recharge areas to discharge areas for the seven principal flow directions, based purely on advection alone are presented in Table 4.1.

The estimated velocity field in the area ranges from 0.002 m day^{-1} to 11.2 m day^{-1}, and the travel time ranges from 7 years to 833 years. However, the velocity is below 0.85 m day^{-1} for much of the area (Figure 4.8a). The high velocities recorded in the western sections of the domain are outliers. The spatial distribution of the velocity field ties in well with the hydraulic conductivity field. For instance, the high velocities recorded in the western sections of the domain coincide with the high hydraulic conductivities observed in Figure 4.7. Similarly, the observation that most of the area has low velocities mimics the observed HK field.

The velocity field observed gives an indication of the rate at which contaminants would travel, solely by advection, along the identified principal flowpaths in the modelled domain. However, some contaminants would travel faster than the speed of the groundwater by diffusion or dispersion. The observed velocity field is significant in relation to contaminant transport in the domain. We see from the data in Table 4.1, that contaminants (from the landfill at Pantang, small rubbish dumps, broken sewage systems, pesticides and/or weedicides applied on farms, and other potential sources) get leached

into the subsurface by rainfall and transported across the study area. The rate at which this happens must be a cause for worry because the quality of groundwater resources serving as source of portable water in the study area is potentially at risk of contamination/pollution, posing a threat to the well-being of inhabitants in the area.

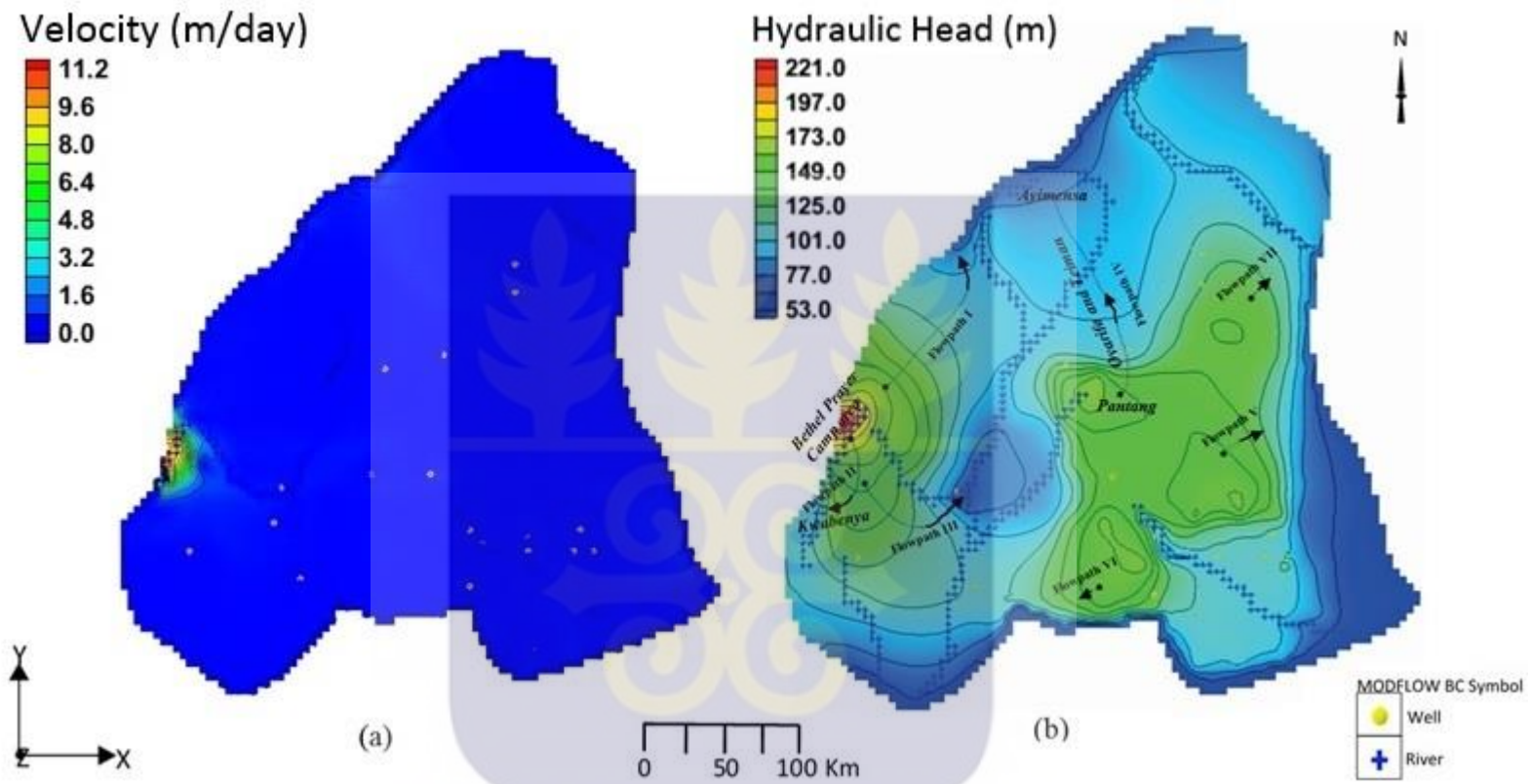

Figure 4.8 (a) Velocity field in the modelled domain

(b) Flowpaths in the modelled domain (plan views)

Table 4.1 Flowpaths, lengths, travel times, and average velocities for the study area

Flowpaths	Lengths (m)	Travel Time (days)	Travel time (years)	Average Velocity (m day^{-1})
I	1543.36	50797.62	139.17	0.030
II	934.96	130697.74	358.08	0.007
III	1111.63	236317.20	647.44	0.005
IV	2081.23	2445.57	6.70	0.851
V	456.47	304223.16	833.49	0.002
VI	137.13	19183.88	52.56	0.007
VII	163.15	73097.46	200.27	0.002

Referring to Figure 4.8 and Table 4.1, contaminants/pollutants leached into the aquifer zone through recharge by rainfall at the Pantang community will travel at approximately 0.85 m day^{-1} along flowpath IV. It would take approximately 7 years for these contaminants to pollute the subsurface water downstream at Ayimensa. However, it will take a shorter time for the contamination to occur at Oyarifa and Teiman due to their proximity to Pantang.

Considering flowpath II, contaminants from the Bethel Camp area would travel at approximately 0.007 m day^{-1}, and it will take about 358 years for groundwater drawn in the Kwabenya township to get contaminated. This is a considerable amount of time, but the eventual impact will be felt.

Contaminants transported along flowpath I will affect groundwater drawn by inhabitants at Otopram and Berekuso. Contaminants transported along flowpaths III and V will pollute the subsurface water at Ashongman and Santeo, respectively, while those transported along flowpaths VI and VII will contaminate groundwater at Madina and Katamanso, respectively. The average velocities and estimated travel times for the respective flowpaths are presented in Table 4.1 above.

The landfill cited at Pantang remains a relevant source of groundwater contamination in the study area and beyond. Municipal solid waste landfills emit large amounts of landfill gas and leachate to the environment. Such emissions present significant adverse impacts on the general public health and safety, as well as groundwater quality. According to The Groundwater Foundation, landfills are supposed to have a protective layer to prevent contaminants from getting into the water (The Groundwater Foundation, n.d.). However, if there is no layer or it is cracked, contaminants from the landfill can leach into the groundwater. Though there is the possibility of sorption of some of the contaminants as they are transported along the trajectory of the groundwater flow, some appreciable levels of the contaminants would be accessed at the destination discharge areas. For example, heavy metals such as Al, As, Cd, Cr, Hg, Mn, Sb, V, and Zn can pose serious health hazards when they occur beyond their acceptable limits in water, especially when such water is used over a considerable period of time.

Other potential sources of the contaminants could be smaller dumping sites, broken sewage systems cited in homes and public facilities, oil spills at garages, and pesticides used on farms in the study area. For instance, an improperly designed or maintained sewage system can leak viruses, bacteria, household chemicals, and other contaminants into the groundwater causing serious problems. Additionally, storage tanks at the various petroleum filling stations in the study area can corrode, crack and develop leaks over time. Serious contamination would occur with the accompanying health implications when the contaminants leak into the groundwater.

The effects of the potential contamination of groundwater on both humans and animals can be far-reaching. Drinking contaminated groundwater can pose serious health implications. Diseases such as dysentery, hepatitis may be the result of contamination from sewage waste. Poisoning may result from toxins that have been leached into dug wells. Wildlife can also be harmed by contaminated groundwater. Other long term effects such as certain types of cancers could result from exposure to contaminated water.

4.3 The recharge rate estimates

Groundwater recharge is key in modelling groundwater flow. Accurate estimation of groundwater recharge is imperative to proper management and protection of valuable groundwater resources. As noted in section 3.1.2.3, in estimating the recharge rates for the domain under investigation, a recharge coverage was set up using 1% to 3% of the average annual rainfall value for Accra, for the period January 2005 to December 2014.

The calculated range of values were slightly varied and the model simulated during the calibration process. The average annual rainfall value for the stated period was computed to be 825.6 mm.

The city of Accra lies within the coastal-savannah, and is reported to have low annual rainfall varying between 600 mm and 900 mm, with an annual average of about 800 mm distributed over less than 80 days (Obuobie et al., 2006; Oppong & Badu, 2013). At calibration, groundwater recharge in the domain ranges from 2.70×10^{-5} m day^{-1} to 3.78×10^{-4} m day^{-1} (Figure 4.9). From Figure 4.9, the groundwater recharge is less than 8.10×10^{-5} m day^{-1} for much of the area. Hence, using the range 2.70×10^{-5} m day^{-1} to 8.10×10^{-5} m day^{-1}, the groundwater recharge represents 1.2% and 3.6% of the average annual precipitation in the area (consistent with the calculated range of values).

These low estimates reflect the barrage of construction projects impeding aquifer recharge through rainfall. The low recharge rates occurring in most parts of the study area can be attributed to the very low or non-existence of vertical hydraulic conductivity which restricts the vertical percolation of precipitation into the aquifer system.

However, there were high recharge values observed in some isolated parts of the domain which may be regarded as outliers, attributable to open systems and/or dug-outs enhancing recharge. Specifically, the highest recharge rate in the terrain occurred mostly

within the topographic high areas in the western portions of the study area. This observation can be ascribed to the fact that the rocks occurring there are extensively fractured, thickly foliated and highly deformed. This implies that there are a lot of weaker zones in those areas, facilitating the movement and flow of water in the terrain.

The estimated groundwater recharge distribution in the area corresponds to the distribution of the groundwater hydraulic potential suggested in Figure 4.5. This observation is consistent with the general hydrogeological knowledge that highlands and lowlands serve as recharge and discharge zones in groundwater flow systems. Thus, the surface topography is a subdued replica of the groundwater table elevation (Fetter, 2001; Freeze & Cherry, 1979; Yidana et al., 2011).

Comparatively, recharge rates estimated for this study varies marginally to recharge estimates obtained from numerical simulations in a similar terrain (cf. Yidana et al., 2014). Results from the cited work conducted on the Densu basin, had recharge estimates for part of the terrain with similar lithologies ranging from 2.2×10^{-4} m day^{-1} to 5.8×10^{-4} m day^{-1}. The difference can be attributed to the variations in the extent of deformations at the different study areas. Additionally, this model is calibrated under steady-state conditions while that by Yidana et al. (2014) is a transient model.

The observed groundwater recharge appears to be significant compared to the observed abstraction rates in the area, as depicted by the water budget presented in section 4.5.

However, climate change could affect the spatial distribution of groundwater recharge in the terrain. Transient groundwater flow simulation would be required to analyse such trends. Currently, the time-variable hydraulic head and flow data necessary for such analysis is unavailable.

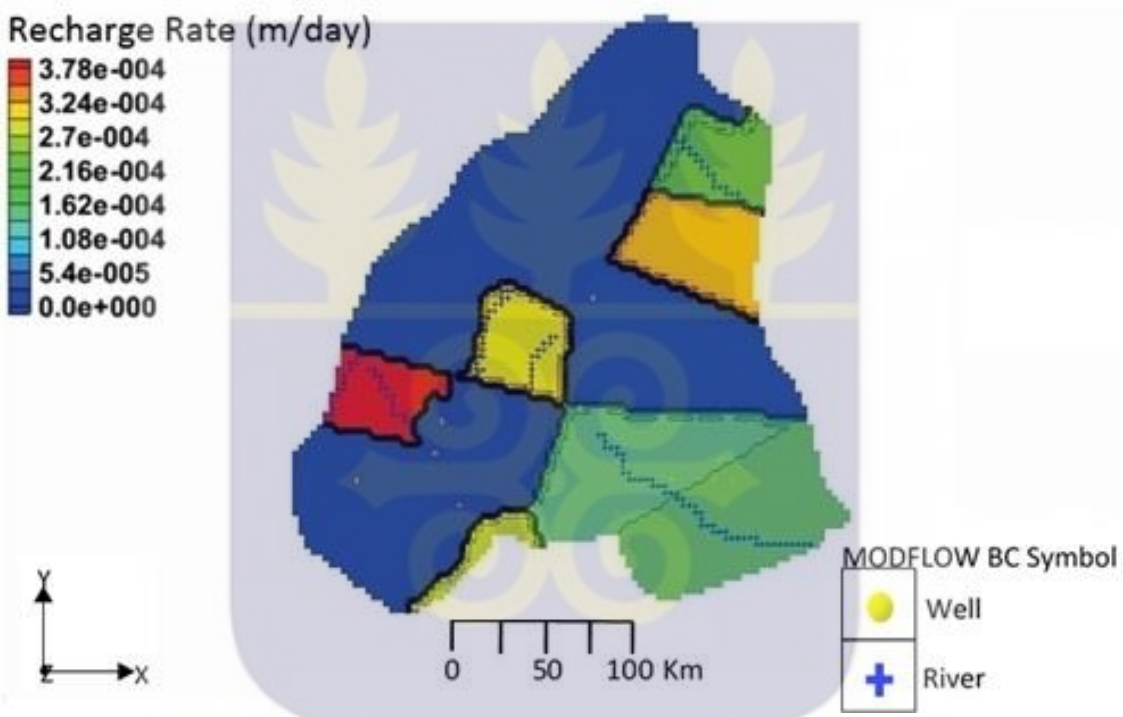

Figure 4.9 Distribution of groundwater recharge in the study area (plan view)

4.4 Parameter sensitivity analysis

In groundwater flow simulation, sensitivity analysis is carried out on a calibrated model to determine its stability with respect to small changes in aquifer input parameters (Yidana et al., 2015b). The sensitivity analysis was conducted on HK and recharge, automatically through PEST. A histogram (Figure 4.10) was generated at the end of the

model calibration to illustrate parameter sensitivities. The histogram reveals that the calibrated model is insensitive to the HK while there is some level of sensitivity to recharge in an isolated zone. Thus, the model can be considered to be stable to HK and recharge, except for the isolated zone in the recharge field. It is safe, therefore, to conclude that the model is very useful and suitable for predicting scenarios.

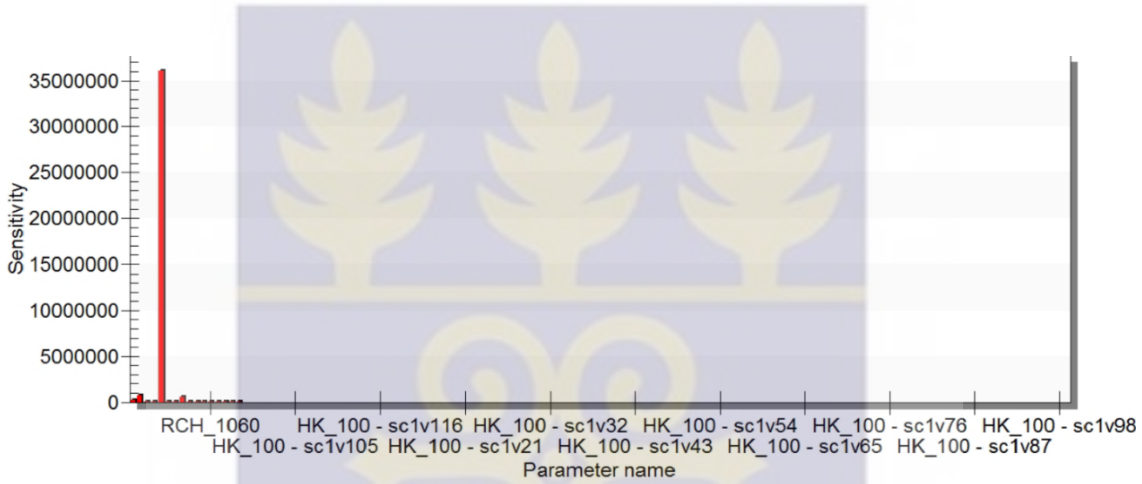

Figure 4.10 Parameter sensitivity plot of the calibrated steady-state model

4.5 Groundwater budget in the domain

The law of conservation of mass requires that the total amount of water inflow, outflow, and storage for a groundwater system is conserved. As stated in section 2.4, equation (1.1) describing the general flow of groundwater simplifies to equation (2.16) under steady-state conditions.

From Table 4.2, there is a percentage discrepancy of 0.004 between the inflows and outflows. The low value indicates that the flow system conserves mass. Thus, the volume of water entering the model through recharge and flow equals the volume of water leaving the model through drainage.

From the water budget, the simulated groundwater recharge in the area is 23366.23 $m^3\ day^{-1}$, while the base flow for the modelled domain is 10773.31 $m^3\ day^{-1}$. Also, the rivers drain 26109.19 $m^3\ day^{-1}$ of the aquifer's water, while the drain on the aquifer's resource through abstraction wells is 944.64 $m^3\ day^{-1}$. The surface flows in the terrain were computed by multiplying the head stages by the conductances of the rivers. The abstraction rates were obtained from the total estimated yield from the pumping test data for the various boreholes (Table 3.1).

Table 4.2 indicates that the quantum of recharge through rainfall to the aquifer can adequately cater for the current levels of abstraction in the modelled domain.

Table 4.2 Groundwater flow budget of the modelled domain under steady-state condition

Sources/Sinks	Inflow ($m^3\ day^{-1}$)	Outflow ($m^3\ day^{-1}$)	Difference ($m^3\ day^{-1}$)	Percent Discrepancy (%)
General heads	1495624.78	1528886.864	-33262.08425	
Rivers	36882.50363	26109.18981	10773.31382	
Abstraction wells	0	944.6400032	-944.6400032	
Recharge	23366.23151	0	23366.23151	
Total	1555873.515	1555940.694	-67.17891862	-0.004317669

4.6 Stochastic simulation of groundwater flow in the domain

Stochastic simulations were conducted on the steady-state calibrated model to enhance confidence in the groundwater flow model for the terrain under investigation. The weakness of numerical models relates to their apparent non-uniqueness, especially where the data relied upon are relatively scanty (Yidana et al., 2015a). This is further compounded where there is insufficient field investigation to properly conceptualise the physical domain, resulting in unreliable outcomes and bad decisions.

Uncertainty in groundwater systems can be classified into two: intrinsic and information uncertainties (Dettinger & Wilson, 1981). The first class derives from the variability of certain natural properties (such as recharge rate and HK defy exact description) and is an irreducible uncertainty (by observations) inherent in the system. The second class is the result of incomplete information (in quantity and/or quality) about the aquifer system and could be reduced by various strategies, notably further measurements and analysis.

In this study, the PEST Null Space Monte Carlo approach was used to simulate a set of nine hundred and ninety-five (995) equally probable models as a means of enhancing confidence in the calibrated groundwater flow model for the study area. The Monte Carlo method employs numerous replications of flow system simulations, with the parameters and inputs of each simulation generated at random from their respective probability distributions (Dettinger & Wilson, 1981). The results of the simulations are compiled to form estimates of the probability distribution of the aquifer flow or piezometric heads.

Monte Carlo simulations have been applied to the investigation of the effects of spatial variability of physical properties inflow through porous media by several authors, including Warren and Price (1961), Freeze (1975), and Smith and Freeze (1979) (as cited in Dettinger & Wilson, 1981).

Moore and Doherty (2005) provides a theoretical basis of the role of the calibration null space that is comprised of all differences between the simplified (or regularised) parameter field represented in a model and the complexity of the natural world. Since the calibration null space is comprised of the combinations of parameters whose sensitivity to the model output during calibration is negligible, these combinations in the null space often pertain to the fine-scale information (Yoon et al., 2013). The Null Space Monte Carlo (NSMC) approach (Tonkin & Doherty, 2009) utilises this concept where, based on the parameter sensitivities during calibration, the null space of the calibration parameter field is identified. Stochastically generated parameter fields are then projected through the null space. The perturbation of the null space components does not significantly change the overall calibration, and the solution-space components are retained.

A recent study (Keating et al., 2010) has shown that the NSMC possesses the computational efficiency necessary to explore the predictive uncertainty of strongly nonlinear groundwater models which are highly parameterized. This suggests that the NSMC approach can serve as a practical tool for predictive uncertainty analysis in strongly nonlinear environmental problems.

From the stochastic simulations carried out, no significant differences were observed in the hydraulic heads, HKs, and recharge rates. The statistical analysis gives the standard deviations in the heads as ranging from 0.00011 to 0.00224 (Figure 4.11). The standard deviations in the HK and recharge parameters are also illustrated by Figures 4.12 and 4.13, respectively. The standard deviations displayed, show little or no variations in the three hydraulic parameters (heads, HK, and recharge) used in calibrating the steady-state model. Thus, the steady-state model is unique for the hydraulic parameters, and hence, provides sufficient information to assist in the regional hydrogeological characterisation of the aquifer.

Since all the nine hundred and ninety-five (995) realisations generated by the stochastic simulations have similar outcome, results for the first and final realisations are displayed in Figures 4.14 and 4.16.

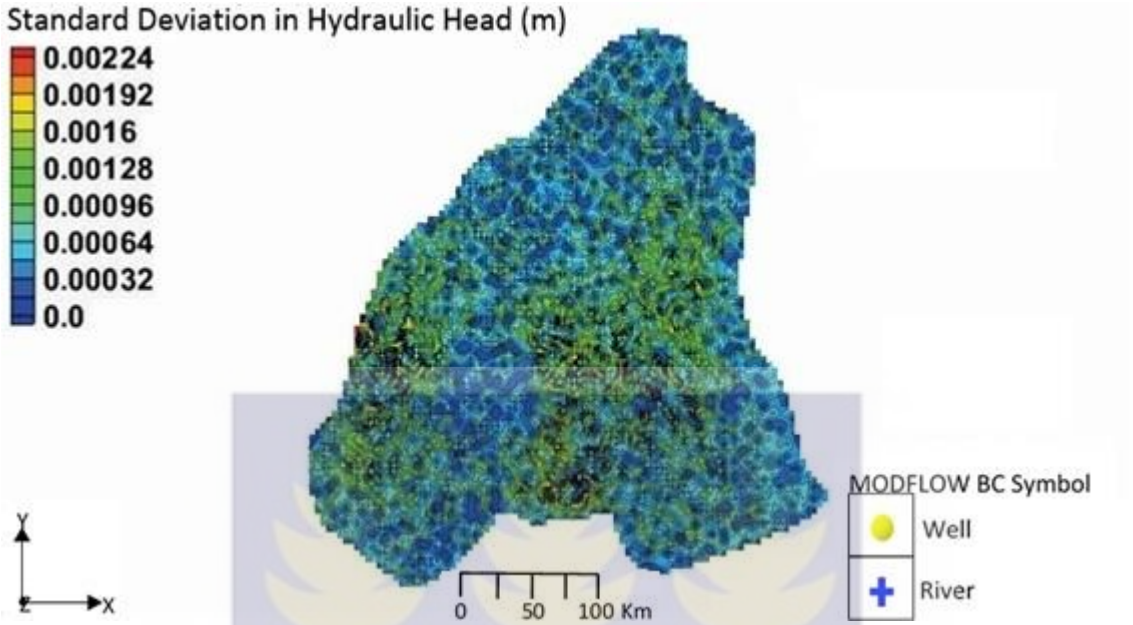

Figure 4.11 Standard deviation in computed hydraulic heads from stochastic MODFLOW models

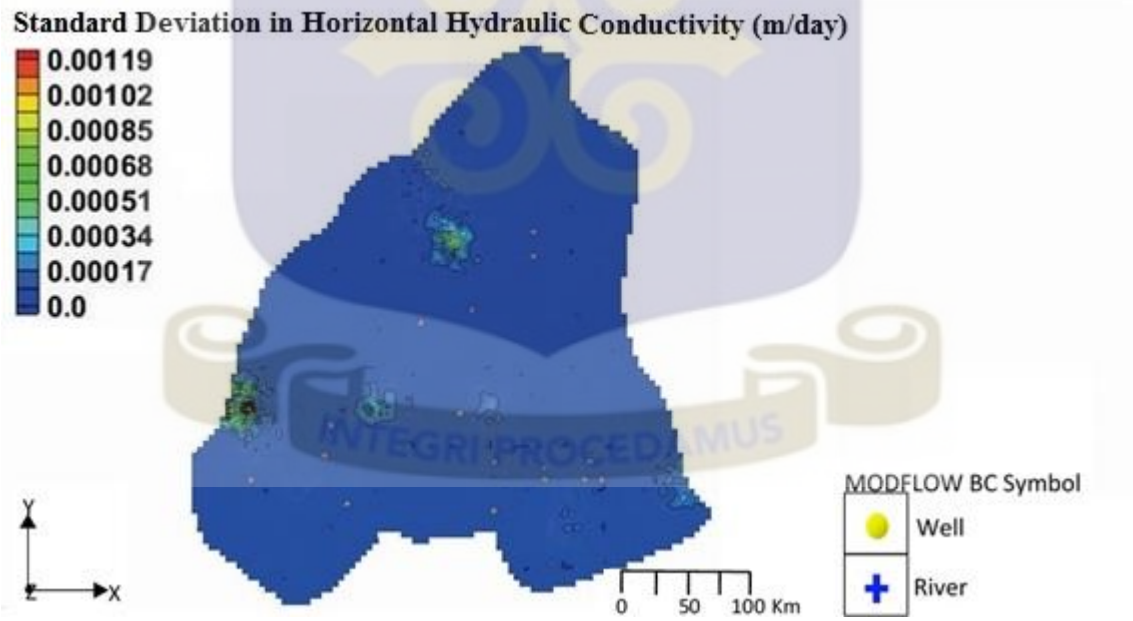

Figure 4.12 Standard deviation in the HK input array

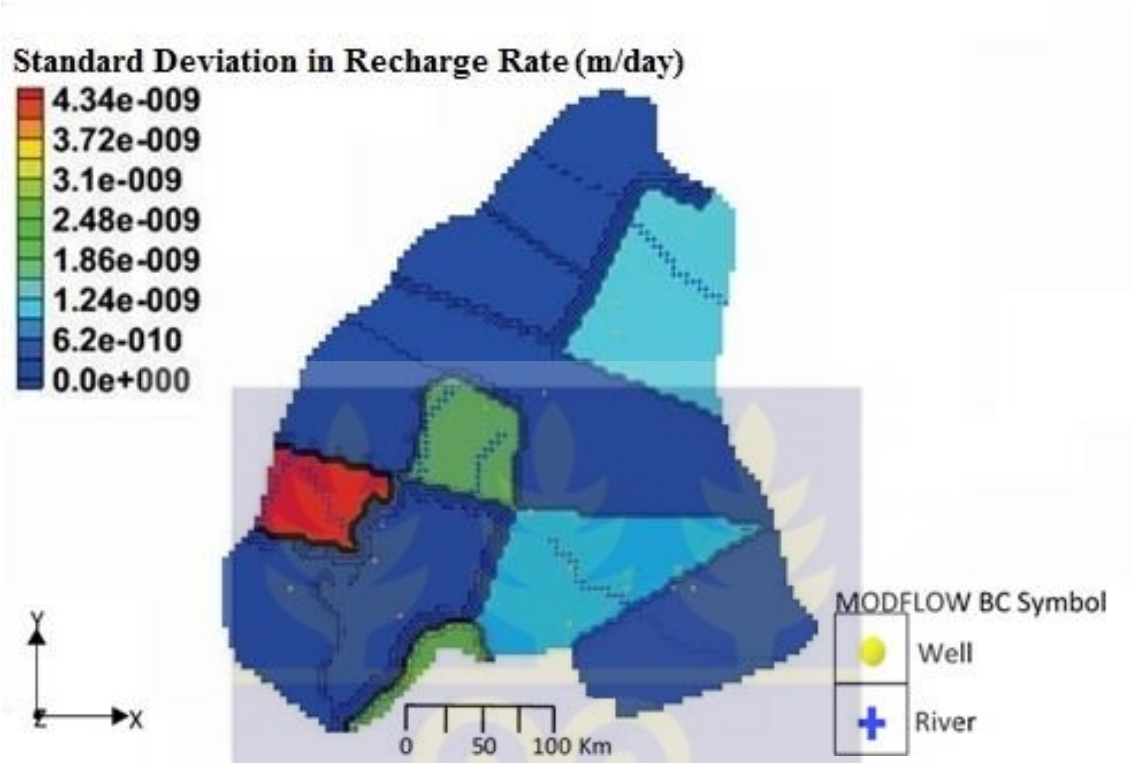

Figure 4.13 Standard deviation in recharge rate from stochastic MODFLOW models

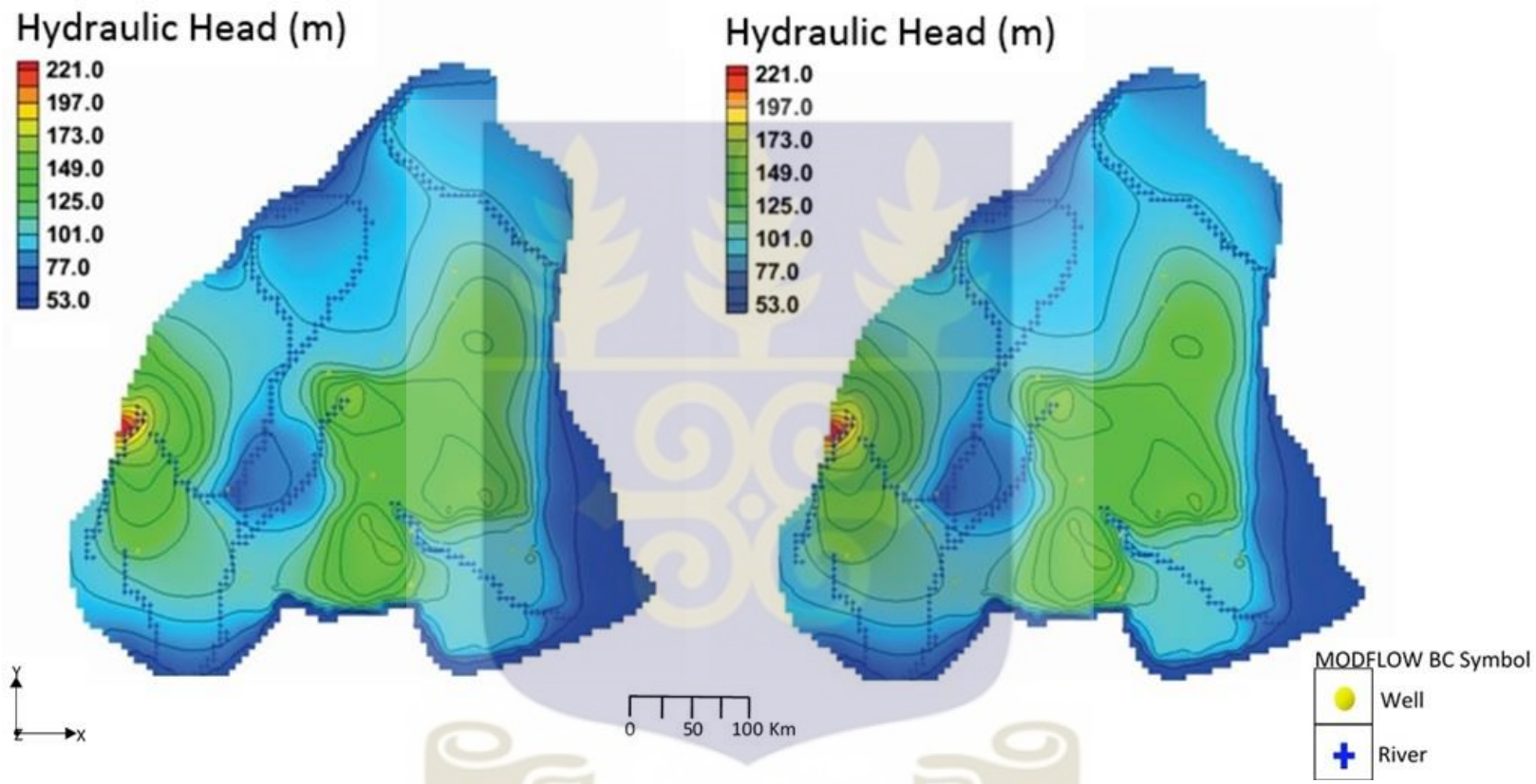

L-H: Figure 4.14 The hydraulic heads from the stochastic simulation for realisation number 1 and 995, respectively

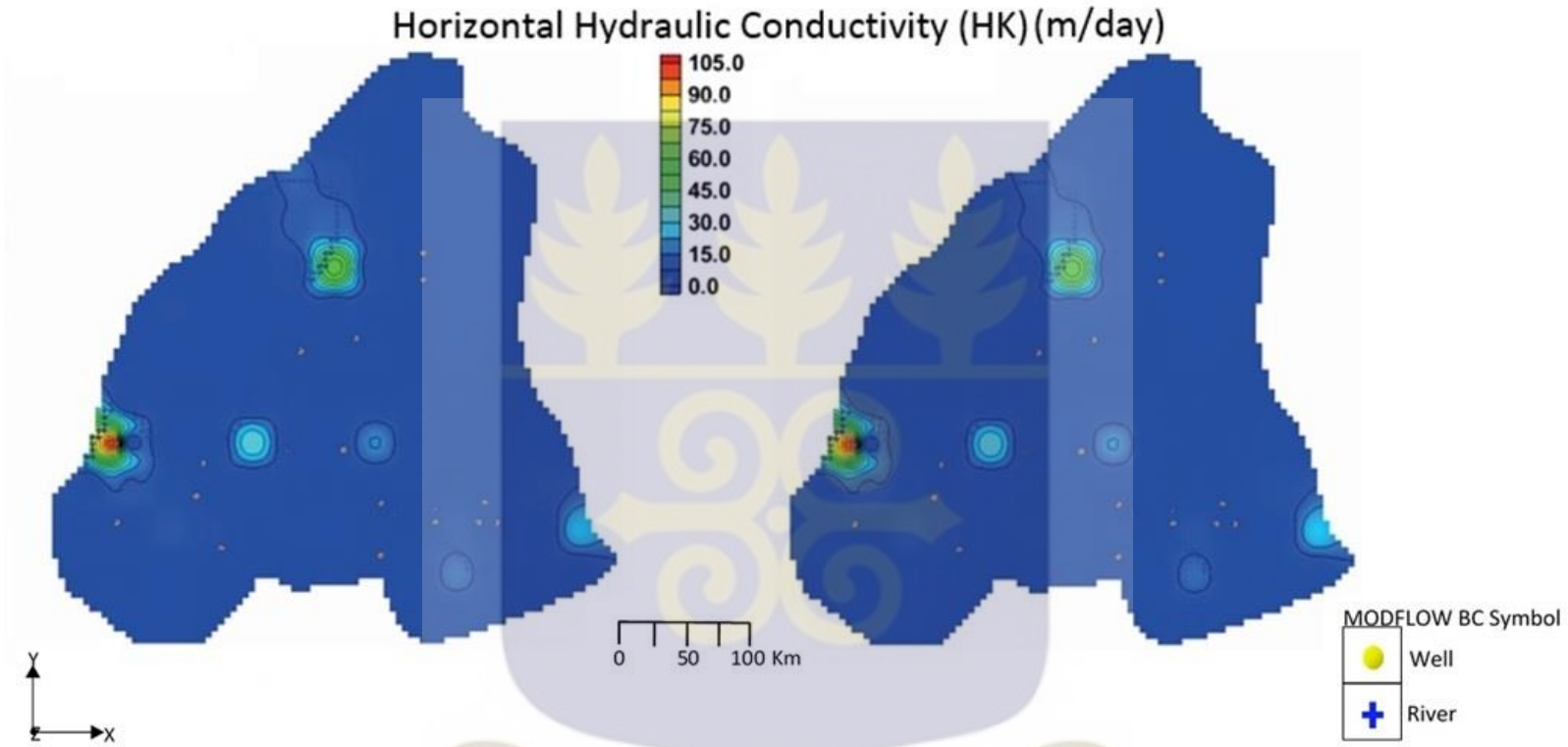

L-H: Figure 4.15 The HKs from the stochastic simulation for realisation number 1 and 995, respectively

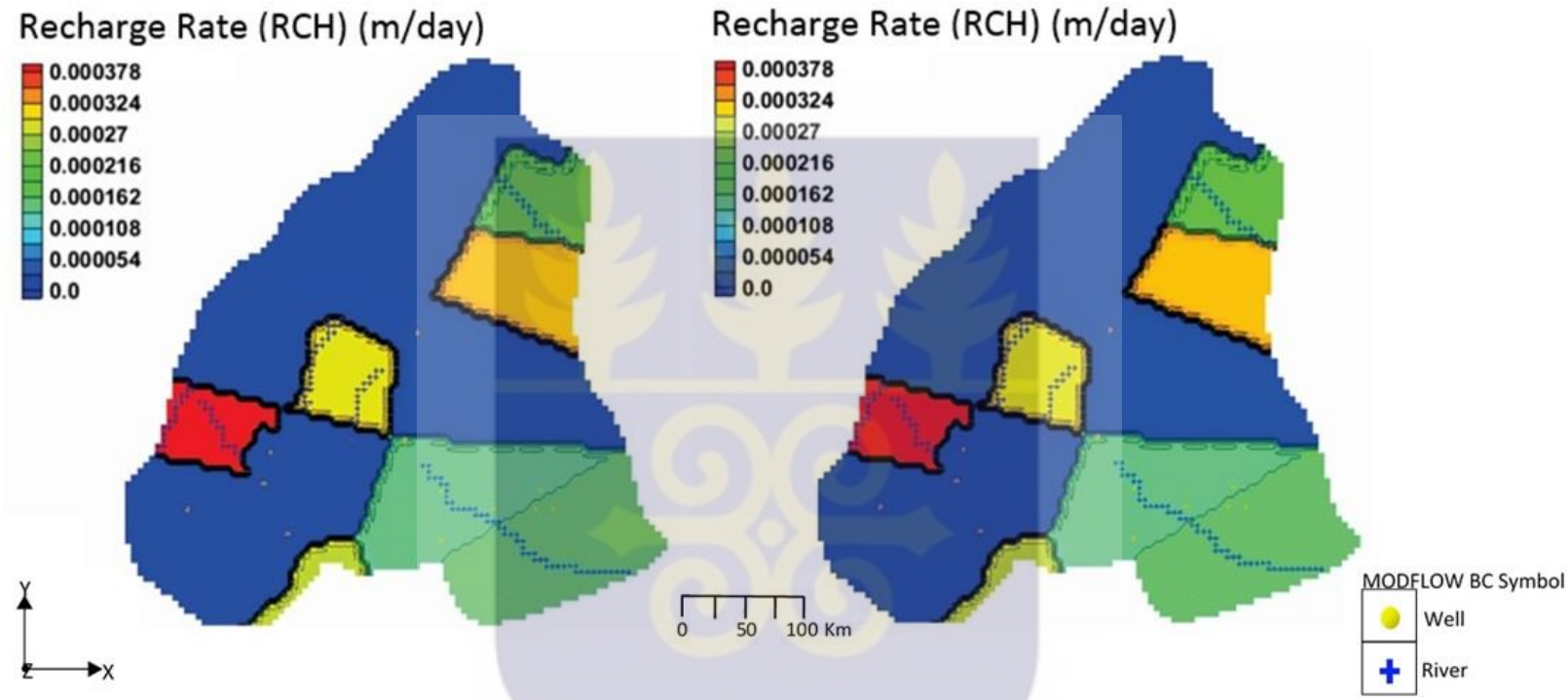

L-H: Figure 4.16 The RCHs from the stochastic simulation for realisation number 1 and 995, respectively

4.7 Scenario analysis

Different scenarios were simulated using the results from the stochastic runs to predict possible changes, if any, in the general configuration of the flow system on different water management conditions. The scenarios centered on variations in groundwater recharge and abstraction.

The first scenario entailed progressively increasing the groundwater abstraction from all the twenty production wells by 10%, 20%, 30%, 40% up to 100%; then 200%, 300%, and 400% above the current abstraction rates. The recharge rates at calibration were, however, kept constant. The model was simulated after each increment, on the forward run, and the flow patterns observed for any possible variations. The objective was to observe variations in the hydraulic head with increase in population with an accompanying increase in groundwater abstraction, as recharge to the basin stays at the current rates. It is observed that an increase in the current abstraction rates (Table 3.1) by up to 200% show no major variations in the flow system, except for some marginal changes towards the south-eastern portion of the domain.

Figure 4.17 illustrates the hydraulic head distribution and flow pattern after 10% increase in the current groundwater abstraction rates. Illustrations for the other percentage increments are captured in Appendix B. The observation is consistent for all the probable realisations generated by the stochastic simulations for each of the percentage increments. This observation implies, the existing rates of recharge of the aquifers in the terrain can

sustain up to a three times increase in the current rates of abstraction of groundwater in the area for both domestic and commercial purposes.

However, noticeable changes are observed in the steady-state model when abstraction rates increase by 300% and 400%. Figure 4.18 illustrates the observed variations after a 400% increase. Illustration of the observed changes after a 300% increase is captured in Appendix B. For instance, dry cells emerge indicating a considerable drawdown in the terrain. Also, the marginal variations in the flow pattern within the south-eastern portion of the domain are more pronounced. The observations point to the fact that the existing rates of recharge cannot sustain up to a four times increase in the current rates of abstraction of groundwater in the area. This suggests that increased groundwater recharge is required to sustain an increase in the current abstraction rates by four times and beyond if groundwater would be the only source of water for domestic and commercial usage.

The Ghana Meteorological Agency reports that, Accra experiences a bi-modal rainfall regime; a major rainy season, which occurs from March to July, and minor rainy season, which occurs from September to November (Amoako & Frimpong Boamah, 2015). The rains are usually intensive with short storms. Karley (2009) also reports that, the seasonal rainfall in Accra (measured – June, July and August) over the period between 1935 and 2007 depicts a relatively flat mean trend over the period. Recent happenings also show that the levels of rainfall in Accra may not decline as a result of climate variabilities.

However, groundwater recharge from rainfall could reduce over time if the increase in development projects in probable local groundwater recharge areas of Accra is not constrained. Again, the incessant paving of almost every available open space in Accra could eventually result in a drastic decline in aquifer recharge through precipitation in the study area. It is necessary therefore, to conduct more detailed research to identify and secure local and regional groundwater recharge sources. Also, the development of local groundwater recharge dugouts would help reduce the annual quantities of rainwater lost through evapotranspiration and runoffs as a result of floods. This will help have more water stored in the aquifers for use during the periods of need.

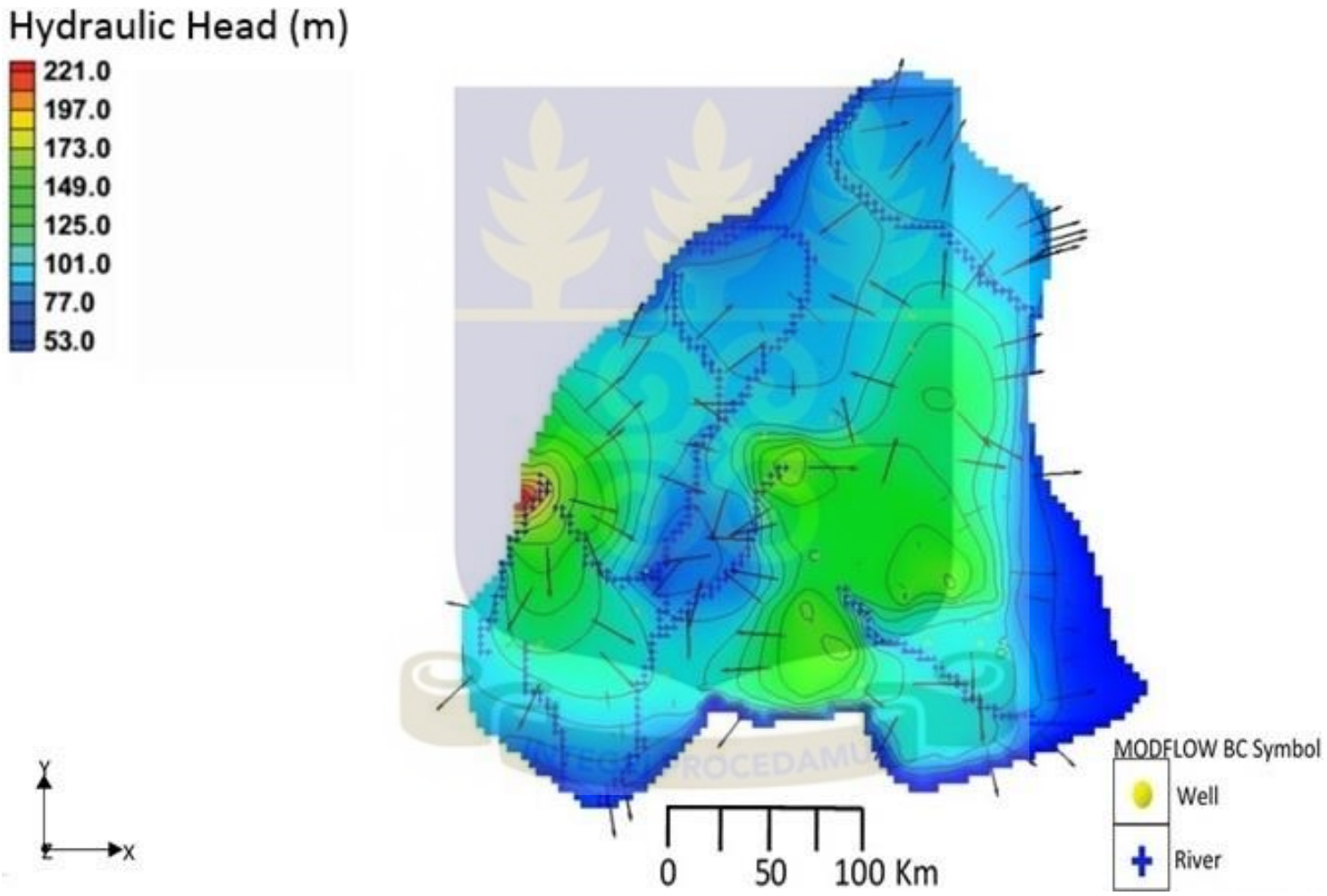

Figure 4.17 Hydraulic head distribution and flow pattern after 10% increase in groundwater abstraction

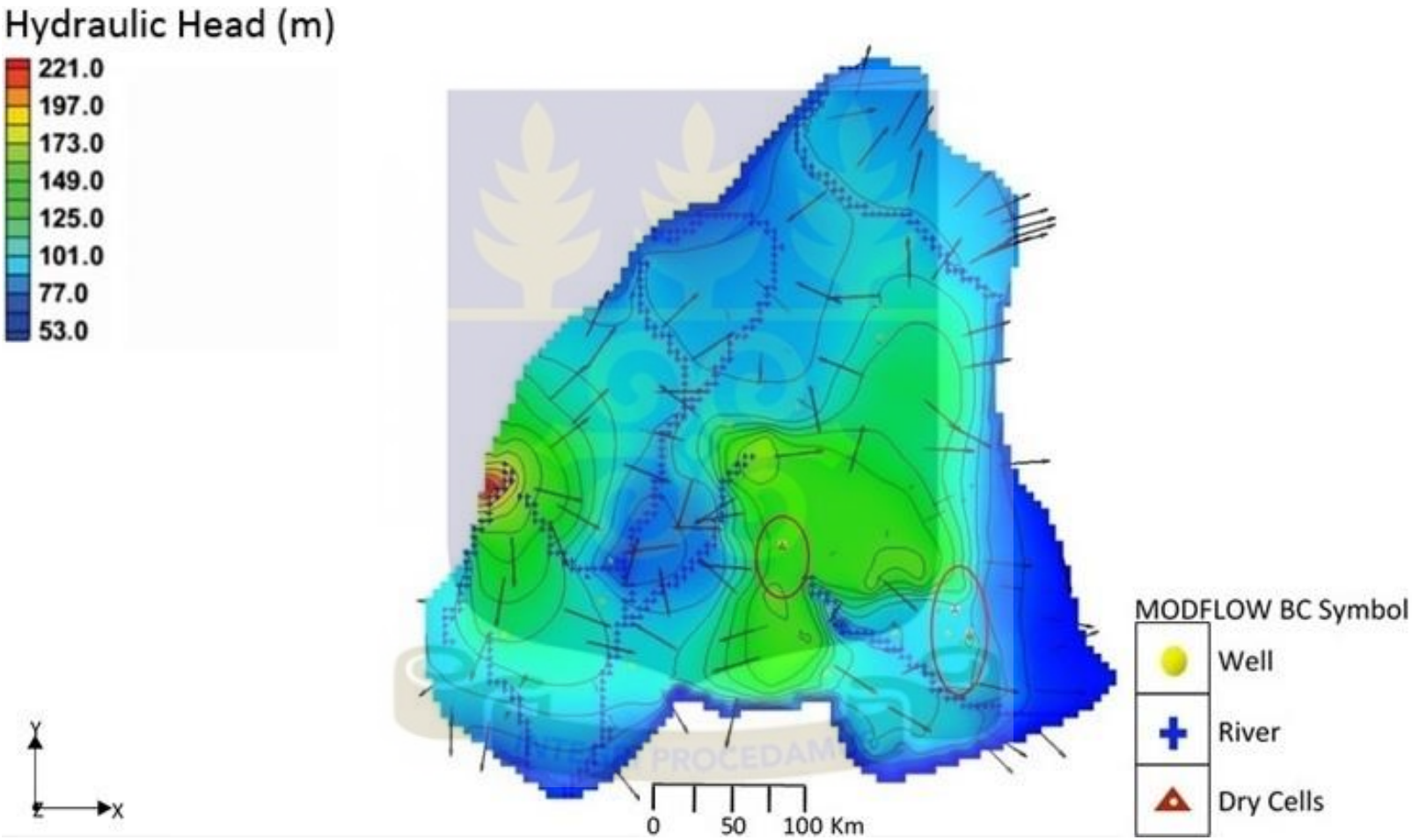

Figure 4.18 Hydraulic head distribution and flow pattern after 400% increase in groundwater abstraction

The second scenario involved successively decreasing the groundwater recharge rates at calibration by 10%, 20% up to 90% below the current recharge rates while keeping the current abstraction rates unchanged. After each decrease, the model was simulated on forward run and the flow patterns observed for any possible changes. The intent was to capture the possible effects of a decline in rainfall patterns on groundwater resource in the domain. The general flow patterns observed after a 10% decrease in recharge rates is illustrated by Figure 4.19. Illustrations for the other percentage decreases are captured in Appendix B. There are no observable changes in hydraulic head. However, there are some marginal changes in the flow vectors towards the south-eastern portion of the domain when the current recharge rates are reduced by up to 40% (Figure 4.19). This variation intensifies, as the recharge rates are further reduced by 50% up to 90% at the current abstraction rates (Figure 4.20).

In addition, subtle changes in hydraulic head in the north-eastern portion towards the south-eastern portion of the domain was noticed when the current recharge rates were reduced by 50% up to 90% (Figures 4.20). There is also the incidence of dry cells when the recharge rates are reduced by 70% up to 90% at the current abstraction rates (Figures 4.20). The implication is that when the current rates of recharge decline by half or more, there would be considerable drawdown if the current abstraction rates are to be sustained solely by groundwater resource in the study area.

The foregoing observations are consistent for all the probable realisations generated by the stochastic simulations for each of the percentage decrements. Additional illustrations of the observed variations are presented in Appendix B.

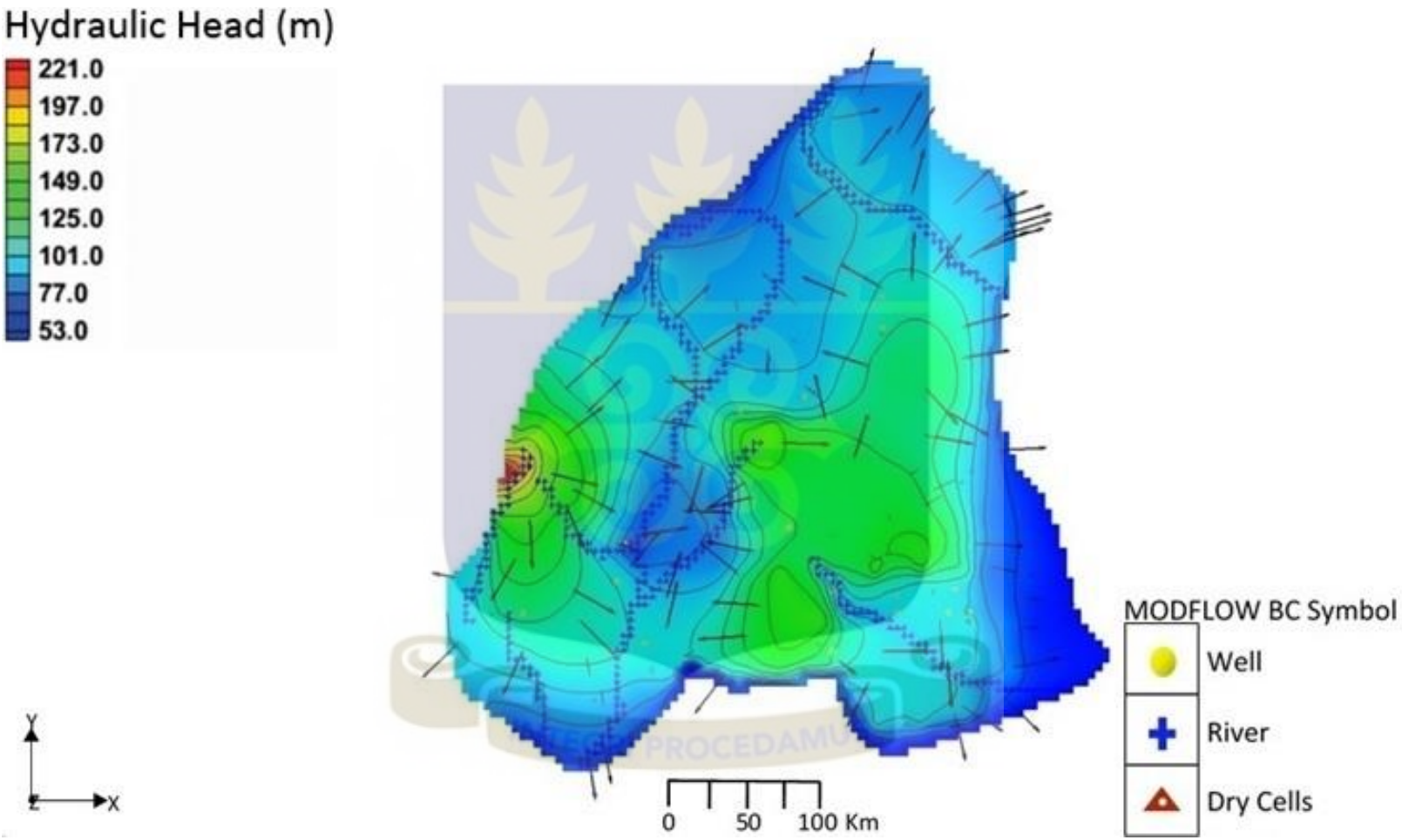

Figure 4.19 Hydraulic head distribution and flow pattern after 10% to 40% reduction in groundwater recharge

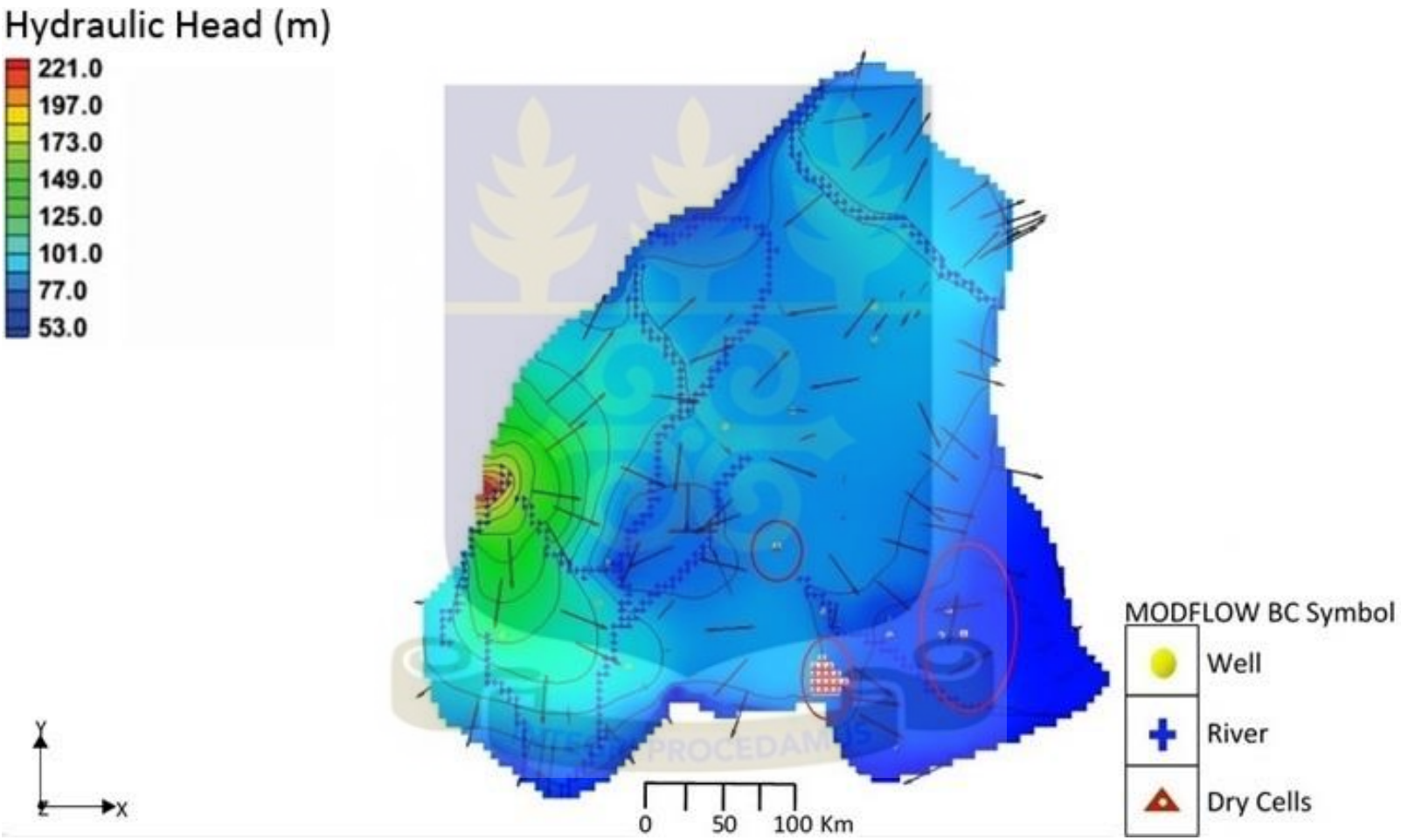

Figure 4.20 Hydraulic head distribution and flow pattern after 90% reduction in groundwater recharge

The third scenario simulated the effects of a 10% reduction in the current groundwater recharge rates with a subsequent progressive increase in the abstraction rates by 10%, 20% up to 100%, and then 200%, 300%, and 400%. The noticeable effects, when abstractions rates are increased by 10% up to 40%, are the changes in the contours that form within the south-eastern portion of the terrain. This can be attributed to a decline in the hydraulic heads. Figure 4.21 illustrates the observed changes after a 10% increase in the current abstraction rates. That for the other percentage increments in the current abstraction rates are presented in Appendix B.

Flow vectors towards the south-eastern portion of the terrain show some amount of change in direction as the abstraction rates are increased further by 50% to 100%. Illustrations of these observed changes are captured in Appendix B.

However, when the current abstraction rates are increased by 200%, 300%, and 400% with the recharge rates still reduced by 10%, dry cells emerge in addition to new contours forming within the south-eastern portion of the study area (Figure 4.22). Since rainfall is the main source of recharge of the aquifer, a reduction in the current rainfall figures coupled with an increase in the current abstraction rates by three to five times, would result in considerable drawdown hence, the incidence of the dry cells. Additional illustrations of the observed effects are presented in Appendix B.

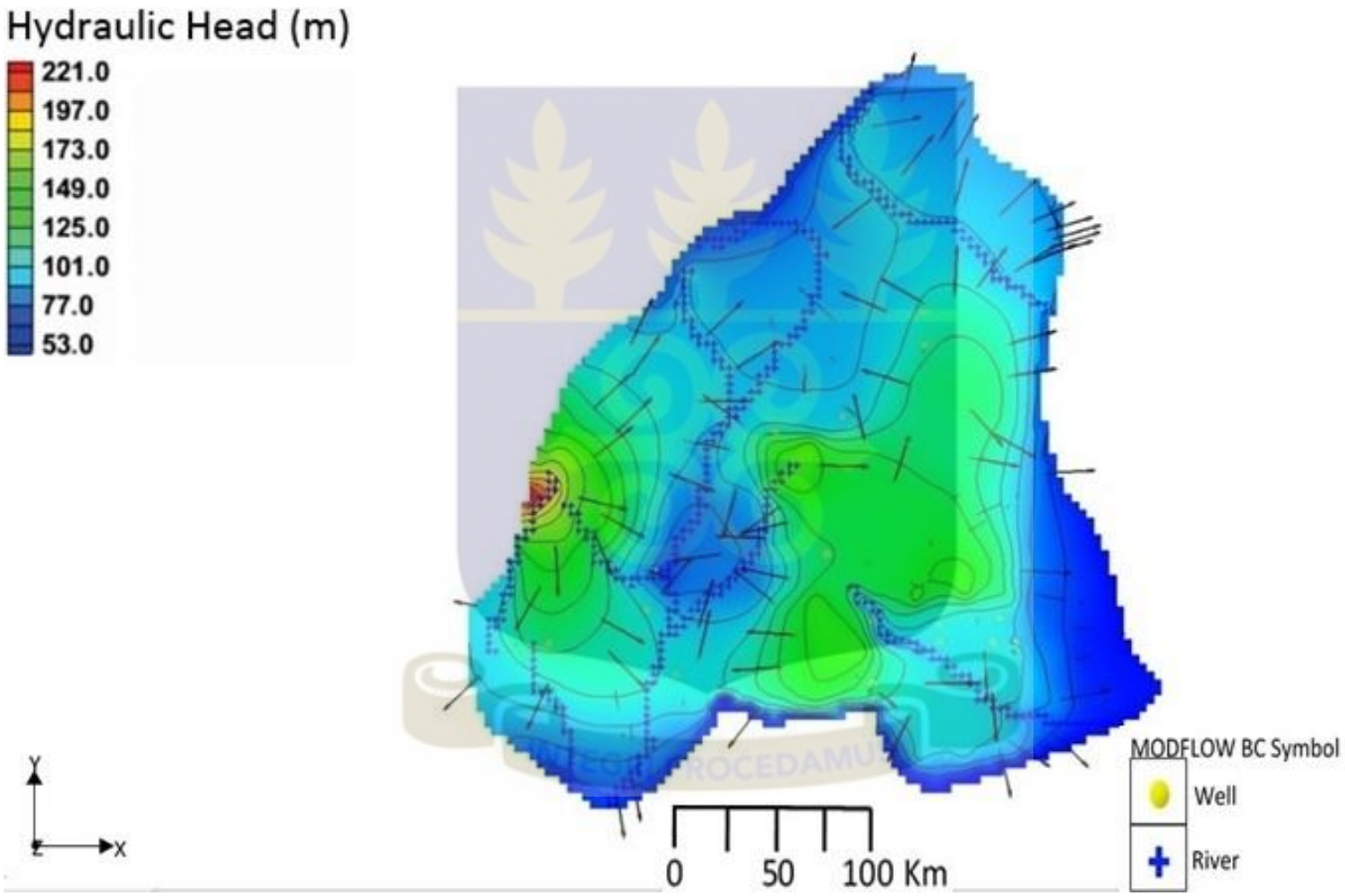

Figure 4.21 Hydraulic head distribution and flow pattern after 10% reduction in groundwater recharge and 10% increase in abstraction

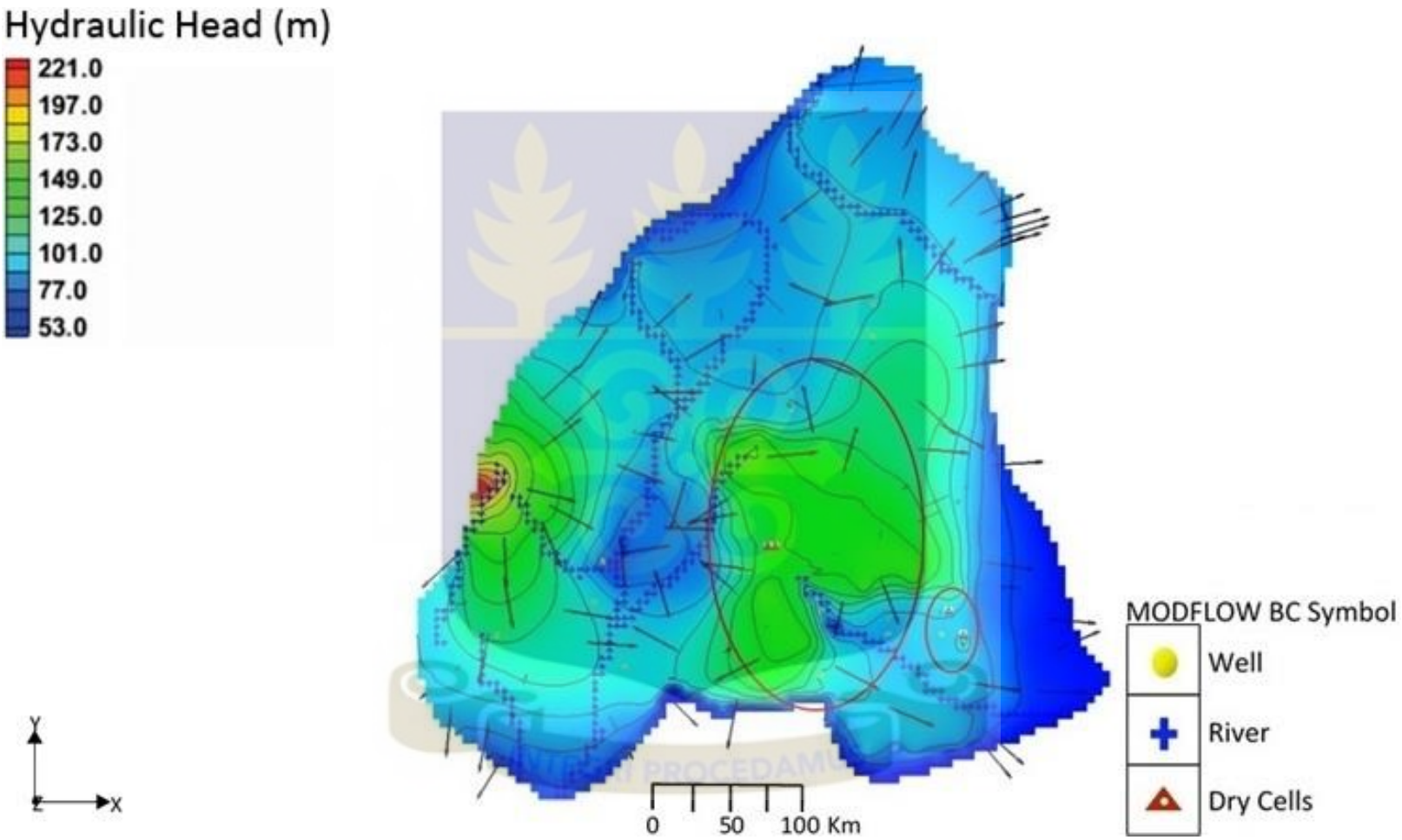

Figure 4.22 Hydraulic head distribution and flow pattern after 10% reduction in groundwater recharge and 400% increase in abstraction

4.8 Chapter summary

In this chapter I have presented, analysed and discussed the major findings from the study. First, the stratigraphy, general groundwater levels and flow patterns in the domain were discussed. Four lithologies namely, clay, laterite, quartzite, and schist, were identified. The terrain has been argued to have a single aquifer made of a quartzite-schist formation. The linear plot of the relationship between the model computed and the observed head data, at calibration, depicts a close fit. The cross-section cutting procedure adopted revealed local and intermediate flow systems in the terrain. It also assisted in identifying potential recharge areas in the study area.

Second, estimates of the hydraulic conductivity and velocity field simulated at calibration were discussed. The observed linear relationship between the spatial distributions of the two fields tied in well with the established theoretical relationship that exists between the hydraulic conductivity parameter and the seepage velocity of groundwater flow. Next, I generated seven unique flowpaths for contaminant transport using the particle tracking technique in MODPATH. The respective lengths, travel times, and average velocities for contaminant transport along each of the flowpaths were generated. The analysis indicated that the estimated velocity field is significant for contaminant transport in the domain.

Third, I discussed the estimated recharge rate simulated at calibration for the domain. The estimated range represents 1.2% and 3.6% of the average annual precipitation in the area. This low range is a true reflection of occurrences in the GAR, notably flood

runoffs and the volume of construction projects impeding aquifer recharge through precipitation. However, the water budget for the domain indicates that the current abstraction rates can be adequately catered for by the estimated recharge rates of the aquifer through rainfall.

Fourth, results of the stochastic simulations indicate that the steady-state flow model is unique for the hydraulic parameters (head, recharge, and HK) simulated. Additionally, the parameter sensitivity analysis also indicates that the flow model is insensitive to both HK and recharge.

Finally, I delved into the analysis of results from the three management scenarios centered on variations in groundwater recharge and abstraction simulated to investigate the sustainability of the groundwater resource in the domain. Details of the conclusions from the analysis of the scenarios are given in the next chapter.

CHAPTER FIVE

CONCLUSIONS AND OUTLOOK

5.0 Introduction

This concluding chapter presents a summary of the research work done, highlighting significant results and their implications (section 5.1). Recommendations are made to the two municipal assemblies and further work in this area of research in the study area and other areas in the GAR are outlined (section 5.2).

5.1 Summary of major findings of the study

5.1.1 The stratigraphy of the domain

This study, being the first of its kind in the study area, has successfully characterised the hydrogeology of the area, using historical hydrogeological and groundwater monitoring data. A solid stratigraphy of the domain has been developed using data on pumping test and borehole lithological logs of twenty wells drilled in the Ga East and Adentan municipalities under the GoG 20,000 Borehole Drilling Project carried out in 2012.

The model, within the limit of available data, identifies a single aquifer system made up of quartzite-schist formations. Four lithological units were identified in the domain, viz. laterite, schist, quartzite, and clay. Subsequently, a numerical groundwater flow

model, calibrated under steady-state conditions, for the Ga East and Adentan municipalities was achieved using MODFLOW in the GMS package version 10.0 (Aquaveo, 2014).

5.1.2 The hydraulic conductivity estimates

The model suggests that the aquifer hydraulic conductivity falls within the range of 7.5 m day^{-1} to 105.0 m day^{-1}, with a mean of 13.1 m day^{-1}. The conductivities are lower than 15.0 m day^{-1} in much of the area, which is consistent with observed hydraulic conductivity values for lithologies of the aquifer material. The observed outliers are attributable to the fractured and jointed quartzite within the weathered zone, enhancing the conduits within the materials for rapid flow of groundwater. The hydraulic conductivity field is based on secondary structural entities created in the wake of fracturing and/or weathering of the rocks. The range of values depict homogeneity in the hydraulic conductivity field.

5.1.3 The velocity field and flow systems

The estimated velocity field in the area ranges from 0.002 m day^{-1} to 11.2 m day^{-1}, with much of the area having a velocity below 0.85 m day^{-1}. The spatial distribution of the velocity field ties in well with the hydraulic conductivity field observed for the terrain. The estimated velocity field is significant for contaminant transport in the area.

Seven principal groundwater flowpaths have been identified in the study area using particle tracking technique under MODPATH. The travel times, based purely on advection, along the flowpaths from recharge to discharge locations range from 7 years to 833 years. The cross-section cutting technique reveals cases of local and intermediate flow systems. Potential recharge areas have been identified as well.

5.1.4 Recharge estimates

The calibrated aquifer recharge, through precipitation, ranges from 2.70 $\mathrm{m\ day^{-1}}$ to 3.78×10^{-4} $\mathrm{m\ day^{-1}}$. However, the groundwater recharge is less than 8.10×10^{-5} $\mathrm{m\ day^{-1}}$ for much of the area. Hence, using the range 2.70×10^{-5} $\mathrm{m\ day^{-1}}$ to 8.10×10^{-5} $\mathrm{m\ day^{-1}}$, the groundwater recharge represents 1.2% and 3.6% of the average annual precipitation in the area. These low estimates are expected, considering the inundation of Accra with construction projects impeding aquifer recharge through rainfall. Additionally, the flooding situation in Accra over the years has resulted in high runoffs, which adversely affects aquifer recharge through precipitation.

The water budget indicates the flow system conserves mass, confirming that the flow model was calibrated under steady-state conditions. The water budget also shows that current abstraction levels of groundwater in the area can be sustained by recharge through rainfall to the aquifer system with minimal net drawdown in the hydraulic head. A number of recharge areas are identified in parts of the study area, namely, the Bethel Prayer Camp area, Mango Lane, and Santeo.

5.1.5 Stochastic and scenario analyses

Stochastic simulations carried out on the calibrated model indicate that it is unique for the aquifer recharge, HK and hydraulic head. The steady-state model can therefore be relied upon to assist in the regional hydrogeological characterisation of the aquifer.

The first of the three management scenarios centering on variations in groundwater recharge and abstraction simulated to investigate the sustainability of the groundwater resource indicate that the existing recharge rates can sustain up to a three times increase in the current rates of abstraction of groundwater for both domestic and commercial purposes. The second reveals that, when the current rates of recharge decline by half or more, there would be considerable drawdown if the current abstraction rates are to be sustained solely by groundwater resource. And the third shows that, having rainfall as the main source of recharge to the aquifer, a reduction in the current rainfall figures coupled with an increase in the current abstraction rates by three to five times would result in considerable drawdown.

5.1.6 Implications of the major findings

This research was conducted into groundwater hydraulics in the Ga East and Adentan municipalities, and as discussed in section 4.2, the transportation of contaminants is likely to proceed at an appreciable pace under the influence of the velocity and hydraulic conductivity fields. The resulting effect is that the quality of groundwater is likely to be compromised, hence, the need to treat the water before use in domestic and commercial activities.

From the simulated management scenarios conducted to ascertain the sustainability of the resource, a decline in the current recharge rates (through reducing precipitation rates) with an accompanying increase in the current abstraction rates by three to five times would result in considerable drawdown in the aquifer resource. This would require the construction of local groundwater recharge dugouts to stem the amount of rainwater lost annually through evapotranspiration and flood runoffs.

5.2 Recommendations and further works

It is recommended that wells/dugouts should be sited at the identified discharge areas to boost aquifer recharge in the study area. There is also the need to protect identified recharge areas against the siting of construction projects. Additionally, steps should be taken by the two municipal assemblies to control the excessive paving of open spaces in the area to enhance aquifer recharge through precipitation. Developers are encouraged to comply with directives from the assemblies in this regard for the greater good of all.

Groundwater recharge from rainfall could reduce over time if development projects in probable local groundwater recharge areas are not constrained. It is necessary, therefore, to conduct more detailed research to identify and secure local and regional groundwater recharge sources. Also, the development of local groundwater recharge dugouts would help reduce the annual quantities of rainwater lost through evapotranspiration and runoffs as a result of floods. This will help have more water stored in the aquifers for use during the periods of need.

On a personal level, I would carry out further studies to incorporate fully the landfill cited at Pantang in the model to track the transport of contaminants from the landfill to parts of the study area more comprehensively. Samples from the landfill will be analysed to identify some potential contaminants leached into the subsurface flow by rainfall.

The management scenarios simulated in this study are based on steady-state conditions, which may not necessarily account for conditions that may prevail in the event of increasing groundwater abstraction rates and decreasing recharge. It will be prudent, therefore, to develop a transient model, which takes into account the time-variable nature of groundwater storage in the area, to simulate the time varying patterns in groundwater storage.

It is my firm conviction that this work needs to be replicated in other municipalities/districts in the GAR to allow for gaining insight into the state and fate of groundwater resource in the entire region. The results of the various studies may be compared to gain understanding into the trend of groundwater abstraction and recharge, as well as the implications of the velocity fields for contaminant transport, so that appropriate legislation may be formulated to regulate the use of this valuable resource.

REFERENCES

Adarkwa, K.K. (2012). The changing face of Ghanaian towns. *African Review of Economics and Finance*, 4(1), 1-29.

Amoako, C., & Frimpong Boamah, E. (2015). The three-dimensional causes of flooding in Accra, Ghana. *International Journal of Urban Sustainable Development*, 7(1), 109-129.

Anderson, M.P. (1986). Field verification of groundwater models. In W.Y. Garner et al. (Eds.), *American Chemical Society Symposium Series*, 315, *in Evaluation of Pesticides in Groundwater* (pp. 396-412).

Anderson, M.P., & Woessner, W.W. (1992). Applied groundwater modeling of flow and advective transport. San Diego, CA: Academic Press.

Anderson, M.P., & Woessner, WW. (2002). Applied groundwater modelling - Simulation of flow and advective transport. San Diego, CA: Academic Press.

Appelo, C.A.J., & Postma, D. (2010). *Geochemistry, Groundwater and Pollution* (2nd ed.). Amsterdam, The Netherlands: Balkema Publishing.

Aquaveo. (2010). Groundwater Modeling System Version 7.1. Aquaveo, Provo, Utah.

Aquaveo. (2014). Groundwater Modeling System Version 10.0. Aquaveo, Provo, Utah.

Attandoh, N., Yidana, S.M., Abdul-Samed, A., Sakyi, P.A., Banoeng-Yakubo, B., & Nude, P.M. (2013). Conceptualization of the hydrological system of some sedimentary aquifers in Savelugu-Nanton and surrounding areas, Northern Ghana. *Hydrological Processes*, 27(11), 1664-1676. doi:10.1002/hyp.9308

Attoh, K., Dallmeyer, R.D., & Affaton, P. (1997). Chronology of nappe assembly in the Pan-African Dahomeyideorogen, West Africa: evidence from 40Ar/39Ar mineral ages. *Precambrian Research*, 82**,** 153-171.

Banoeng-Yakubo, B., Yidana, S.M., Akabzaa, T., & Asiedu, D. (2008). Groundwater flow modeling in the Akyem Area, Southeastern, Ghana. *Journal of Environmental Hydrology*, 16(13), 1-9.

Bethke, C.M. (1989). Modeling subsurface flow in sedimentary basins. *Geologische Rundschau*, 78, 129-154.

Blay, P.K. (1991). Applying subduction tectonics to the evolution of the Pan-African Dahomeyide deformed belt of Ghana, West Africa. In *Proceedings of the First Local Conference on Mineral Exploration and Development and their Impact on the Economy of Ghana*, (52-75). Accra: Minerals Commission.

Connel, L.D. (2007). Simple models for subsurface solute transport that combine unsaturated and saturated zone pathways. *Journal of Hydrology*, 332, 361-373.

Dapaah-Siakwan, S., & Gyau-Boakye, P. (2000). Hydrogeologic framework and borehole yields in Ghana. *Journal of Hydrogeology*, 8, 405-416.

Dettinger, M.D., & Wilson, J.L. (1981). First order analysis of uncertainty in numerical models of groundwater flow. Part 1. Mathematical development. *Water Resources Research*, 17(1), 149-161.

Dickson, K.B., & Benneh, G. (1988). *A new geography of Ghana*. London, England: Longman.

Doherty, J. (2005). PEST: *Model Independent Parameter Estimation. User Manual* (5th ed.). Corinda, Australia: Watermark Numerical Computing.

Domenico, P.A. (1972). *Concepts and models in groundwater hydrology*. New York, NY: McGraw-Hill.

Domenico, P.A., & Schwartz, F.W. (1998). *Physical and chemical hydrogeology* (2nd ed.). New York, NY: John Wiley and Sons, Inc.

Ebraheem, A.M., Garamoon, H.K., Raid, S., Wycisk, P., & Seif El Nasr, A.M. (2003). Numerical modelling of groundwater resource management options in the East Oweinat area, SW, Egypt. *Environmental Geology*, 44, 433-447.

Farthing, M.W., Sassen, D.R., Prins, J.F., & Miller, C.T. (2004). A problem-solving environment for subsurface flow and transport phenomena. *Developments in Water Science*, 55(2), 1117-1130. doi:10.1016/S0167-5648(04)80129-1

Fetter, C.W. (2001). *Applied hydrogeology* (4th ed.). New Jersey, NJ: Prentice Hall.

Field, D.A. (1991). Generic delaunay triangulation algorithm for finite element meshes. *Advances in Engineering Software*, 13(5/6), 263-272.

Fitts, C.R. (2002). *Groundwater science*. London, England: Elsevier Science Ltd.

Franke, O.L., & Reilly, T.E. (1987). The effects of boundary conditions on steady-state response of three hypothetical groundwater systems – results and implications of numerical experiments. *U.S. Geological Survey Water-Supply Paper*, 2315.

Freeze, R.A. (1972). Role of subsurface flow in generating surface runoff. Base flow contributions to channel flow. *Water Resource Research*, 8, 609-623.

Freeze, R.A., & Witherspoon, P.A. (1966). Theoretical analysis of regional groundwater flow: 1. Analytical and numerical solutions to the mathematical model. *Water Resources Research*, 2(4), 641-656.

Freeze, R.A., & Witherspoon, P.A. (1967). Theoretical analysis of regional groundwater flow: 2. Effect on water-table configuration and subsurface permeability variation. *Water Resources Research*, 3(2), 623-634.

Freeze, R.A., & Cherry, J.A. (1979). *Groundwater*. Upper Saddle River, NJ: Prentice Hall, Inc.

Ghana Statistical Service (2012). *2010 Population and Housing Census Final Results*. Retrieved from www.statsghana.gov.gh/docfiles/2010/phc_population_and_housing_census_final_results.pdf

Grant, N.K. (1969). The late precambrian to early paleozoic orogeny in Ghana, Togo, Dahomey and Nigeria. *Geological Society of America Bulletin*, 80(1), 45-55.

Harbaugh, A.W. (2005). MODFLOW-2005, The U.S. Geological Survey modular ground-water model - the ground-water flow process. *U.S. Geological Survey Techniques and Methods*, (06-A16).

Hayatu, A.I., Nura, Y., & Nuhu, I. (2013). Physics of groundwater flow for confined and unconfined aquifers in relation to measurement of groundwater level variation with time. *Journal of Physical Science and Innovation*, 5(1), 23-34.

Hill, M.C. (1990). Preconditioned conjugate-gradient 2 (PCG2), a computer program for solving ground-water flow equations. *Water- Resources Investigations Report* (90-4048). Denver, CO: USGS.

Hill, M.C., Banta, E.R., Harbaugh, A.W., & Anderman, E.R. (2000). MODFLOW-2000, The U.S. Geological Survey modular ground-water model. User guide to the observation, sensitivity, and parameter-estimation processes and three post processing programs. *Open-File Report* (00-184). Reston, VA: USGS.

Hornberger, G.M., Raffensperger, J.P., Wiberg, P.L., & Eshleman, K.N. (1998). *Elements of physical hydrology*. Baltimore: Johns Hopkins University Press.

Hubbert, M.K. (1940). The theory of ground-water motion. *Journal of Geology*, 48(8), 758-944.

Hubbert, M.K. (1956). Darcy's law and the field equations of the flow of underground fluids. *Trans. Amer. Inst. Min. Met. Eng.*, 207, 222-239.

Jones, N.L., Budge, T.J., Lemon, A.M., & Zundel, A.K. (2002). Generating MODFLOW grids from boundary representation solid models. Groundwater, 40(2), 194-200. doi:10.1007/s1266-5010-0740-y

Kai-Yuan, K. (2014). Application of an integrated surface water-groundwater model to multi-aquifers modelling in Choushui river alluvial fan, Taiwan. *Hydrological Processes*, 28(3), 1409-1421. doi:10.1002/hyp.9678

Karley, N.K. (2009). Flooding and physical planning in urban areas in West Africa: situational analysis of Accra, Ghana. *Theoretical and Empirical Researches in Urban Management*, 4(13), 25-41.

Kesse, G.O. (1985). *The mineral and rock resources of Ghana*. Rotterdam, The Netherlands: Balkema Publishing.

Konikow, L.F. (1996). Numerical models of groundwater flow and transport. Manual on mathematical models in isotope hydrogeology. *International Atomic Energy Agency Report*, (IAEA-TECDOC-910). Vienna, Australia: IAEA.

Konikow, L.F., & Reilly, T.E. (1998). Groundwater modelling. In J.W. Delleur (Ed.), *The Handbook of Groundwater Engineering* (1-20.40). Boca Raton, Florida: CRC.

Kumar, C.P. (2002). Groundwater flow models. *Scientist "E1" National Institute of Hydrology* Roorkee, 247667.

Kumar, C.P. (2015). Modelling of groundwater flow and data requirements. *International Journal of Modern Sciences and Engineering Technology*, 2(2), 18-27.

Lawson, C.L. (1986). Properties of n-dimensional triangulation. *Computer-Aided Geometric Design*, 3, 231-246.

Lewis, M.A. (1989). Water. In G.J.H. McCall, & B.R. Maker (Ed.), *Earth science mapping for planning, development and conservation*. Boston, London: Graham and Trotman.

Lutz, A., Thomas, J.M., Pohll, G., & McKay, A. (2007). Groundwater resource sustainability in the Nabogo basin of Ghana. *Journal of African Earth Sciences*, 49, 61-70.

Mani, R. (1978). The geology of the Dahomeyan of Ghana.Geology of Ghana Project. *Ghana Geological Survey Bulletin*, 45.

Maxey, G.B. (1964). Hydrogeology. In V.T. Chow (Ed.), *Handbook of Applied Hydrology*. New York, NY: McGraw-Hill.

Mercer, J.W., & Faust, C.R. (1981). *Ground-water modeling*. Dublin, Ohio: National Water Well Association.

Ministry of Local Government and Rural Development. (2006). *A repository of all districts in the Republic of Ghana*. Retrieved from http://gaeast.ghanadistricts.gov.gh/?arrow=atd&_=2&sa=6329

Moltyaner, G.L., Klukas, M.H., Wills, C.A., & Killey, R.W.D. (1993). Numerical simulations of Twin lake natural-gradient tracer test: a comparison of methods. *Water Resources Research*, 29, 3433-3452.

Moore, J.E. (1979). Contributions of groundwater modelling to planning. *Journal of Hydrology*, 43, 121-128.

Moore, C., & Doherty, J. (2005). Role of the calibration process in reducing model predictive error. *Water Resources Research*, 41(5). doi:10.1029/2004WR003501

Moore, C., & Doherty, J. (2006). The cost of uniqueness in groundwater model calibration. *Advances in Water Resources*, 29(4), 605-623. doi:10.1016/j.advwatres.2005.07.003

Obuobie, E., Keraita, B., Danso, G., Amoah, P., Olufunke, O.C., Raschid-Sally, L., & Drechsel, P. (2006). *Irrigated urban vegetable production in Ghana: characteristics, benefits and risks*. Accra, Ghana: IWMI-RUAF-CPWF.

Ophori, D.U. (1999). Constraining permeabilities in a large-scale groundwater system through model calibration. *Journal of Hydrology*, 224, 1-20.

Oppong, R.A., & Badu, E. (2013). Building material preferences in warm-humid and hot-dry climates in Ghana. *Journal of Science and Technology*, 32(3), 24-37.

Panday, S. & Huyakorn, P.S. (2004). A fully coupled physically-based spatially-distributed model for evaluating surface/subsurface flow. *Advances in Water Resources*, 27, 361-382.

Seaber, P.R. (1988). Hydrostratigraphic units. *Geological Society of America*, 0-2, 9-14.

Senthilkumar, M., & Elango, L. (2004). Three-dimensional mathematical model to Simulate groundwater flow in the lower Palar river basin, southern India. *Journal of Hydrogeology*, 12, 197-208.

Spitz, K. & Moreno, J. (1996). *A practical guide to groundwater and solute transport modeling*. United States: John Willey and Sons Ltd.

Tairou, M.S., Affaton, P., Anum, S., & Fleury, T.J. (2012). Pan-African paleo-stresses and reactivation of the Eburnean basement complex in southern Ghana (West Africa). *Journal of Geological Research*, 938927, 1-15. doi:10.1155/2012/938927

The Community Water and Sanitation Agency Act 1998 (Act 564). Retrieved from http://www.cwsa.gov.gh/cwsa_subcat_select.cfm?corpnews_catid=3&corpnews_scatid=4

The Groundwater Foundation. (n.d.). *Potential threats to our groundwater*. Retrieved from http://www.groundwater.org/get-informed/groundwater/contamination.html

Todd, D.K. (1959). *Ground water hydrology*. New York, NY: John Wiley & Sons.

Todd, D.K. (1980). *Groundwater hydrology* (2nd ed.). New York, NY: John Wiley & Sons.

Todd, D.K., & Mays, L.W. (2005). *Groundwater hydrology* (3rd ed.). New York, NY: John Wiley & Sons.

Tonkin, M.J., & Doherty, J. (2009). Calibration-constrained Monte Carlo analysis of highly parameterized models using sunspace techniques. *Water Resources Research*, 45(12). doi:10.1029/2007WR006678

Tóth, J.A. (1962). A theory of groundwater motion in small drainage basins in Central Alberta, Canada. *Journal of Geophysical Research*, 67(11), 4375-4387.

Tóth, J.A. (1963). A theoretical analysis of groundwater flow in small drainage basins. *Journal of Geophysical Research*, 68(16), 4795-4812.

Uddameri, V., &Kuchanur, M. (2007). Simulation-optimisation approach to assess groundwater availability in Refugio County, TX. *Environmental Geology*, 51, 921-929.

Wang, H.F., & Anderson, M.P. (1982). *Introduction to groundwater modeling – finite difference and finite element methods*. San Francisco: W.H. Freeman.

Watson, D.F. (1981). Computing the n-dimension delaunay tessellation with application voronoi and polytopes. *Computer Journal*, 24(2), 167-172.

Weight, W.D. (2008). *Hydrological field manual*. New York, NY: McGraw-Hill.

Yidana, S.M. (2011). Groundwater flow modelling and particle tracking for chemical transport in the southern Voltaian aquifers. *Environmental Earth Sciences*, 63(4), 709-721. doi:10.1007/s12665-010-0740-y

Yidana, S.M., Banoeng-Yakubo, B., Akabzaa, T., & Asiedu, D. (2011). Characterization of the flow regime and hydrochemistry of groundwater from the Buem formation, eastern Ghana. *Hydrological Processes*, 25, 2288-2301. doi:10.1002/hyp.7992

Yidana, S.M., & Chegbeleh, L.P. (2013). The hydraulic conductivity field and groundwater flow in the unconfined aquifer system of the Keta Strip, Ghana. *Journal of African Earth Science*, 86, 45-52.

Yidana, S.M., Alfa, B., Banoeng-Yakubo, B., Addai, M.O. (2014). Simulation of groundwater flow in a crystalline rock aquifer system in southern Ghana. An evaluation of effects of increased groundwater abstraction on the aquifers using a transient groundwater flow model. *Hydrological Processes*, 28, 1084-1094.

Yidana, S.M., Alo, C., Addai, M.O., Fynn, O.F., & Essel, S.K. (2015a). Numerical analysis of groundwater flow and potential in parts of a crystalline aquifer system in northern Ghana. *International Journal of Environmental Science and Technology*, 12(12), 3805-3818. doi:10.1007/s13762-015-0805-2

Yidana, S.M., Essel, S.K., Addai, M.O., & Fynn, O.F. (2015b). A preliminary analysis of the hydrogeological conditions and groundwater flow in some parts of a crystalline aquifer system: Afigya Sekyere South District, Ghana. 104, 132-139.

Zhang, Q., & Werner, A. (2009). Integrated surface-subsurface modelling of Fuxianhu Lake catchment Southwest China. *Water Resources Management*, 23, 2189-2204.

Zhou, Q., Liu, H.H., Bodvarsson, G.S., & Oldenburg, C.M. (2003). Flow and transport in unsaturated fractured rock: effects of multiscale heterogeneity of hydrogeological properties. *Journal of Contaminant Hydrology*, 60(1/2), 1-30. doi:10.1016/s0169-7722(02)00080-3

APPENDIX A: Derivation of the total mechanical energy of a unit volume of groundwater

Considering a unit volume of groundwater of nearly constant temperature, the total mechanical energy of the water would have three components – kinetic, gravitational potential and fluid-pressure energy (Fetter, 2001, p. 114). The kinetic energy which is as a result of its motion is given by equation (A.1).

$$E_k = \frac{1}{2}mv^2 \tag{A.1}$$

where

E_k is the kinetic energy

v is the velocity

m is the mass

When a weightless container is filled with this unit volume of water of mass m and moved vertically a distance z from a datum (a reference surface), work is done in moving the mass of water upward. The work done is given by equation (A.2).

$$W = Fz = (mg)z \tag{A.2}$$

where

W is the work done

z is the elevation of the centre of gravity of the water above the datum

g is the acceleration due to gravity

F is the applied force

The mass of water acquires an amount of energy equal to the work done in lifting it above the datum. This energy is a potential energy. It is due to the position of the fluid mass with respect to the datum and is referred to as *gravitational potential energy* E_g expressed as shown in equation (A.3).

$$W = E_g = mgz \tag{A.3}$$

The mass of water possesses another source of potential energy due to the *pressure* of the surrounding fluid acting upon it (Fetter, 2001). The pressure is given by the expression shown in equation (A.4).

$$P = {}^{F}/_{A} \tag{A.4}$$

where

P is the pressure

Thus, from the units of pressure in equation (A.4), pressure could be thought of as potential energy per unit volume of fluid.

For a unit volume of fluid, the mass, m, is numerically equal to the density ρ. Applying this to the three components, the total mechanical energy of the unit volume of water from equations (A.1), (A.3) and (A.4) is given by equation (A.5).

$$E_{tv} = \frac{1}{2}\rho v^2 + \rho g z + P \tag{A.5}$$

where

E_{tv} is the total mechanical energy per unit volume.

Dividing equation (A5) by ρ, yields total mechanical energy per unit mass, E_{tv} as expressed in equation (A.6). The expression shown in equation (A.6) is referred to as the Bernoulli equation (Freeze & Cherry, 1979; Weight, 2008).

$$E_{tm} = \frac{v^2}{2} + gz + \frac{P}{\rho} \tag{A.6}$$

An ideal fluid has the three components of the total energy to be constant while real fluids do not. Real fluids are compressible and do suffer frictional flow losses. Dividing equation (A.6) by g for the case of an ideal fluid will result in the expression shown in equation (A.7).

$$\frac{v^2}{2g} + z + \frac{P}{\rho g} = \text{constant} \tag{A.7}$$

APPENDIX B: Results from the Scenario Analysis Simulations

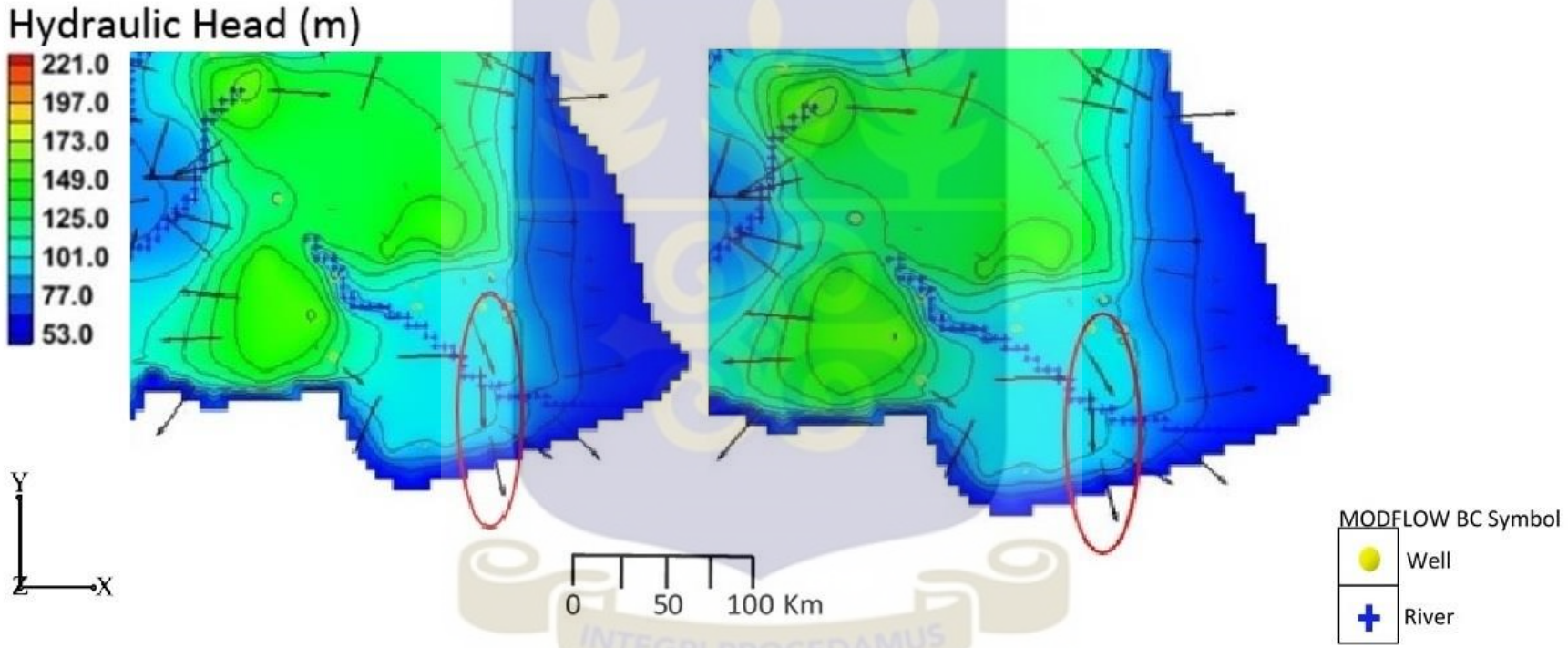

L-R: Figure B1 Hydraulic head distributions and flow patterns after 70% and 80% increase in groundwater abstraction, respectively

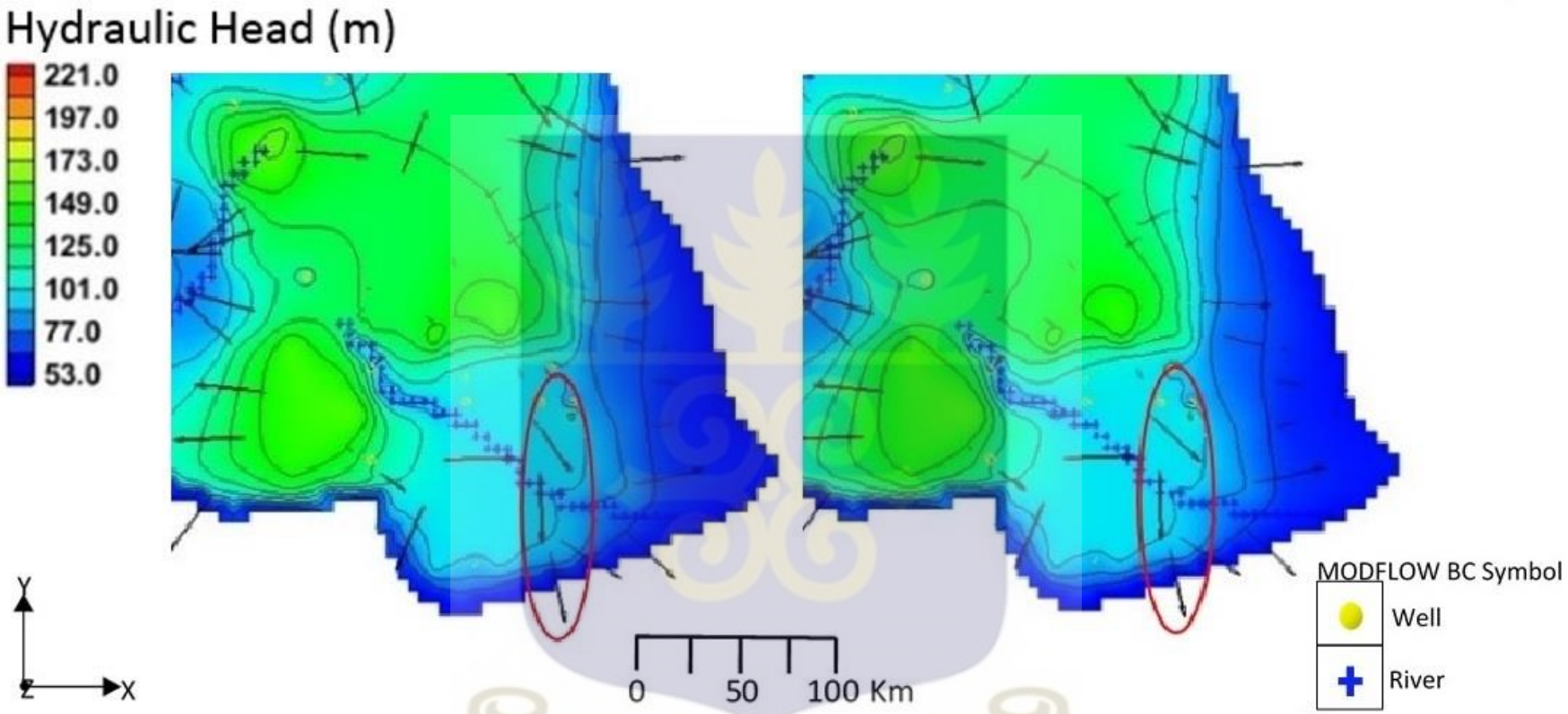

L-R: Figure B2 Hydraulic head distributions and flow patterns after 90% and 100% increase in groundwater abstraction, respectively

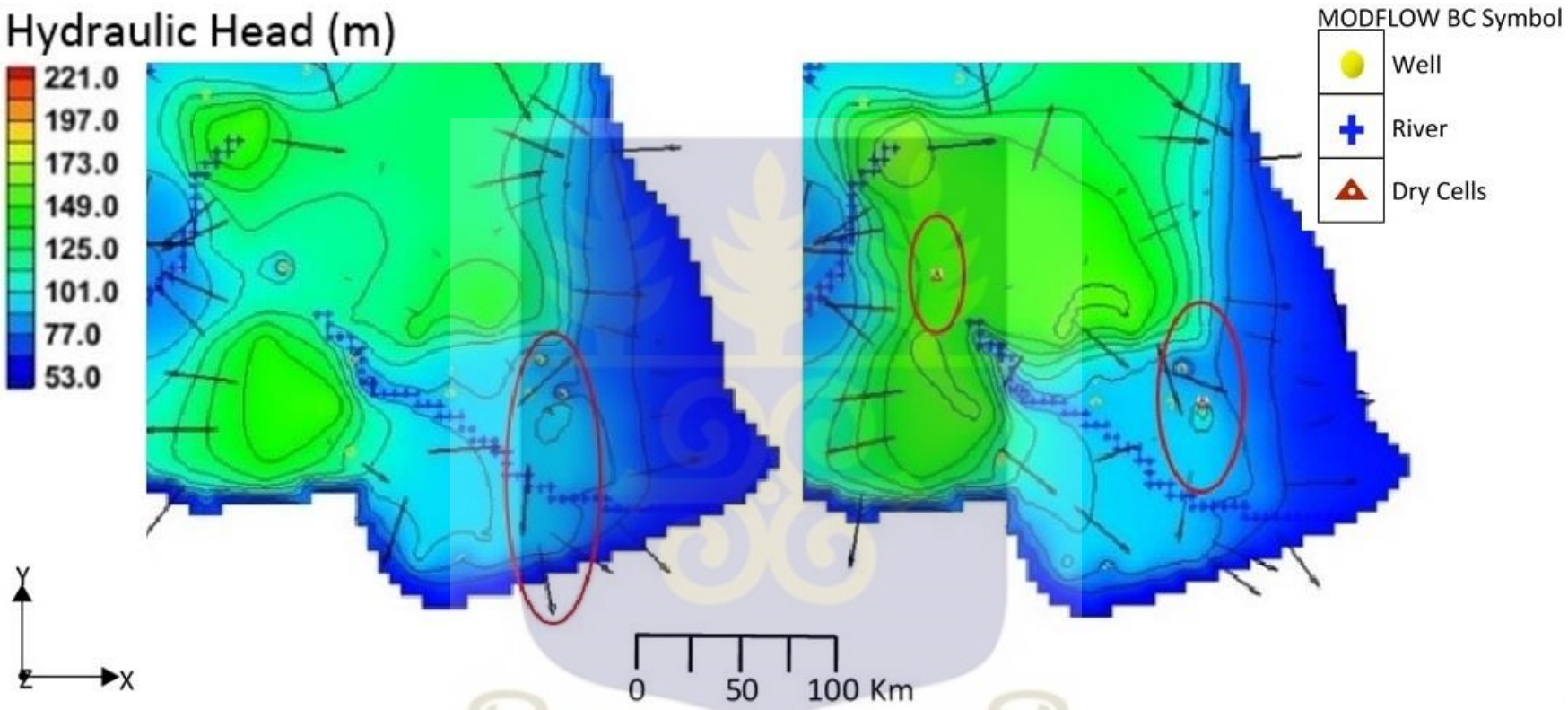

L-R: Figure B3 Hydraulic head distributions and flow patterns after200% and 300% increase in groundwater abstraction, respectively

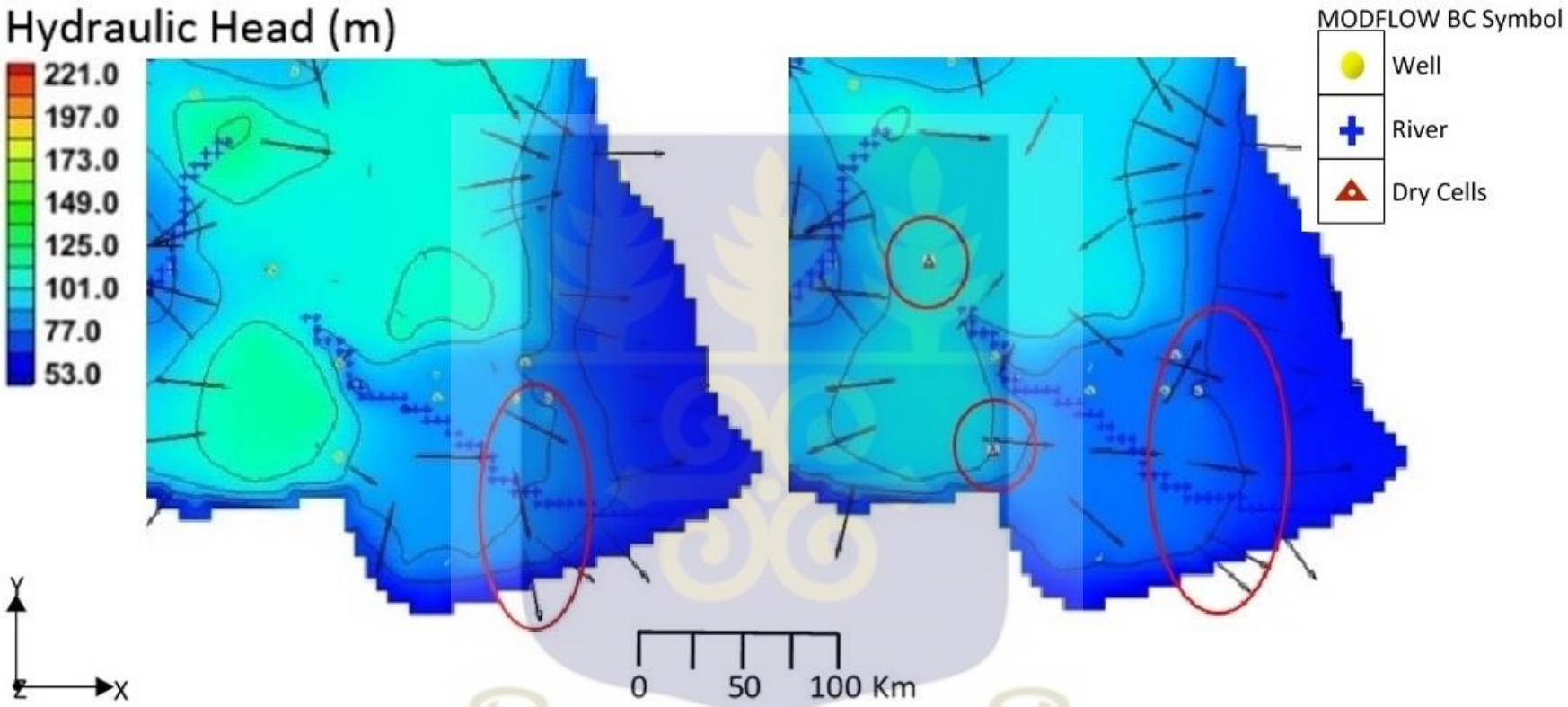

L-R: Figure B4 Hydraulic head distributions and flow patterns after 50% and 70% reduction in groundwater recharge, respectively

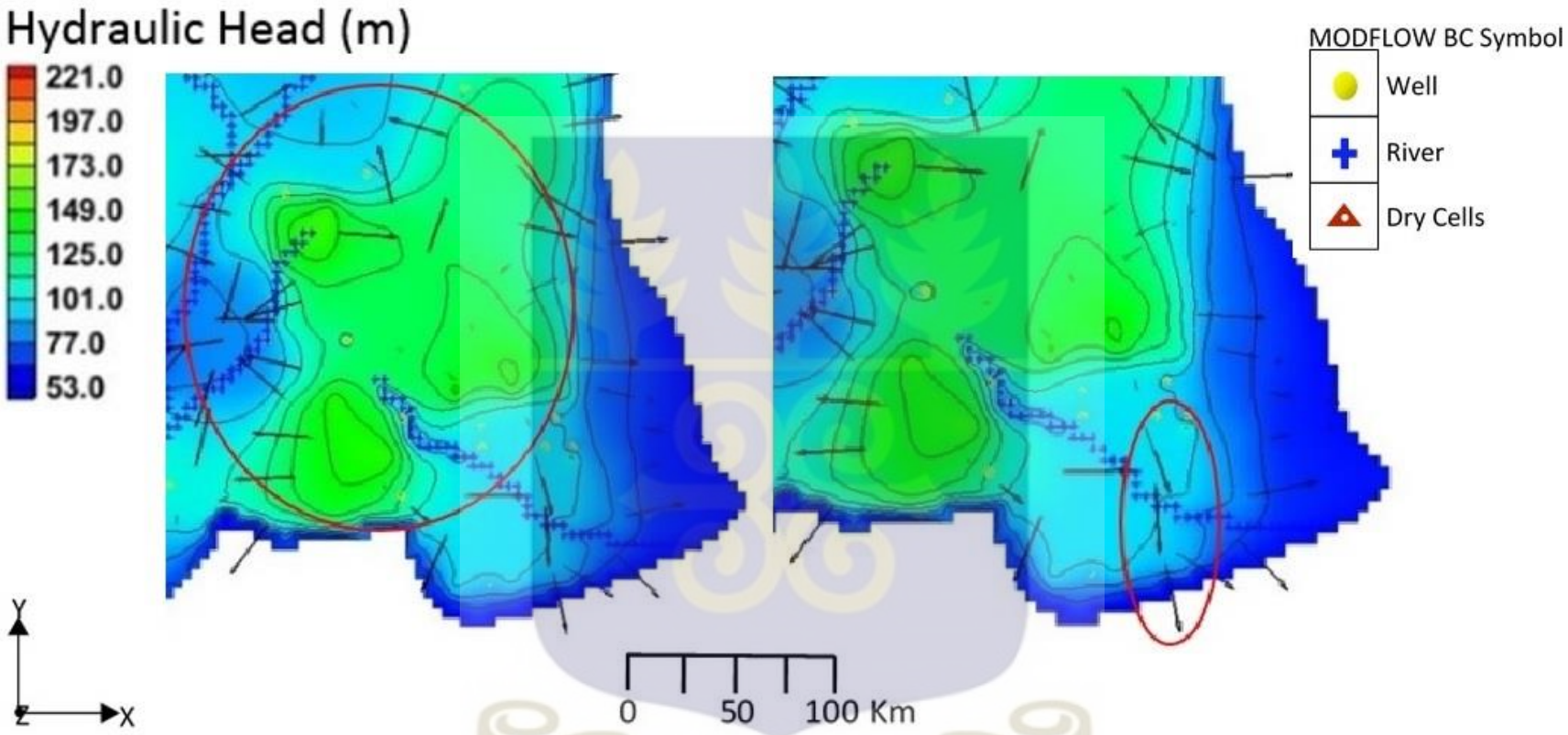

L-R: Figure B5 Hydraulic head distributions and flow patterns after 10% reduction in groundwater recharge with 40% and 50% increase in abstraction, respectively

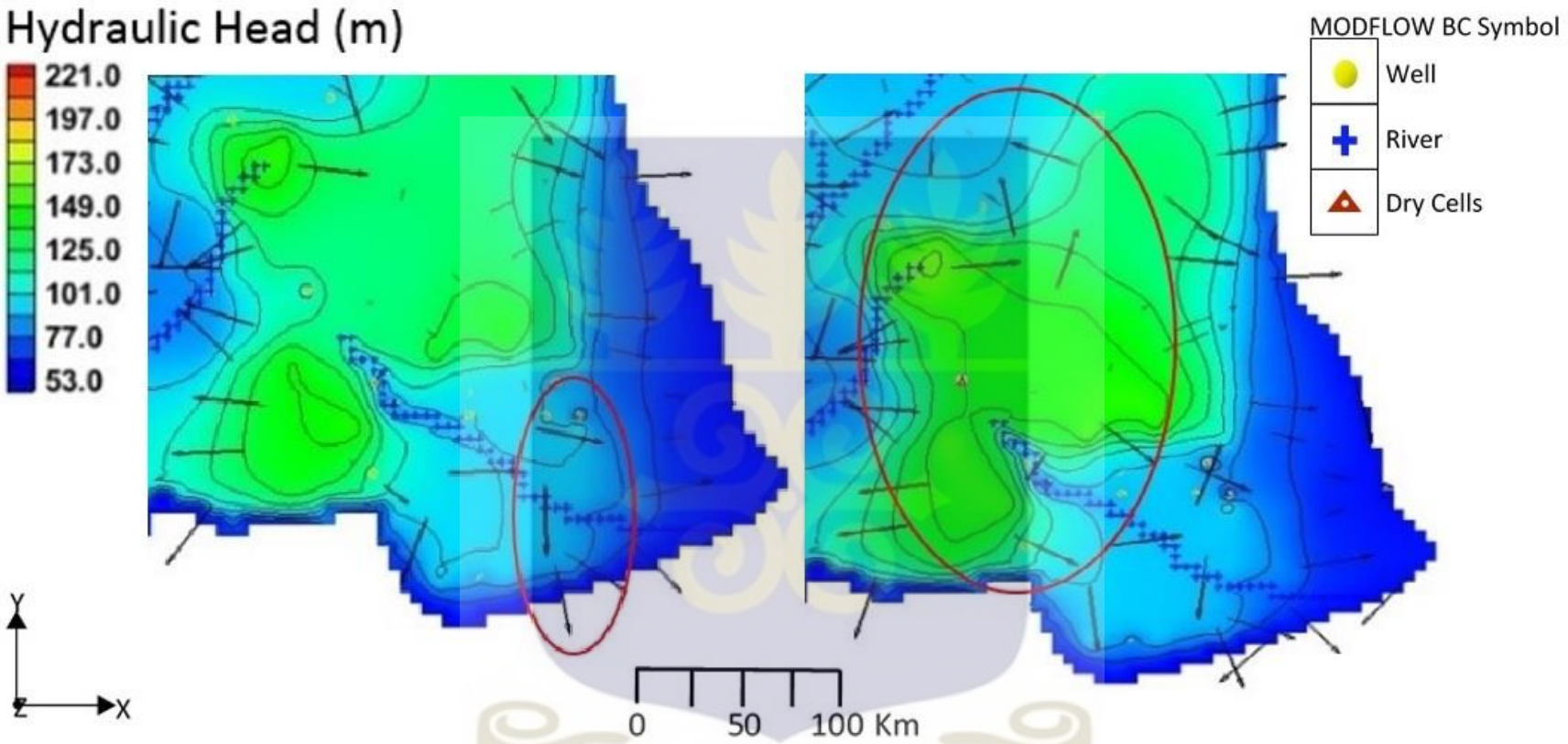

L-R: Figure B6 Hydraulic head distributions and flow patterns after 10% reduction in groundwater recharge with 100% and 200% increase in abstraction, respectively

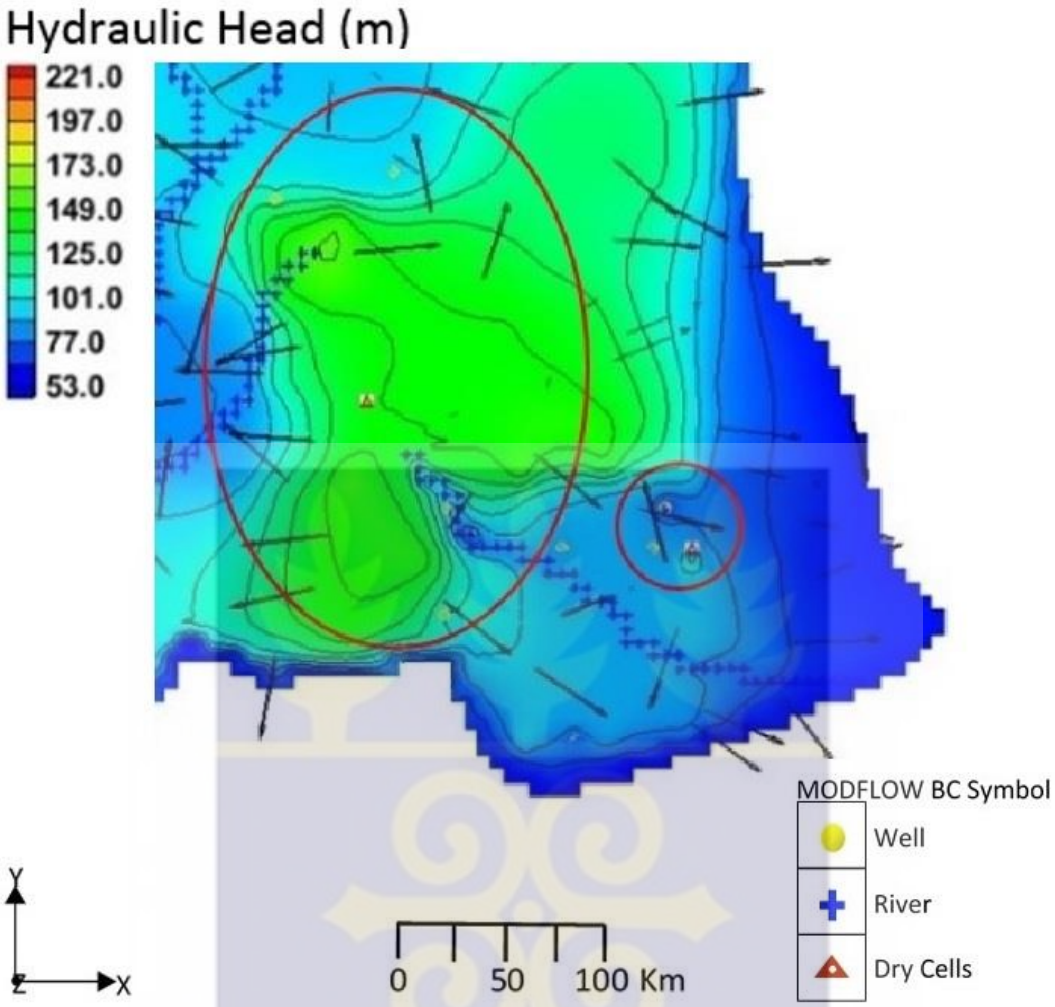

Figure B7 Hydraulic head distribution and flow pattern after 10% reduction in groundwater recharge and 300% increase in abstraction